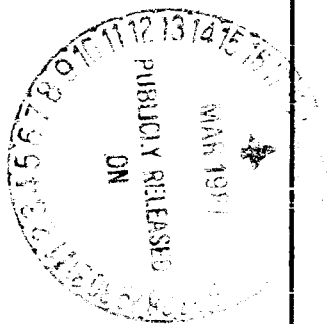


**NASA
Technical
Paper
2392**

February 1985

Effects of Empennage Surface
Location on Aerodynamic
Characteristics of a Twin-
Engine Afterbody Model With
Nonaxisymmetric Nozzles

Francis J. Capone and
George T. Carson, Jr.



Date for general release February 1987



**NASA
Technical
Paper
2392**

1985

Effects of Empennage Surface
Location on Aerodynamic
Characteristics of a Twin-
Engine Afterbody Model With
Nonaxisymmetric Nozzles

Francis J. Capone and
George T. Carson, Jr.

*Langley Research Center
Hampton, Virginia*

NASA

National Aeronautics
and Space Administration

Scientific and Technical
Information Branch

Summary

The effects of empennage surface location and vertical tail cant angle on the aft-end aerodynamic characteristics of a twin-engine fighter-type configuration have been determined in an investigation conducted in the Langley 16-Foot Transonic Tunnel. The configuration featured two-dimensional convergent-divergent nozzles and twin vertical tails. The investigation was conducted at different empennage locations that included two horizontal and three vertical tail positions. Vertical tail cant angle was varied from -10° to 20° for one selected configuration. Tests were conducted at Mach numbers from 0.60 to 1.20 and at angles of attack from -3° to 9° . Nozzle pressure ratio was varied from jet off (1) to approximately 9, depending upon Mach number. An analysis of the results of this investigation was made at a tail deflection of 0° .

Tail interference effects were present throughout the test range of Mach numbers and were found to be either favorable or adverse, depending upon test condition and model configuration. At a Mach number of 0.90, adverse interference effects accounted for a significant percentage of total aft-end drag. Interference effects on the nozzle were generally favorable but became adverse as the horizontal tails were moved from a mid to an aft position. The effects of vertical tail position on aft-end drag were usually dependent on Mach number and configuration. Generally a forward position of the vertical tails produced the lowest total aft-end drag. The configuration with nonaxisymmetric nozzles had lower total aft-end drag with tails off than a similar configuration with axisymmetric nozzles at Mach numbers of 0.60 and 0.90. At a Mach number of 0.60, the nonaxisymmetric nozzle configuration had lower drag with tails-on than the axisymmetric nozzle configuration but unfavorable interference caused higher drag at a Mach number of 0.90. A decrease in total aft-end drag occurred as vertical tail cant angle was varied from -10° to 20° .

Introduction

The mission requirements for the next generation fighter aircraft may dictate a highly versatile vehicle capable of operating over a wide range of flight conditions. These aircraft will most likely be designed for high maneuverability and agility, will operate in a highly hostile environment, and will possess short take-off and landing characteristics to operate from bomb-damaged airfields. These aircraft require variable geometry nozzles to provide high internal nozzle performance; thus, important aft-end parameters such as closure and local boattail angles continuously change throughout the operating range of Mach number, angle of attack, and engine pressure ratios. Large drag penalties can result from integration of the propulsion system into the air-

craft because of adverse interactions originating from empennage surfaces, base areas, actuator fairings, and tail booms (refs. 1 to 5).

A comprehensive program to study the interference effects of empennage surfaces on single- and twin-engine fighter afterbody/nozzle drag has been conducted at the Langley Research Center (refs. 6 to 11) because these interference effects can account for a major portion of total aft-end drag. These studies, which are summarized in references 12 and 13, were conducted with configurations with conventional axisymmetric nozzles. Little information is currently available on empennage effects on configurations with advanced nozzle concepts.

This paper presents results from an investigation of the effects of horizontal and vertical tail position on twin-engine fighter aft-end drag with a model which had nonaxisymmetric (two-dimensional convergent-divergent) nozzles. This exhaust system has the potential to satisfy many different mission requirements with less installation penalties than axisymmetric nozzles (refs. 14 to 16). The present study was part of an overall research program that also determined nonaxisymmetric nozzle thrust reverser performance (ref. 17) and effects of thrust reversing on horizontal tail effectiveness (ref. 18). This investigation was conducted in the Langley 16-Foot Transonic Tunnel at Mach numbers from 0.60 to 1.20, at angles of attack from -3° to 9° , and at nozzle pressure ratios up to 9. Horizontal tail incidence angle was varied from 0° to -10° .

Symbols

Model forces and moments are referred to the stability axis system with the model moment reference center located 4.45 cm above the model centerline at fuselage station 91.6 cm, which corresponds to $0.25\bar{c}$. All coefficients are nondimensionalized with respect to $q_\infty S$ or $q_\infty S\bar{c}$. A discussion of the data reduction procedure and definitions of the aerodynamic force and moment terms and the propulsion relationships used herein are presented in the appendix. The symbols used in the computer-generated tables are given in parentheses in the second column.

$A_{mb,1}$	model cross-sectional area at FS 113.67 and FS 122.56, cm^2
$A_{mb,2}$	model cross-sectional area at FS 168.28, cm^2
$A_{seal,1}$	cross-sectional area enclosed by seal strip at FS 113.67 and FS 122.56, cm^2

$A_{\text{seal},2}$		cross-sectional area enclosed by seal strip at FS 168.28, cm^2	C_m	(CM)	total aft-end aerodynamic pitching-moment coefficient
C_D	(CD)	total aft-end drag coefficient	$C_{m,\text{aft}}$	(CMAFT)	afterbody (plus tails) pitching-moment coefficient
$C_{D,\text{aft}}$	(CDAFT)	afterbody (plus tails) drag coefficient	$C_{m,n}$	(CMN)	nozzle pitching-moment coefficient
$C_{D,n}$	(CDN)	nozzle drag coefficient	$C_{m,t}$	(CMT)	total aft-end pitching-moment coefficient (including thrust component), $C_{m,t} \equiv C_m$ at NPR = 1
$C_{D,\text{tails}}$		tail drag coefficient			
$C_{(D-F)}$	(C(D-F))	drag-minus-thrust coefficient, $C_{(D-F)} \equiv C_D$ at NPR = 1 (jet off)			
$C_{D,o}$		C_D at $C_L = 0$	\bar{c}		wing mean geometric chord, 44.42 cm
$\Delta C_{D,ia}$		increment in empennage interference drag coefficient on afterbody (eq. (A13))	D_f		friction drag, N
$\Delta C_{D,in}$		increment in empennage interference drag coefficient on nozzle (eq. (A12))	F_A		total aft-end axial force, N
$\Delta C_{D,it}$		increment in empennage interference drag coefficient on total aft end (eq. (A11))	$F_{A,\text{Mbal}}$		axial force measured by main balance, N
$(\Delta C_{D,ia})_o$		increment in empennage interference drag coefficient on afterbody at $C_L = 0$	$F_{A,\text{mom}}$		momentum tare axial force due to bellows, N
$(\Delta C_{D,in})_o$		increment in empennage interference drag coefficient on nozzle at $C_L = 0$	$F_{A,\text{Sbal}}$		axial force measured by afterbody shell balance, N
$(\Delta C_{D,it})_o$		increment in empennage interference drag coefficient on total aft end at $C_L = 0$	F_{aft}		afterbody (plus tails) axial force, N
$C_{F,i}$		ideal isentropic gross thrust coefficient	F_i		ideal isentropic gross thrust
C_L	(CL)	total aft-end aerodynamic lift coefficient	F_j		thrust along body axis, N
$C_{L,\text{aft}}$	(CLAFT)	afterbody (plus tails) lift coefficient	M	(MACH)	free-stream Mach number
$C_{L,n}$	(CLN)	nozzle lift coefficient	NPR		nozzle pressure ratio, $p_{t,j}/p_\infty$
$C_{L,t}$	(CLT)	total aft-end lift coefficient (including thrust component), $C_{L,t} \equiv C_L$ at NPR = 1	\dot{m}		measured mass-flow rate, kg/sec
			\dot{m}_i		ideal mass-flow rate, kg/sec
			$\bar{p}_{es,1}$		average static pressure at external seal at FS 113.67, Pa
			$\bar{p}_{es,2}$		average static pressure at external seal at FS 122.56, Pa
			$\bar{p}_{es,3}$		average static pressure at external seal at FS 168.28, Pa

\bar{p}_i		average internal static pressure, Pa
$p_{t,j}$		average jet total pressure, Pa
p_∞		free-stream static pressure, Pa
q_∞		free-stream dynamic pressure, Pa
S		wing reference area, 4290.00 cm ²
R		gas constant, 287.3 J/kg-K
t/c		thickness-chord ratio
$T_{t,j}$		jet total temperature, K
α	(ALPHA)	angle of attack, deg
γ		ratio of specific heats, 1.3997 for air at 300 K
δ_h		horizontal tail deflection, positive leading edge up, deg
Λ_{te}		leading-edge sweep angle, deg
ϕ_t		vertical tail cant angle, positive tip out, deg

Abbreviations:

ASME	American Society of Mechanical Engineers
BL	buttock line, cm
FS	fuselage station (axial location described by distance in centimeters from model nose)
Fwd	forward
HT	horizontal tails
VT	vertical tails
WL	water line, cm

Apparatus and Procedure

Wind Tunnel

This investigation was conducted in the Langley 16-Foot Transonic Tunnel, a single-return atmospheric wind tunnel with a slotted octagonal test section and continuous air exchange. The wind tunnel has continuously variable airspeed up to a Mach number of 1.30.

Test-section plenum suction is used for speeds above a Mach number of 1.05. A complete description of this facility and operating characteristics can be found in reference 19.

Model and Support System

Details of the general research, twin-engine fighter afterbody model and wing-tip-mounted support system used in this investigation are presented in figure 1. Photographs of the model and support system installed in the Langley 16-Foot Transonic Tunnel are shown in figure 2. A sketch of the wing planform geometry is presented in figure 3.

The wing-tip model support system shown in figure 1 consisted of three major portions: the twin support booms, the forebody (nose), and the wing-centerbody combination. These pieces made up the nonmetric portion (that portion of the model not mounted on the force balance) of the twin-engine fighter model. The fuselage centerbody was essentially rectangular in cross section having a constant width and height of 25.40 cm and 12.70 cm, respectively. The four corners were rounded by a radius of 2.54 cm. Maximum cross-sectional area of the centerbody (fuselage) was 317.04 cm². The support system forebody (or nose) was typical of a powered model in that the inlets were faired over. For these tests, the wings were mounted above the model centerline (model has capability for both high or low wing mount). The wing had a 45° leading-edge sweep, a taper ratio of 0.5, an aspect ratio of 2.4, and a cranked trailing edge (fig. 3). The NACA 64-series airfoil had a thickness ratio of 0.067 near the wing root to provide a realistic wake on the afterbody. From BL 27.94 outboard to the support booms, however, wing thickness ratio increased from 0.077 to 0.10 to provide adequate structural support for the model and to permit transfer of compressed air from the booms to the model propulsion system.

The metric portion of the model aft of FS 113.67, supported by the main force balance, consisted of the internal propulsion system, afterbody, tails (not shown in fig. 1), and nozzles. The afterbody lines (boattail) were chosen to provide a length of constant cross section aft of the nonmetric centerbody and to enclose the force balance and jet simulation system while fairing smoothly downstream into the closely spaced nozzles. The afterbody shell from FS 122.56 to FS 168.28 and tail surfaces (when installed) were attached to an afterbody force balance which was attached to the main force balance (fig. 1). The main force balance in turn was grounded to the nonmetric wing-centerbody section. The nozzles were attached directly to the main force balance through the propulsion system piping. Three clearance gaps (metric breaks) were provided between

the nonmetric and the individual metric portions (afterbody and nozzles) of the model at FS 113.67, FS 122.56, and FS 168.28, to prevent fouling of the components upon each other. A flexible plastic strip inserted into circumferentially machined grooves in each component impeded flow into or out of the internal model cavity (fig. 1).

In this report, that section of the model aft of FS 122.56 is referred to as the total aft end (includes afterbody, tails when installed, and nozzles). That section of the model from FS 122.56 to FS 168.28 is referred to as the afterbody, and that section aft of FS 168.28 is considered the nozzles. A skin-friction drag adjustment to the axial force results of the main balance was made for the section of the model from FS 113.67 to FS 122.56. (See appendix.)

The afterbody had provisions for mounting both the twin vertical tails and horizontal tails in three axial positions. The vertical tails at a cant angle of 0° , were tested in three positions—forward, mid, and aft—as shown in figure 4. With the vertical tails in the mid position, cant angles of -10° , 10° , and 20° were also tested. The horizontal tails were only tested in the mid and aft positions which are about at the same positions as those of references 9 to 12. Note that both the vertical and horizontal tails have smaller tail spans when installed in the aft position than when they are installed in the other positions.

Sketches of the horizontal and vertical tails are presented in figures 5 and 6, respectively. These tail surfaces were sized to be representative of current twin-engine fighter aircraft. Individual root fairings (fillers) contoured the tails to the afterbody at each tail position. Clearance gaps were provided between the nozzles and horizontal and vertical tails (aft position) in order to prevent fouling between the main and afterbody balances (fig. 4). These tail surfaces (without fairings) were also used in the investigations of references 9 to 11.

Twin-Jet Propulsion Simulation System

The twin-jet propulsion simulation system is shown in figure 1. An external high-pressure air system provides a continuous flow of clean, dry air at a controlled temperature of about 306 K at the nozzles. This high-pressure air is brought into the wind-tunnel main support strut where it is divided into two separate flows and passed through remotely operated flow-control valves. These valves are used to balance the total pressure in each nozzle.

The divided compressed airflows are piped through the wing-tip support booms, through the wings, and into the flow-transfer bellows assemblies (fig. 1). A sketch of a single flow-transfer bellows assembly is shown in figure 7. The air in each supply pipe is discharged perpendicularly to the model axis through eight

sonic nozzles equally spaced around the supply pipe. This method is designed to eliminate any transfer of axial momentum as the air is passed from the nonmetric to the metric portion of the model. Two flexible metal bellows are used as seals and serve to compensate the axial forces caused by pressurization. The cavity between the supply pipe and bellows is vented to model internal pressure. The airflow is then passed through the tailpipes into the transition sections and then to the exhaust nozzles. (See fig. 1.)

The nonaxisymmetric (two-dimensional convergent-divergent) nozzle used in this investigation is shown in figure 8. The nozzle simulated a dry-power or cruise operating mode with a design NPR of about 3.5. The nozzle throat area (17.48 cm^2) and expansion ratio (1.15) were sized to be consistent with advanced mixed flow turbofan cycles. The ratio of total throat area to maximum body cross-sectional area was 0.11, and the nozzle throat aspect ratio was 3.45. This nozzle was one of a series of nozzles tested in the study reported in reference 20. Nozzle static performance, ideal thrust coefficients, and scheduled pressure ratios are presented in figure 9.

Instrumentation

Forces and moments on the metric portions of the model were measured by two six-component strain-gauge balances. The main balance measured forces and moments resulting from nozzle gross thrust and the external flow field over that portion of the model aft of FS 113.67. The tandem afterbody shell balance measured forces and moments resulting from the external flow field over the afterbody and empennage surfaces from FS 122.56 to FS 168.28. The tandem balance arrangement permits the separation of model component forces for data analysis.

Eight external seal static pressures were measured in the seal gap at the first metric break (FS 113.67). All orifices were located on the nonmetric centerbody and spaced symmetrically about the model perimeter. An additional five orifices, positioned symmetrically about the right side of the model measured seal gap pressures at the second metric break (FS 122.56). The final seal pressures were measured by two sets of surface taps, both consisting of two orifices, each an equal distance fore and aft of the third metric break (FS 168.28). In addition to these external pressures, two internal pressures were measured at each metric seal. These pressure measurements were then used to correct measured axial force and pitching moment for pressure-area tares as discussed in the appendix.

Chamber pressure and temperature measurements taken in the supply pipe, upstream of the eight sonic nozzles (fig. 7), were used to compute mass-flow rates for each nozzle. Instrumentation in each charging sec-

tion consisted of a stagnation-temperature probe and a total-pressure rake. Each rake contained four total-pressure probes. (See fig. 8.)

All pressures were measured with individual pressure transducers. Data obtained during each tunnel run were recorded on magnetic tape and reduced with standard data reduction procedures. Typically, for each data point, 50 samples of data were recorded over a period of 5 sec and the average was used for computational purposes.

Tests

This investigation was conducted in the Langley 16-Foot Transonic Tunnel at Mach numbers from 0.60 to 1.20 and at angles of attack from -3° to 9° . Nozzle pressure ratio varied from 1 (jet off) to 9, depending upon Mach number. Basic data were obtained by varying nozzle pressure ratio at zero angle of attack and by varying angle of attack at fixed nozzle pressure ratios. The investigation was conducted with different empennage locations that included two horizontal and three vertical tail positions. Vertical tail cant angle was varied from -10° to 20° for one selected configuration. Horizontal tail incidence was varied for selected configurations from 0° to -10° . Reynolds number based on the wing mean geometric chord varied from 4.4×10^6 to 5.28×10^6 .

All tests were conducted with 0.26-cm-wide boundary-layer transition strips consisting of No. 120 silicon carbide grit sparsely distributed in a thin film of lacquer. These strips were located 2.54 cm from the tip of the forebody nose and on both upper and lower surfaces of the wings and empennage at 5 percent of the root chord to 10 percent of the tip chord.

Presentation of Results

The results of this investigation are presented in both tabular and plotted form. Table 1 is an index to the tabular results contained in tables 2 to 17. The computer symbols appearing in these tables are defined in the section "Symbols" with their corresponding mathematical symbols which are described in the appendix. Plotted data are presented only at $\delta_h = 0^\circ$ because subsequent analysis cannot be made at a constant lift coefficient. Because this investigation was conducted with a partially metric model, data were obtained at essentially three different ranges of lift coefficient as tail deflection was varied from 0° to -10° . Basic and summary data for selected conditions at $\delta_h = 0^\circ$ are presented in figures 10 to 22 as follows:

Figure

Variation of aft-end aerodynamics at $\alpha = 0^\circ$ with NPR for—	
Horizontal tails mid, variable vertical tail position, and $\phi_t = 0^\circ$	10

Horizontal tails aft, variable vertical tail position, and $\phi_t = 0^\circ$	11
Horizontal tails aft, vertical tails mid, and variable ϕ_t	12
Variation of total aft-end aerodynamics with α for—	
Horizontal tails mid, variable vertical tail position, and $\phi_t = 0^\circ$	13
Horizontal tails aft, variable vertical tail position, and $\phi_t = 0^\circ$	14
Horizontal tails aft, vertical tails mid, and variable ϕ_t	15
Summary data:	
Total aft-end drag, $C_L = 0$, and empennage location	16
Interference drag terms, $C_L = 0$, and empennage location	17
Interference drag terms, $\alpha = 0^\circ$, and horizontal tails mid	18
Interference drag terms, $\alpha = 0^\circ$, and horizontal tails aft	19
Comparison with axisymmetric nozzle configurations with $\alpha = 0^\circ$	20
Total aft-end drag, $C_L = 0$, and vertical tail cant angle	21
Interference drag terms, $\alpha = 0^\circ$, and vertical tail cant angle	22

Discussion

Basic Data

The basic data obtained during this investigation are presented in figures 10 to 15 for the various configurations tested at $\delta_h = 0^\circ$ only. Two types of data presentation are made to illustrate the effects of nozzle pressure ratio and angle of attack. First, the variation of total aft end, afterbody, and nozzle aerodynamic drag and lift coefficients with nozzle pressure ratio at $\alpha = 0^\circ$ is presented in figures 10 to 12. Second, the variation of total aft-end aerodynamic lift and drag coefficients with angle of attack is presented in figures 13 to 15 at jet-off conditions and at a scheduled pressure ratio for each Mach number (fig. 9(c)). Test parameters not shown in plotted form, such as total aft-end pitching-moment coefficient, or obtained on configurations investigated at tail deflections other than 0° have been tabulated (tables 2 to 17).

In general, the variation of total aft-end drag coefficient C_D with nozzle pressure ratio for any particular configuration (figs. 10 to 12), follows expected trends (e.g., see refs. 6 and 9). Total aft-end drag decreases with initial jet operation up to nozzle pressure ratios of 2 to 3. This decrease in total aft-end drag is primarily a result of a decrease in drag on the nozzles particularly at $M = 0.60$ and 1.20. This decrease in nozzle

drag is caused by a reduction in the external flow expansion required at the nozzle exit as the exhaust flow fills the nozzle base region. As nozzle pressure ratio is further increased, there is an increase in nozzle drag and, hence, total aft-end drag. Except at $M = 0.60$, nozzle drag subsequently decreases again with additional increases in NPR. The change in drag trend with increasing NPR (generally a drag increase) at NPR above 2 to 3 is probably caused by exhaust flow entrainment effects on the external nozzle flow, whereas the drag decreases at the higher nozzle pressure ratios ($NPR > 3$) are caused by a compression at the nozzle exit created by the increased thickness of the exhaust flow plume. These trends with increasing nozzle pressure ratio are typical for jet-powered models (ref. 6).

The effects of angle of attack on total aft-end aerodynamic characteristics shown in figures 13 to 15 are also typical for partially metric afterbody propulsion models. A single break occurs in the lift curves at $\alpha \approx 3^\circ$ at $M = 0.60$, whereas at $M = 1.20$, there are breaks at $\alpha = 0^\circ$ and 3° . At $M = 0.90$, the lift curves are nonlinear. Total aft-end drag polars also exhibit characteristics that are typical for afterbody propulsion models. A typical shape of the drag at $M = 0.90$ probably results from changes in the wing downwash on the afterbody and empennage surfaces in the transonic range.

Effect of Empennage Location

The effects of twin vertical tail longitudinal position on total aft-end zero-lift drag coefficients and individual zero-lift interference drag increments are presented in figures 16 and 17, respectively, for the two horizontal tail positions investigated. These values were determined by interpolation at $C_L = 0$ from data obtained as angle of attack was varied at constant nozzle pressure ratio (fig. 13(b), typical). These nozzle pressure ratios correspond to the schedule shown in figure 9(c). In addition, the effect of nozzle pressure ratio on individual interference drag coefficients at $\alpha = 0^\circ$ is shown in figures 18 and 19 for the various configurations tested. Note that these interference drag data are at $\alpha = 0^\circ$ (because of the method used to obtain data) rather than $C_L = 0$; thus, absolute levels may differ from those presented in figure 17.

Horizontal tails mid. There are no definite trends to total aft-end zero lift drag $C_{D,o}$ as the vertical tails are moved from the forward to the mid position (fig. 16) for the test Mach numbers. The lowest value of $C_{D,o}$ was measured for this investigation at $M = 0.60$ and $NPR = 3.5$ with all tail surfaces in the mid position (fig. 16). The lowest jet-off ($NPR = 1$) value of $C_{D,o}$ also occurred for this configuration (fig. 13(a)).

The trends of zero-lift total aft-end empennage interference drag coefficient (fig. 17) are the same as for $C_{D,o}$ as vertical tail position is varied for the test Mach numbers. Note that $(\Delta C_{D,it})_o$ is negative at $M = 0.60$ and 1.20 ; this indicates favorable interference. At $M = 0.60$, this favorable interference is due to the tails-on nozzle drag being lower than the tails-off nozzle drag. At this Mach number, favorable interference is a result of favorable interference on the nozzles. However, the favorable interference effects on the total aft end at $M = 1.20$ are caused from favorable interference on the afterbody and not the nozzles (fig. 17). Similar results at $M = 1.20$ were found in reference 9.

At $M = 0.90$, favorable interference on the nozzles also occurred. However, the favorable interference effects on the nozzles are negated by adverse interference now present on the afterbody (fig. 17), which is greatly aggravated as the vertical tails are moved from the forward to the mid position. With the vertical tails in the mid position, afterbody interference drag is 57 percent and total aft-end interference drag is 47 percent of the total aft-end zero-lift drag $C_{D,o}$. As the vertical tails are moved from the forward to mid location at $M = 0.60$ and 0.90 , there is a decrease in nozzle drag (fig. 10) and a favorable increase (more negative) in nozzle interference drag increment. This trend is similar to that obtained previously on a single-engine configuration (ref. 6) but opposite to that obtained on a twin-engine configuration (ref. 9). Both of these studies utilized models with axisymmetric nozzles.

Horizontal tails aft. As shown in figure 16, a large increase in total aft-end zero-lift drag occurs subsonically as the vertical tails are moved from the forward to mid position. Further movement of the vertical tails to the aft position then results in a decrease in $C_{D,o}$. A similar trend was observed at $M = 1.20$, but the changes in $C_{D,o}$ are small. With the horizontal tails aft, the configuration with the vertical tails forward produced the lowest total aft-end drag at all Mach numbers. In general, configurations with staggered tail arrangements (vertical tails forward, horizontal tails aft) have been found to have lower total aft-end drag for both single- and twin-engine configurations (refs. 6 and 9).

Examination of zero-lift individual interference drag increments shows a large effect of moving the horizontal tail from the mid to aft position (fig. 17). With the horizontal tails in the aft position, the increment in empennage interference drag coefficient on the nozzle is always unfavorable, even though nozzle drag coefficient is still negative at $M = 0.60$ and 0.90 (fig. 11). This probably indicates a reduction in pressure recovery on the nozzles or flow separation on the nozzle sidewalls when the horizontal tails are located adjacent to the

nozzles. As the vertical tails are moved from the forward to the aft position, there is an increase in empennage interference drag on the nozzle (except at $M = 0.6$ with vertical tails aft) and an increase in nozzle drag (fig. 11). This trend is opposite to the one noted with the horizontal tails mid and is the same as that reported in reference 9.

At $M = 0.9$, there is a sharp increase in both the total and afterbody empennage interference drag terms (fig. 17) as the vertical tails are moved from the forward to mid position. Similar results were also found with the horizontal tails in the mid position. Although the reasons for this behavior are not known, one possible explanation is that the adverse interference is a result of the vertical tails being misaligned with the local flow field of the wing/forebody at the mid position. Reference 10 indicates that total aft-end drag was extremely sensitive to vertical tail toe angle. The vertical tail toe angle was 0° for the present investigation.

At lifting conditions (figs. 13 and 14), the configuration with the vertical tails forward generally had the lowest jet-on drag coefficient throughout the Mach number and angle-of-attack ranges except at $M = 0.60$. At this Mach number, the configuration with the vertical and horizontal tails mid had the lowest drag over the angle-of-attack range.

Comparison with other data. A comparison of the total aft-end drag coefficient at $\alpha = 0^\circ$ of the present study with that of the configuration of reference 9 is made in figure 20. Both of these configurations were identical up to FS 122.56 and used the same tail surfaces. The afterbody (FS 122.56 to FS 168.28) of reference 9 was designed to have axisymmetric nozzles installed at FS 168.28. Since the nozzles of both these investigations had the same nozzle throat areas and expansion ratios, the afterbody closure ratios (ratio of twice throat area to maximum body cross-sectional area) were the same.

In order to make the comparisons between the two configurations, it is first necessary to discuss the total aft-end drag characteristics of both configurations without tails. Additional drag differences between the two configurations are caused by tail interference effects since the drag of the tails is essentially the same. Tails-off total aft-end drag coefficients at $\alpha = 0^\circ$ are presented in the table on this page. As can be seen, the nonaxisymmetric nozzle configuration of the present study has lower drag at $M = 0.60$ and 0.90 because of the nozzle installation. The higher drag at $M = 1.20$ is attributed to poor cross-sectional area distribution characteristics.

As seen in figure 20, the present configuration always had lower total aft-end drag than that of reference 9 for all the combinations of empennage surfaces tested at

M	Drag from present study for—		Drag from reference 9 for—	
	Jet off	Schedule NPR	Jet off	Schedule NPR
0.60	0.0039	0.0035	0.0050	0.0041
.90	.0032	.0028	.0040	.0030
1.20	.0166	.0158	.0150	.0122

$M = 0.60$. However, at $M = 0.90$ and $M = 1.20$, the configurations of the present study nearly always had higher drag than that of reference 9 because of unfavorable tail interference effects. In general, the trends in C_D with vertical tail movement are similar to that of reference 9.

Effect of Vertical Tail Cant Angle

The effects of vertical tail cant angle on total aft-end zero-lift drag coefficient and increments in empennage interference drag coefficient at $\alpha = 0^\circ$ are presented in figures 21 and 22. As can be seen, increasing tail cant angle from -10° to 20° reduced total aft-end zero-lift drag coefficient and, in general, reduced each of the drag interference terms over the test Mach number range. Figure 15 also shows that reductions in drag coefficient from increasing tail cant angle also occur over the test angle-of-attack range. Similar results were obtained in reference 10.

Conclusions

An investigation has been conducted in the Langley 16-Foot Transonic Tunnel to determine the effects of empennage surface location and vertical tail cant angle on the aft-end aerodynamic characteristics of a twin-engine fighter-type configuration. The configuration featured two-dimensional convergent-divergent nozzles and twin vertical tails. The investigation was conducted at different empennage locations that included two horizontal and three vertical tail positions. Vertical tail cant angle was varied from -10° to 20° for one selected configuration. Tests were conducted at Mach numbers from 0.60 to 1.20 over an angle-of-attack range from -3° to 9° . Nozzle pressure ratio was varied from jet off (1) to approximately 9, depending upon Mach number. An analysis of the results of this investigation at a tail deflection of 0° indicates the following conclusions:

1. Tail interference effects were present throughout the test range of Mach numbers and were found to be either favorable or adverse, depending upon test condition and model configuration. At Mach number of 0.90, adverse interference effects accounted for a significant percentage of total aft-end drag.

2. Interference effects on the nozzle were generally favorable but became adverse as the horizontal tails were moved from a mid to an aft position.

3. The effects of vertical tail position on aft-end drag were usually dependent on Mach number and configuration. Generally, a forward position of the vertical tails produced the lowest total aft-end drag.

4. The configuration with nonaxisymmetric nozzles had lower total aft-end drag with tails off than a similar configuration with axisymmetric nozzles at Mach numbers of 0.60 and 0.90.

5. At a Mach number of 0.60, the nonaxisymmetric nozzle configuration had lower drag with tails on than

the axisymmetric nozzle configuration but unfavorable interference caused higher drag at a Mach number of 0.90.

6. A decrease in total aft-end drag occurred as vertical tail cant angle was varied from -10° to 20° .

Langley Research Center
National Aeronautics and Space Administration
Hampton, VA 23665
October 3, 1984

Appendix

Data Reduction and Calibration Procedure

Calibration Procedure

The main balance measured the combined forces and moments due to nozzle gross thrust and the external flow field of that portion of the model aft of FS 113.67. The tandem shell balance measured forces and moments due to the external flow field exerted over the afterbody and tails between FS 122.56 and FS 168.28.

Force and moment interactions exist between the flow-transfer bellows system (fig. 7) and the main force balance because the centerline of this balance was below the jet centerline (fig. 1). Consequently, single and combined loadings of normal and axial force and pitching moment were made with and without the jets operating with ASME calibration nozzles. These calibrations were performed with the jets operating because this condition gives a more realistic effect of pressurizing the bellows than capping the nozzles and pressurizing the flow system. Thus, in addition to the usual balance-interaction corrections applied for a single force balance under combined loads, another set of interactions were made to the data from this investigation to account for the combined loading effect of the main balance with the bellows system. These calibrations were performed over a range of expected normal forces and pitching moments. Note that this procedure is not necessary for the afterbody forces because the flow system is not bridged by the tandem shell balance.

Data Adjustments

In order to achieve desired axial-force terms, the axial forces measured by both force balances must also be corrected for pressure-area tare forces acting on the model and the main balance corrected for momentum tare forces caused by flow in the bellows. The external seal and internal pressure forces on the model were obtained by multiplying the difference between the average pressure (external seal or internal pressures) and free-stream static pressure by the affected projected area normal to model axis. The momentum tare force was determined from calibrations with the ASME nozzle prior to the wind-tunnel investigation.

Axial force minus thrust was computed from the main balance axial force with the following relationship:

$$F_A - F_j = F_{A,Mbal} + (\bar{p}_{es,1} - p_\infty)(A_{mb,1} - A_{seal,1}) + (\bar{p}_i - p_\infty)A_{seal,1} - F_{A,mom} + D_f \quad (A1)$$

where $F_{A,Mbal}$ includes all pressure and viscous forces, internal and external, on both the afterbody and thrust system. The second and third terms account for the

forward seal rim and interior pressure forces, respectively. In terms of an axial-force coefficient, the second term ranges from -0.0001 to -0.0007 and the third term varies ± 0.0075 , depending upon Mach number and pressure ratio. The internal pressure at any given set of test conditions was uniform throughout the inside of the model; thus, no cavity flow was indicated. The momentum tare force $F_{A,mom}$ is a momentum tare correction with jets operating and is a function of the average bellows internal pressure that is a function of the internal chamber pressure in the supply pipes just ahead of the sonic nozzles (fig. 7). Although the bellows were designed to minimize momentum and pressurization tares, small bellows tares still exist with the jet on. These tares result from small pressure differences between the ends of the bellows when internal velocities are high and also from small differences in the forward and aft bellows spring constants when the bellows are pressurized. The last term D_f (eq. (A1)) is the friction drag of the section from FS 113.67 to FS 122.68. A friction drag coefficient of 0.0004 was applied at all Mach numbers.

Afterbody axial force is computed from a similar relationship as follows:

$$F_{aft} = F_{A,Sbal} + (\bar{p}_{es,2} - p_\infty)(A_{mb,1} - A_{seal,1}) + (\bar{p}_i - p_\infty)A_{seal,2} + (\bar{p}_{es,3} - p_\infty)(A_{mb,2} - A_{seal,2}) \quad (A2)$$

Since both balances are offset from the model centerline, similar adjustments are made to the pitching moments measured by both balances. These adjustments are necessary because both the pressure area and bellows momentum tare forces are assumed to act along the model centerline. The pitching-moment tare is determined by multiplying the tare force by the appropriate moment arm and subtracting the value from the measured pitching moments.

Model Attitude

The adjusted forces and moments measured by both balances were transferred from the body axis (which lies in the horizontal tail chord plane) of the metric portion of the model to the stability axis. Attitude of the nonmetric forebody relative to gravity was determined from a calibrated attitude indicator located in the model nose. Angle of attack α , which is the angle between the afterbody centerline and the relative wind, was determined by applying terms for afterbody deflection, caused when the model and balance bent under aerodynamic load, and by a flow angularity term to the angle measured by the attitude indicator. The flow angularity adjustment was 0.1° , which is the average angle measured in the Langley 16-Foot Transonic Tunnel.

Ideal Thrust

The ideal isentropic gross thrust of each nozzle can also be determined if the mass-flow rate for each nozzle is known. The effective discharge coefficients of the eight sonic nozzles (fig. 7) forward of each of the nozzle tail pipes were determined and used for measuring mass flow.

The total ideal isentropic gross thrust or exhaust jet momentum for both nozzles is

$$F_i = \dot{m} \sqrt{RT_{t,j} \frac{2\gamma}{\gamma-1} \left[1 - \left(\frac{p_\infty}{p_{t,j}} \right)^{\frac{\gamma-1}{\gamma}} \right]} \quad (\text{A3})$$

where \dot{m} is the mass-flow rate measured in the flow-transfer assemblies and $p_{t,j}$ is the average jet stagnation pressure for both nozzles.

Thrust-Removed Characteristics

The resulting force and moment coefficients (including thrust components) from the main balance include total lift coefficient $C_{L,t}$, drag-minus-thrust coefficient $C_{(D-F)}$, and total pitching-moment coefficient $C_{m,t}$. Force and moment coefficients from the tandem shell balance are afterbody (plus tails) lift coefficient $C_{L,\text{aft}}$, afterbody drag coefficient $C_{D,\text{aft}}$, and afterbody pitching-moment coefficient $C_{m,\text{aft}}$.

Thrust-removed aerodynamic force and moment coefficients for the entire model were obtained by determining the components of thrust in axial force, normal force, and pitching moment and subtracting these values from the measured total (aerodynamic plus thrust) forces and moments. These thrust components at forward speeds were determined from measured static data and were a function of the free-stream static and dynamic pressure. Thrust-removed aerodynamic coefficients are

$$C_L = C_{L,t} - \text{Jet lift coefficient} \quad (\text{A4})$$

$$C_D = C_{(D-F)} + \text{Thrust coefficient} \quad (\text{A5})$$

$$C_m = C_{m,t} - \text{Jet pitching moment coefficient} \quad (\text{A6})$$

Nozzle coefficients are obtained by simply combining the measured results from both force balances as follows:

$$C_{L,n} = C_L - C_{L,\text{aft}} \quad (\text{A7})$$

$$C_{D,n} = C_D - C_{D,\text{aft}} \quad (\text{A8})$$

$$C_{m,n} = C_m - C_{m,\text{aft}} \quad (\text{A9})$$

Tail Interference Terms

Vertical and horizontal tail drag was defined as the sum of form drag plus skin-friction drag for $M < 0.90$ and wave drag plus skin-friction drag for $M > 1.00$. The subsonic form factors for the tails were calculated with the equation:

$$\text{Form factor} = 1 + 1.44(t/c) + 2(t/c)^2 \quad (\text{A10})$$

The individual fairings required for each tail location were also included in the skin-friction and wave-drag calculations. Values of $C_{D,\text{tails}}$ are given in table 18.

The tail interference terms used in this report are consistent with those used in references 6 and 9. The total tail interference increment on the aft end was determined from

$$\Delta C_{D,it} = (C_D)_{\text{tails on}} - (C_D)_{\text{tails off}} - C_{D,\text{tails}} \quad (\text{A11})$$

where $(C_D)_{\text{tails on}}$ is the measured total aft-end drag for a given configuration, $(C_D)_{\text{tails off}}$ is the measured aft-end drag for the same afterbody/nozzle configuration with the tails removed, and $C_{D,\text{tails}}$ is the computed value of tail drag as discussed previously. Hence this total tail interference increment includes the interference effects of one empennage surface on another, of the afterbody/nozzles on empennage surfaces, and of empennage surface on the afterbody/nozzles. It also includes drag increments associated with misalignment of the empennage surfaces with the afterbody flow field. The empennage interference effects on the nozzles alone were found from the following equation:

$$\Delta C_{D,in} = (C_{D,n})_{\text{tails on}} - (C_{D,n})_{\text{tails off}} \quad (\text{A12})$$

where the nozzle drags are obtained from equation (A8). This empennage interference increment, then, is the result of changes in nozzle external pressure distributions resulting from adding empennage surfaces to an afterbody/nozzle configuration. The empennage interference increment on the afterbody alone was then defined to be the difference between the empennage interference increments on the total aft end and the nozzles alone or

$$\Delta C_{D,ia} = \Delta C_{D,it} - \Delta C_{D,in} \quad (\text{A13})$$

References

1. Nichols, Mark R.: *Aerodynamics of Airframe-Engine Integration of Supersonic Aircraft*. NASA TN D-3390, 1966.
2. Glasgow, E. R.: Integrated Airframe-Nozzle Performance for Designing Twin-Engine Fighters. AIAA Paper No. 73-1303, Nov. 1973.
3. Runckel, Jack F.: *Interference Between Exhaust System and Afterbody of Twin-Engine Fuselage Configurations*. NASA TN D-7525, 1974.
4. Richey, G. K.; Surber, L. E.; and Laughrey, J. A.: Airframe/Propulsion System Flow Field Interference and the Effect on Air Intake and Exhaust Nozzle Performance. *Airframe/Propulsion Interference*, AGARD-CP-150, Mar. 1975, pp. 23-1-23-31.
5. Berrier, Bobby L.; and Staff, Propulsion Integration Section: *A Review of Several Propulsion Integration Features Applicable to Supersonic-Cruise Fighter Aircraft*. NASA TM X-73991, 1976.
6. Berrier, Bobby L.: *Effect of Nonlifting Empennage Surfaces on Single-Engine Afterbody/Nozzle Drag at Mach Numbers From 0.5 to 2.2*. NASA TN D-8326, 1977.
7. Burley, James R., II; and Berrier, Bobby L.: *Investigation of Installation Effects on Single-Engine Convergent-Divergent Nozzles*. NASA TP-2078, 1982.
8. Burley, James R., II; and Berrier, Bobby L.: *Effects of Tail Span and Empennage Arrangement on Drag of a Typical Single-Engine Fighter Aft End*. NASA TP-2352, 1984.
9. Leavitt, Laurence D.: *Effect of Empennage Location on Twin-Engine Afterbody/Nozzle Aerodynamic Characteristics at Mach Numbers From 0.6 to 1.2*. NASA TP-2116, 1983.
10. Leavitt, Laurence D.; and Bare, E. Ann: *Effects of Twin-Vertical-Tail Parameters on Twin-Engine Afterbody/Nozzle Aerodynamic Characteristics*. NASA TP-2158, 1983.
11. Bare, E. Ann; and Berrier, Bobby L.: *Investigation of Installation Effects on Twin-Engine Convergent-Divergent Nozzles*. NASA TP- 2205, 1983.
12. Leavitt, Laurence D.: Effects of Various Empennage Parameters on the Aerodynamic Characteristics of a Twin-Engine Afterbody Model. AIAA-83-0085, Jan. 1983.
13. Berrier, Bobby L.: Empennage/Afterbody Integration for Single and Twin-Engine Fighter Aircraft. AIAA-83-1126, June 1983.
14. Capone, Francis J.: The Nonaxisymmetric Nozzle—It Is for Real. AIAA Paper 79-1810, Aug. 1979.
15. Nelson, B. D.; and Nicolai, L. M.: Application of Multi-Function Nozzles to Advanced Fighters. AIAA-81-2618, Dec. 1981.
16. Capone, Francis J.; and Reubush, David E.: *Effects of Varying Podded Nacelle-Nozzle Installations on Transonic Aeropropulsive Characteristics of a Supersonic Fighter Aircraft*. NASA TP-2120, 1983.
17. Carson, George T., Jr.; Capone, Francis J.; and Mason, Mary L.: *Aeropropulsive Characteristics of Non-axisymmetric-Nozzle Thrust Reversers at Mach Numbers From 0 to 1.20*. NASA TP- 2306, 1984.
18. Capone, Francis J.; and Mason, Mary L.: *Interference Effects of Thrust Reversing on Horizontal Tail Effectiveness of a Twin-Engine Fighter Aircraft at Mach Numbers From 0.15 to 0.90*. NASA TP-2350, 1984.
19. Peddrew, Kathryn H., compiler: *A User's Guide to the Langley 16-Foot Transonic Tunnel*. NASA TM-83186, 1981.
20. Yetter, Jeffery A.; and Leavitt, Laurence D.: *Effects of Sidewall Geometry on the Installed Performance of Nonaxisymmetric Convergent-Divergent Exhaust Nozzles*. NASA TP-1771, 1980.

TABLE 1. INDEX TO DATA TABLES

Table	Position of—		ϕ_t , deg	δ_h , deg
	Horizontal tails	Vertical tails		
2	Off	Off		
3	Mid	Forward	0	0
4	Mid	Mid	0	0
5	Aft	Forward	0	0
6	Aft	Forward	0	-5
7	Aft	Forward	0	-10
8	Aft	Mid	0	0
9	Aft	Mid	0	-5
10	Aft	Mid	0	-10
11	Aft	Aft	0	0
12	Aft	Aft	0	-5
13	Aft	Mid	-10	0
14	Aft	Mid	10	0
15	Aft	Mid	20	0
16	Aft	Mid	20	-5
17	Aft	Mid	20	-10

ORIGINAL PAGE IS
OF POOR QUALITY

TABLE 2. AERODYNAMIC CHARACTERISTICS FOR TAILS OFF

MACH	NPR	ALPHA	CLT	C(D-F)	CMT	CL	CD	CM	CLAFT	CDRAFT	CMRAFT	CLN	CDN	CMN
1.197	9.95	11	.0029	.0170	.0016	.0029	.0166	.0016	.0040	.0086	.0040	.0012	.0081	.0024
1.201	2.99	.12	.0046	.0051	.0043	.0038	.0159	.0019	.0045	.0066	.0047	.0007	.0073	.0026
1.198	5.01	.12	.0063	.0265	.0075	.0051	.0163	.0031	.0047	.0087	.0050	.0004	.0076	.0019
1.199	7.02	.10	.0069	.0482	.0094	.0054	.0158	.0031	.0033	.0086	.0033	.0021	.0072	.0003
1.199	9.00	.12	.0075	.0706	.0116	.0056	.0145	.0033	.0034	.0086	.0035	.0022	.0059	.0002
1.195	9.4	3.10	.0210	.0188	.0170	.0210	.0184	.0170	.0167	.0093	.0151	.0043	.0090	.0019
1.200	9.4	.11	.0029	.0171	.0006	.0029	.0167	.0006	.0030	.0087	.0031	.0001	.0079	.0025
1.199	9.1	2.91	.0171	.0204	.0088	.0171	.0200	.0188	.0099	.0094	.0080	.0072	.0106	.0108
1.201	8.4	5.91	.0360	.0276	.0377	.0360	.0272	.0377	.0217	.0122	.0197	.0143	.0150	.0180
1.201	8.0	8.92	.0481	.0348	.0499	.0481	.0344	.0499	.0323	.0156	.0314	.0157	.0188	.0184
1.202	6.99	3.09	.0239	.0466	.0184	.0190	.0165	.0121	.0168	.0092	.0155	.0022	.0073	.0034
1.201	6.98	.10	.0063	.0481	.0089	.0048	.0153	.0026	.0028	.0087	.0030	.0020	.0067	.0004
1.200	7.00	2.92	.0114	.0472	.0004	.0096	.0164	.0067	.0102	.0094	.0083	.0007	.0069	.0016
1.199	7.03	5.91	.0276	.0451	.0102	.0224	.0207	.0166	.0221	.0122	.0201	.0004	.0083	.0036
1.198	7.02	8.89	.0434	.0370	.0227	.0349	.0266	.0291	.0324	.0156	.0315	.0025	.0110	.0025
1.899	1.10	.11	.0060	.0036	.0024	.0060	.0032	.0024	.0000	.0065	.0033	.0020	.0033	.0009
1.897	2.00	.08	.0072	.0182	.0067	.0061	.0024	.0039	.0048	.0061	.0044	.0014	.0036	.0005
1.904	3.00	.09	.0074	.0382	.0080	.0060	.0023	.0037	.0042	.0062	.0036	.0018	.0040	.0001
1.903	5.04	.08	.0082	.0733	.0121	.0062	.0028	.0042	.0041	.0062	.0035	.0021	.0033	.0007
1.902	6.98	.09	.0094	.1102	.0160	.0067	.0023	.0049	.0041	.0060	.0035	.0026	.0037	.0014
1.902	1.10	3.12	.0051	.0036	.0009	.0051	.0032	.0009	.0013	.0065	.0002	.0038	.0032	.0007
1.904	1.10	.09	.0044	.0033	.0018	.0044	.0029	.0018	.0042	.0064	.0034	.0002	.0035	.0016
1.904	1.10	2.92	.0052	.0030	.0050	.0052	.0026	.0050	.0043	.0062	.0062	.0011	.0036	.0013
1.899	1.10	5.91	.0057	.0028	.0035	.0057	.0024	.0030	.0049	.0059	.0050	.0008	.0035	.0015
1.902	1.11	8.93	.0044	.0048	.0039	.0044	.0044	.0039	.0019	.0065	.0043	.0063	.0021	.0082
1.902	5.00	3.12	.0112	.0719	.0098	.0051	.0033	.0020	.0021	.0061	.0011	.0030	.0028	.0009
1.895	4.98	.09	.0082	.0737	.0120	.0062	.0026	.0042	.0042	.0061	.0037	.0020	.0035	.0005
1.901	5.01	2.92	.0056	.0739	.0151	.0075	.0018	.0073	.0062	.0058	.0064	.0013	.0040	.0010
1.902	5.01	5.91	.0027	.0745	.0167	.0046	.0010	.0090	.0067	.0054	.0076	.0019	.0044	.0014
1.901	5.01	8.93	.0085	.0728	.0123	.0014	.0023	.0045	.0028	.0061	.0058	.0014	.0037	.0013
1.602	1.05	.11	.0059	.0043	.0029	.0059	.0039	.0029	.0027	.0058	.0025	.0032	.0019	.0005
1.597	2.01	.09	.0076	.0432	.0099	.0051	.0028	.0038	.0027	.0055	.0025	.0024	.0028	.0013
1.601	3.01	.09	.0067	.0836	.0119	.0036	.0023	.0020	.0026	.0056	.0023	.0010	.0033	.0003
1.602	3.53	.09	.0071	.1046	.0137	.0036	.0032	.0019	.0023	.0056	.0018	.0010	.0024	.0001
1.603	5.01	.09	.0079	.1661	.0195	.0033	.0035	.0021	.0020	.0055	.0016	.0013	.0020	.0005
1.600	1.04	3.11	.0040	.0041	.0004	.0040	.0037	.0004	.0034	.0059	.0020	.0011	.0021	.0016
1.601	1.05	.10	.0032	.0036	.0021	.0032	.0032	.0021	.0023	.0056	.0018	.0009	.0025	.0003
1.602	1.04	2.91	.0016	.0035	.0033	.0016	.0031	.0033	.0013	.0057	.0017	.0003	.0027	.0016
1.599	1.05	5.89	.0011	.0041	.0009	.0011	.0037	.0009	.0007	.0061	.0000	.0004	.0024	.0008
1.600	1.05	8.91	.0038	.0051	.0015	.0038	.0047	.0015	.0035	.0069	.0028	.0003	.0022	.0012
1.601	3.52	3.11	.0139	.1034	.0139	.0047	.0038	.0021	.0036	.0057	.0024	.0012	.0019	.0003
1.602	3.50	.10	.0059	.1036	.0131	.0024	.0031	.0014	.0023	.0054	.0019	.0001	.0023	.0004
1.602	3.51	2.90	.0017	.1042	.0130	.0004	.0028	.0013	.0011	.0054	.0015	.0008	.0026	.0003
1.600	3.50	5.91	.0089	.1042	.0125	.0011	.0030	.0007	.0005	.0057	.0004	.0006	.0026	.0003
1.597	3.50	8.92	.0183	.1034	.0092	.0048	.0041	.0027	.0029	.0062	.0018	.0019	.0020	.0008

TABLE 3. AERODYNAMIC CHARACTERISTICS FOR HORIZONTAL TAILS MID, VERTICAL TAILS FORWARD, $\phi_t = 0^\circ$, AND $\delta_h = 0^\circ$

MACH	NPR	ALPHA	CLT	C(D-F)	CMT	CL	CD	CM	CLAFT	CDAFT	CMAFT	CLN	CDN	CMN
1.199	93	.00	.0012	.0263	.0048	.0012	.0259	.0048	.0032	.0184	.0031	.0020	.0075	.0016
1.200	3.00	.00	.0035	.0045	.0017	.0028	.0256	.0041	.0040	.0185	.0021	.0012	.0071	.0021
1.200	5.00	.02	.0046	.0165	.0004	.0035	.0259	.0040	.0033	.0184	.0028	.0001	.0075	.0012
1.200	7.00	.00	.0048	.0380	.0018	.0034	.0256	.0045	.0041	.0185	.0018	.0006	.0071	.0026
1.200	8.99	.01	.0061	.0604	.0046	.0043	.0243	.0036	.0039	.0185	.0020	.0004	.0058	.0016
1.199	93	3.02	.0519	.0299	.0559	.0519	.0295	.0559	.0501	.0207	.0567	.0018	.0088	.0008
1.201	.92	.01	.0032	.0267	.0046	.0032	.0263	.0046	.0029	.0186	.0034	.0002	.0077	.0012
1.201	.92	2.99	.0529	.0311	.0679	.0529	.0307	.0679	.0426	.0208	.0617	.0103	.0099	.0062
1.199	.87	5.98	.0910	.0406	.1122	.0910	.0402	.1122	.0755	.0274	.1041	.0154	.0127	.0081
1.198	.84	8.98	.1300	.0549	.1633	.1300	.0545	.1633	.1094	.0370	.1521	.0206	.0175	.0112
1.198	6.99	2.99	.0571	.0348	.0618	.0523	.0289	.0555	.0515	.0208	.0586	.0008	.0080	.0031
1.200	6.99	.01	.0040	.0379	.0007	.0026	.0257	.0056	.0030	.0187	.0032	.0004	.0070	.0024
1.199	7.00	2.99	.0553	.0339	.0629	.0534	.0294	.0692	.0439	.0208	.0633	.0095	.0090	.0059
1.199	7.00	5.96	.0979	.0239	.1087	.0927	.0396	.1150	.0757	.0274	.1040	.0170	.0123	.0110
1.201	7.01	8.97	.1423	.0096	.1638	.1337	.0535	.1701	.1098	.0370	.1524	.0239	.0165	.0177
.899	1.11	.01	.0139	.0118	.0211	.0139	.0114	.0211	.0132	.0142	.0193	.0007	.0028	.0018
.899	2.01	.00	.0081	.0094	.0142	.0091	.0106	.0169	.0123	.0136	.0179	.0032	.0030	.0010
.898	3.01	.01	.0065	.0280	.0109	.0079	.0103	.0153	.0119	.0136	.0173	.0040	.0033	.0020
.901	5.02	.02	.0039	.0653	.0049	.0058	.0106	.0127	.0110	.0137	.0159	.0052	.0032	.0032
.900	7.00	.02	.0025	.1037	.0002	.0050	.0097	.0114	.0108	.0133	.0155	.0058	.0036	.0041
.899	1.11	3.01	.0051	.0102	.0011	.0051	.0098	.0011	.0002	.0132	.0014	.0053	.0035	.0003
.898	1.11	.00	.0101	.0112	.0195	.0101	.0108	.0195	.0131	.0141	.0193	.0030	.0033	.0003
.898	1.11	2.99	.0264	.0128	.0390	.0264	.0124	.0390	.0279	.0155	.0406	.0015	.0031	.0017
.899	1.11	5.99	.0495	.0167	.0699	.0495	.0163	.0699	.0469	.0186	.0691	.0025	.0024	.0008
.900	1.12	8.99	.0866	.0251	.1165	.0866	.0247	.1165	.0755	.0251	.1105	.0011	.0004	.0059
.900	5.01	3.01	.0164	.0670	.0137	.0105	.0087	.0059	.0018	.0127	.0015	.0087	.0040	.0044
.899	5.00	.01	.0020	.0667	.0038	.0040	.0093	.0116	.0101	.0134	.0149	.0061	.0042	.0032
.900	5.00	3.01	.0249	.0648	.0266	.0229	.0110	.0344	.0253	.0149	.0368	.0024	.0039	.0024
.899	4.99	5.99	.0504	.0612	.0541	.0443	.0143	.0619	.0436	.0176	.0638	.0007	.0033	.0020
.899	5.00	8.99	.0925	.0525	.1011	.0825	.0227	.1089	.0737	.0241	.1070	.0088	.0014	.0019
.899	1.04	.01	.0028	.0069	.0113	.0028	.0055	.0113	.0101	.0103	.0134	.0073	.0038	.0022
.601	2.01	.00	.0008	.0399	.0036	.0032	.0065	.0097	.0097	.0101	.0127	.0065	.0046	.0031
.602	3.02	.00	.0024	.0808	.0027	.0054	.0052	.0125	.0103	.0101	.0136	.0049	.0049	.0010
.602	3.52	.01	.0025	.1013	.0010	.0059	.0060	.0128	.0100	.0101	.0133	.0041	.0041	.0005
.604	5.02	.00	.0014	.1637	.0053	.0058	.0062	.0121	.0101	.0101	.0133	.0044	.0039	.0012
.600	1.04	3.00	.0136	.0077	.0114	.0136	.0073	.0114	.0087	.0107	.0111	.0049	.0034	.0003
.601	1.04	.01	.0076	.0082	.0134	.0076	.0078	.0134	.0105	.0103	.0139	.0030	.0026	.0005
.601	1.04	3.02	.0290	.0107	.0381	.0290	.0103	.0381	.0303	.0117	.0397	.0013	.0015	.0015
.599	1.04	6.01	.0612	.0166	.0765	.0612	.0162	.0765	.0561	.0154	.0750	.0051	.0008	.0016
.600	1.04	9.01	.0936	.0249	.1164	.0936	.0245	.1164	.0815	.0216	.1112	.0120	.0029	.0053
.600	3.51	3.01	.0244	.1012	.0261	.0153	.0063	.0142	.0120	.0107	.0155	.0033	.0045	.0012
.600	3.51	.01	.0054	.1009	.0025	.0088	.0069	.0143	.0103	.0101	.0136	.0015	.0032	.0007
.601	3.51	3.01	.0365	.0978	.0323	.0341	.0096	.0441	.0314	.0115	.0414	.0027	.0019	.0027
.599	3.51	6.01	.0747	.0923	.0699	.0667	.0155	.0818	.0567	.0152	.0759	.0101	.0003	.0059
.600	3.51	8.99	.1115	.0834	.1097	.0979	.0237	.1215	.0823	.0214	.1123	.0156	.0023	.0092

TABLE 4. AERODYNAMIC CHARACTERISTICS FOR HORIZONTAL TAILS MID, VERTICAL TAILS MID, VERTICAL TAILS MID,
 $\phi_t = 0^\circ$, AND $\delta_h = 0^\circ$

MACH	NPR	ALPHA	CLT	C(D-F)	CMT	CL	CD	CM	CLAFT	COAFT	CMAFT	CLN	CDN	CMN
.961	1.10	-0.0	.0119	.0139	-.0175	.0119	.0135	-.0175	.0088	.0181	-.0197	.0031	-.0044	.0022
.897	2.01	-.01	.0099	-.0082	-.0150	.0109	.0121	-.0177	.0094	.0167	-.0203	.0015	-.0046	.0026
.899	3.03	-.00	.0083	-.0204	-.0127	.0097	.0121	-.0171	.0086	.0171	-.0193	.0011	-.0050	.0022
.898	5.01	-.02	.0084	-.0630	-.0103	.0104	.0125	-.0182	.0092	.0168	-.0202	.0011	-.0043	.0020
.901	7.01	-.01	.0066	-.1013	-.0054	.0091	.0121	-.0166	.0082	.0168	-.0187	.0009	-.0047	.0021
.898	1.10	-3.01	-.0017	.0115	-.0030	-.0017	.0111	-.0030	-.0002	.0167	-.0041	-.0015	-.0056	.0031
.898	1.10	-.00	.0093	.0132	-.0174	.0093	.0128	-.0174	.0094	.0176	-.0206	-.0001	-.0048	.0032
.901	1.09	2.97	.0207	.0149	-.0317	.0207	.0145	-.0317	.0201	.0187	-.0367	.0006	-.0042	.0050
.898	1.09	5.99	.0425	.0183	-.0600	.0425	.0179	-.0600	.0389	.0206	-.0646	.0035	-.0027	.0046
.898	1.10	8.99	.0815	.0264	-.1085	.0815	.0260	-.1085	.0697	.0263	-.1083	.0118	-.0003	.0002
.899	5.01	-3.01	-.0092	-.0653	-.0055	-.0033	.0106	-.0023	-.0006	.0160	-.0055	-.0026	-.0054	.0031
.899	5.01	-.01	.0058	.0641	-.0087	.0077	.0120	-.0165	.0086	.0170	-.0194	-.0009	-.0050	.0029
.899	5.00	3.00	.0259	-.0621	-.0285	.0239	.0138	-.0363	.0215	.0178	-.0387	.0023	-.0040	.0024
.897	5.00	5.98	.0510	-.0590	-.0564	.0449	.0171	-.0642	.0402	.0199	-.0661	.0047	-.0027	.0019
.900	4.99	8.97	.0922	-.0498	-.1017	.0823	.0251	-.1095	.0685	.0254	-.1064	.0137	-.0003	.0031
.602	1.04	-.01	.0090	.0065	-.0155	.0090	.0061	-.0155	.0112	.0107	-.0172	-.0022	-.0046	.0017
.601	2.01	-.01	.0082	.0400	-.0097	.0106	.0054	-.0157	.0120	.0104	-.0171	-.0007	-.0051	.0014
.600	3.01	-.01	.0099	-.0809	-.0093	.0130	.0050	-.0191	.0120	.0105	-.0182	.0010	-.0055	.0009
.601	3.50	-.02	.0098	-.1012	-.0073	.0132	.0058	-.0191	.0117	.0105	-.0179	.0015	-.0047	.0012
.602	5.02	-.00	.0093	-.1640	-.0015	.0136	.0063	-.0190	.0120	.0104	-.0182	.0017	-.0041	.0008
.601	1.04	-3.02	-.0080	.0061	.0073	-.0080	.0057	.0073	-.0076	.0109	-.0078	-.0003	-.0052	.0005
.602	1.04	.01	.0127	.0075	-.0170	.0127	.0071	-.0170	.0118	.0109	-.0179	.0009	-.0036	.0009
.600	1.04	3.00	.0334	.0109	-.0410	.0334	.0105	-.0410	.0308	.0120	-.0431	.0026	-.0015	.0021
.598	1.04	5.97	.0653	.0171	-.0793	.0653	.0167	-.0793	.0563	.0157	-.0786	.0090	-.0010	.0007
.598	1.04	8.97	.0967	.0261	-.1188	.0967	.0257	-.1188	.0817	.0214	-.1150	.0150	-.0039	.0038
.599	3.51	-3.00	-.0176	-.1025	-.0204	-.0086	.0049	-.0086	-.0084	.0108	-.0089	-.0003	-.0059	.0004
.602	3.51	.01	.0128	-.1006	-.0090	.0161	.0065	-.0207	.0122	.0105	-.0185	.0039	-.0040	.0022
.601	3.51	2.99	.0431	-.0974	-.0384	.0408	.0101	-.0502	.0328	.0119	-.0461	.0081	-.0018	.0041
.599	3.50	5.97	.0812	-.0907	-.0761	.0733	.0170	-.0879	.0578	.0156	-.0809	.0155	-.0014	.0070
.598	3.50	8.98	.1170	-.0813	-.1157	.1034	.0259	-.1275	.0832	.0219	-.1173	.0202	-.0041	.0103
.198	8.98	-.00	.0114	.0273	.0133	-.0114	.0269	.0133	-.0099	.0187	-.0087	-.0016	-.0082	.0046
1.200	3.91	-.02	-.0140	.0047	.0171	-.0133	.0259	.0146	-.0103	.0186	-.0094	-.0030	-.0073	.0052
1.201	5.01	-.01	-.0124	-.0164	.0142	-.0113	.0261	.0098	-.0105	.0185	-.0097	-.0008	-.0076	.0001
1.201	7.00	-.01	-.0097	-.0380	.0107	-.0083	.0255	.0044	-.0107	.0185	-.0101	.0024	-.0071	.0057
1.199	9.00	-.02	-.0097	-.0606	.0116	-.0079	.0249	.0034	-.0089	.0186	-.0079	.0010	-.0058	.0045
1.198	8.98	-3.01	-.0590	.0313	.0717	-.0590	.0204	.0717	-.0530	.0212	-.0647	-.0060	-.0096	.0071
1.202	.87	.01	.0125	.0280	.0128	-.0125	.0276	.0128	-.0091	.0187	-.0078	-.0034	-.0089	.0050
1.200	.87	2.98	.0394	.0307	.0488	.0394	.0303	.0488	.0353	.0205	-.0500	.0000	.0099	.0013
1.197	.85	5.98	.0766	.0396	-.0912	.0766	.0392	-.0912	.0648	.0267	-.0879	.0118	.0124	.0033
1.205	.81	8.97	.1158	.0530	-.1420	.1158	.0526	-.1420	.0982	.0353	-.1354	.0175	-.0174	.0066
1.202	7.01	-3.00	-.0598	.0349	.0696	-.0550	.0285	.0633	-.0546	.0212	-.0671	-.0004	-.0072	.0038
1.199	7.00	-.02	-.0097	-.0382	.0104	-.0083	.0255	.0041	-.0089	.0187	-.0078	.0006	-.0068	.0037
1.200	7.01	2.97	.0481	.0344	-.0521	.0462	.0293	-.0584	.0359	.0205	-.0506	.0103	.0088	.0079
1.201	7.02	5.96	.0872	-.0253	-.0935	.0820	.0383	-.0998	.0657	.0268	-.0888	.0162	.0115	.0110
1.201	7.01	8.97	.1308	-.0116	-.1471	.1222	.0514	-.1534	.0981	.0355	-.1352	.0241	.0159	.0182

ORIGINAL PAGE IS
OF POOR QUALITY.

TABLE 5. AERODYNAMIC CHARACTERISTICS FOR HORIZONTAL TAILS AFT, VERTICAL TAILS FORWARD, $\phi_t = 0^\circ$, AND $\delta_h = 0^\circ$

MACH	NPR	ALPHA	CLT	C(D=F)	CMT	CL	CD	CM	CLAFT	COAFT	CHAFT	CLN	CDN	CMN
1.201	.95	.10	-.0038	.0261	-.0028	-.0038	.0257	-.0028	-.0058	.0173	-.0009	.0020	.0084	-.0019
1.201	3.02	.10	-.0046	.0043	-.0015	-.0038	.0256	-.0040	-.0051	.0173	-.0018	.0013	.0083	-.0021
1.199	4.99	.09	-.0046	-.0165	.0001	-.0036	.0259	-.0042	-.0054	.0173	-.0014	.0018	.0086	-.0020
1.199	7.02	.14	-.0047	-.0391	.0019	-.0035	.0249	-.0045	-.0046	.0173	-.0024	.0011	.0074	-.0020
1.200	9.00	.11	-.0046	-.0616	.0048	-.0044	.0232	-.0034	-.0050	.0171	-.0017	.0007	.0061	-.0016
1.199	.94	-2.91	-.0514	.0294	.0575	-.0514	.0290	.0575	-.0488	.0195	.0582	-.0026	.0095	-.0007
1.197	.94	.10	-.0060	.0267	-.0029	-.0060	.0263	-.0029	-.0050	.0174	-.0022	-.0010	.0069	-.0008
1.199	.93	3.11	.0501	.0315	-.0694	.0501	.0311	-.0694	.0390	.0198	-.0634	.0111	.0114	-.0061
1.202	.88	6.08	.0882	.0403	-.1157	.0882	.0399	-.1157	.0718	.0258	-.1079	.0164	.0141	-.0078
1.199	.85	9.07	.1236	.0545	-.1659	.1236	.0541	-.1659	.1024	.0349	-.1553	.0213	.0192	-.0106
1.199	7.01	-3.08	-.0559	-.0359	.0645	-.0510	.0277	.0581	-.0497	.0195	.0594	-.0013	.0082	-.0012
1.198	7.01	-.09	-.0062	-.0384	.0028	-.0046	.0255	-.0035	-.0054	.0172	-.0013	.0008	.0083	-.0022
1.201	7.01	2.89	.0519	-.0341	-.0639	.0501	.0296	-.0702	.0384	.0193	-.0622	.0116	.0103	-.0081
1.201	7.00	5.90	.0958	-.0243	-.1148	.0907	.0391	-.1211	.0719	.0255	-.1080	.0188	.0136	-.0131
1.200	7.00	8.89	.1371	.0100	-.1701	.1287	.0531	-.1764	.1029	.0346	-.1561	.0258	.0185	-.0203
.900	1.10	-.08	.0094	.0095	.0203	.0094	.0091	.0203	.0117	.0117	-.0197	-.0023	-.0027	-.0005
.900	1.99	-.09	.0671	-.0110	-.0150	.0082	.0087	-.0176	.0106	.0115	-.0176	-.0025	-.0028	.0000
.901	3.01	-.09	.0050	.0295	-.0117	.0072	.0085	-.0161	.0103	.0115	-.0171	-.0031	-.0030	.0010
.902	5.02	-.08	.0041	.0671	-.0065	.0061	.0088	-.0143	.0096	.0113	-.0161	-.0034	-.0025	.0018
.900	7.01	.10	.0030	-.1051	.0020	.0058	.0084	-.0132	.0092	.0113	-.0152	-.0034	-.0029	.0020
.900	1.10	-3.09	-.0028	.0086	.0040	-.0028	.0082	.0040	.0016	.0112	-.0045	-.0044	-.0029	.0006
.902	1.10	-.12	.0103	.0090	.0204	.0103	.0095	-.0204	.0116	.0118	-.0196	-.0013	-.0022	-.0017
.900	1.10	2.92	.0227	.0115	-.0354	.0227	.0111	-.0354	.0230	.0132	-.0371	-.0003	-.0021	.0017
.897	1.10	5.90	.0419	.0152	-.0626	.0419	.0148	-.0626	.0388	.0154	-.0632	.0030	-.0006	.0006
.896	1.11	8.89	.0782	.0237	-.1128	.0782	.0233	-.1128	.0655	.0213	-.1065	.0128	-.0020	-.0062
.900	5.03	-3.09	-.0127	-.0679	.0098	-.0067	.0082	.0020	-.0007	.0108	-.0008	-.0060	-.0026	.0028
.899	4.99	-.09	.0046	-.0670	-.0068	.0067	.0087	-.0146	.0100	.0114	-.0165	-.0033	-.0027	.0019
.899	4.98	2.91	.0241	.0650	-.0267	.0222	.0107	-.0345	.0221	.0124	-.0357	-.0001	-.0017	.0012
.897	4.97	5.90	.0475	.0616	-.0540	.0416	.0140	-.0618	.0389	.0148	-.0627	.0028	-.0008	.0009
.897	4.99	8.91	.0851	.0535	.0994	.0751	.0220	-.1072	.0636	.0206	-.1031	.0115	-.0014	-.0041
.600	1.05	-.09	.0046	.0067	-.0119	.0046	.0063	-.0119	.0105	.0087	-.0146	-.0058	-.0024	.0027
.602	2.01	-.09	.0024	-.0396	-.0046	.0048	.0056	-.0106	.0096	.0085	-.0132	-.0048	-.0029	.0026
.600	3.01	-.09	.0040	.0809	-.0038	.0071	.0053	-.0137	.0103	.0086	-.0143	-.0031	-.0033	.0006
.602	3.50	-.10	.0041	.1006	-.0023	.0076	.0060	-.0140	.0105	.0087	-.0146	-.0029	-.0027	.0006
.602	4.99	-.10	.0029	-.1631	.0040	.0075	.0064	-.0134	.0104	.0086	-.0144	-.0029	-.0022	.0010
.601	1.04	-3.10	-.0108	.0068	.0104	-.0108	.0064	.0104	-.0065	.0092	-.0095	-.0043	-.0028	.0009
.602	1.05	-.10	.0079	.0080	-.0131	.0079	.0076	-.0131	.0104	.0089	-.0148	-.0027	-.0013	.0017
.601	1.04	2.89	.0278	.0107	-.0374	.0278	.0103	-.0374	.0286	.0101	-.0403	-.0008	-.0002	.0029
.600	1.05	5.91	.0587	.0168	-.0764	.0587	.0164	-.0764	.0520	.0136	-.0757	.0067	.0029	.0007
.601	1.05	8.89	.0876	.0254	-.1166	.0876	.0250	-.1166	.0752	.0193	-.1123	.0125	.0058	-.0043
.598	3.50	-3.08	-.0235	-.1021	.0271	-.0143	.0058	.0152	-.0105	.0093	.0151	-.0038	-.0035	.0001
.599	3.49	-.09	.0058	.1003	-.0030	.0094	.0069	-.0147	.0109	.0087	-.0151	-.0015	-.0018	.0004
.599	3.49	2.89	.0366	.0971	-.0348	.0345	.0103	-.0465	.0311	.0100	-.0444	.0034	.0003	-.0022
.600	3.50	5.90	.0741	.0905	-.0740	.0663	.0167	-.0857	.0547	.0137	-.0798	.0116	.0030	-.0059
.602	3.50	8.88	.1077	.0808	-.1144	.0945	.0248	-.1261	.0785	.0195	-.1175	.0160	.0053	-.0086

TABLE 6. AERODYNAMIC CHARACTERISTICS FOR HORIZONTAL TAILS AFT, VERTICAL TAILS FORWARD, $\phi_t = 0^\circ$, AND $\delta_h = -5^\circ$

MACH	NPR	ALPHA	CLT	C(D-F)	CMT	CL	CD	CM	CLAFT	CDAFT	CMAFT	CLN	CDN	CM#
.897	1.09	.01	-.0418	.0122	.0677	-.0418	.011A	.0677	-.0406	.0154	.0680	-.0012	-.0036	-.0003
.896	2.00	-.01	-.0475	-.0091	.0753	-.0464	.0109	.0726	-.0424	.0149	.0709	-.0041	-.0041	.0017
.898	3.01	-.02	-.0522	-.0273	.0834	-.0508	.0109	.0790	-.0442	.0152	.0738	-.0066	-.0043	.0052
.899	4.99	-.00	-.0564	-.0646	.0914	-.0545	.0112	.0836	-.0462	.0151	.0768	-.0083	-.0041	.0068
.899	7.00	-.00	-.0593	-.1030	.0974	-.0568	.0107	.0862	-.0471	.0151	.0781	-.0097	-.0044	.0080
.897	1.08	-3.02	-.0547	.0154	.0848	-.0547	.0150	.0848	-.0512	.0178	.0843	-.0035	-.002A	.0005
.899	1.08	-.02	-.0453	.0130	.0691	-.0453	.0126	.0691	-.0406	.0154	.0681	-.0046	-.0028	.0010
.898	1.08	2.99	-.0314	.0107	.0498	-.0314	.0103	.0498	-.0288	.0136	.0497	-.0026	-.0033	.0001
.897	1.09	5.98	-.0162	.0094	.0230	-.0162	.0090	.0230	-.0123	.0127	.0224	-.0039	-.0037	.0006
.901	1.10	8.99	.0100	.0115	-.0153	.0100	.0111	-.0153	.0082	.0137	-.0111	.0017	-.0025	-.0042
.901	5.02	-3.02	-.0719	-.0614	.1086	-.0659	.0145	.1008	-.056A	.0182	.0932	-.0092	-.0037	.0075
.902	5.01	-.02	-.0582	-.0640	.0923	-.0563	.0115	.0845	-.0462	.0154	.0768	-.0100	-.0039	.0077
.898	5.00	2.97	-.0394	.0672	.0726	-.0414	.0088	.0648	-.0340	.0133	.0582	-.0073	-.0045	.0065
.899	5.01	5.98	-.0204	-.0690	.0471	-.0265	.0068	.0393	-.0198	.0119	.0327	-.0077	-.0051	.0066
.900	5.01	8.99	.0094	-.0674	.0085	-.0006	.0079	.0007	.0048	.0129	-.0044	-.0054	-.0050	.0051
.599	1.04	-.01	-.0499	.0100	.0751	-.0499	.0096	.0751	-.0413	.0130	.0696	-.0086	-.0034	.0055
.601	2.01	-.02	-.0547	-.0372	.0871	-.0524	.0082	.0811	-.0447	.0129	.0745	-.0077	-.0047	.0066
.601	3.00	-.02	-.0555	-.0780	.0911	-.0525	.0075	.0813	-.0456	.0130	.0758	-.0069	-.0055	.0055
.601	3.52	-.00	-.0559	-.0996	.0933	-.0525	.0081	.0815	-.0460	.0130	.0763	-.0065	-.0049	.0052
.600	5.02	-.03	-.0576	.1634	.0996	-.0531	.0081	.0820	-.0471	.0129	.0775	-.0060	-.0049	.0045
.600	1.04	-3.02	-.0638	.0129	.0992	-.0638	.0125	.0992	-.0586	.0164	.0948	-.0052	-.0039	.0044
.601	1.04	-.01	-.0452	.0103	.0737	-.0452	.0099	.0737	-.0414	.0130	.0699	-.0038	-.0031	.0039
.601	1.04	2.97	-.0277	.0089	.0490	-.0277	.0085	.0490	-.0232	.0113	.0435	-.0045	-.002A	.0055
.600	1.04	5.98	-.0041	.0100	.0136	-.0041	.0096	.0136	-.0009	.0114	.0099	-.0032	-.001A	.0037
.600	1.05	9.01	.0189	.0129	-.0207	.0189	.0125	-.0207	.0197	.0126	-.0221	-.0008	-.0001	.0014
.599	3.51	-3.02	-.0803	-.0962	.1216	-.0712	.0120	.109A	-.0646	.0167	.1036	-.0066	-.0048	.0061
.601	3.52	-.03	-.0540	-.0991	.0927	-.0506	.0086	.0809	-.0463	.0129	.0766	-.0044	-.0043	.0063
.602	3.51	2.99	-.0267	.1008	.0615	-.0290	.0060	.0497	-.0260	.0109	.0470	-.0030	-.0043	.0028
.600	3.51	5.98	.0025	-.1002	.0265	-.0054	.0073	.0147	-.0031	.0109	.0128	-.0023	-.0036	.0019
.597	3.50	8.98	.0348	-.0961	-.0116	.0211	.0115	-.0235	.0202	.0124	-.0228	.0010	-.0009	-.0007

ORIGINAL COPY
OF POOR QUALITY

TABLE 7. AERODYNAMIC CHARACTERISTICS FOR HORIZONTAL TAILS AFT, VERTICAL TAILS FORWARD, $\phi_t = 0^\circ$, AND $\delta_h = -10^\circ$

MACH	NPR	ALPHA	CLT	C(D=F)	CMT	CL	CD	CM	CLAFT	CDRAFT	CMRAFT	CLN	CDN	CMN
.601	1.04	-.01	-.1016	.0169	.1713	-.1016	.0165	.1713	-.0969	.0240	.1587	-.0047	-.0075	.0125
.599	2.00	.00	-.1074	-.0294	.1806	-.1051	.0158	.1745	-.0994	.0236	.1621	-.0057	-.0078	.0124
.598	3.00	.00	-.1117	-.0706	.1886	-.1087	.0154	.1787	-.1013	.0238	.1649	-.0074	-.0084	.0138
.597	3.51	-.00	-.1134	-.0924	.1913	-.1100	.0165	.1794	-.1017	.0239	.1654	-.0083	-.0074	.0140
.600	4.99	-.01	-.1159	-.1539	.1972	-.1115	.0170	.1797	-.1025	.0237	.1664	-.0090	-.0068	.0133
.598	1.03	-2.99	-.1181	.0255	.1915	-.1181	.0251	.1915	-.1109	.0306	.1790	-.0071	-.0056	.0125
.599	1.04	.01	-.1035	.0190	.1714	-.1035	.0186	.1714	-.0969	.0238	.1590	-.0066	-.0052	.0125
.600	1.04	3.00	-.0854	.0134	.1459	-.0854	.0130	.1459	-.0795	.0181	.1339	-.0058	-.0050	.0121
.598	1.04	6.00	-.0602	.0111	.1085	-.0602	.0107	.1085	-.0566	.0138	.0998	-.0036	-.0031	.0087
.600	1.05	9.01	-.0367	.0094	.0725	-.0367	.0090	.0725	-.0340	.0120	.0647	-.0027	-.0030	.0078
.599	3.50	-3.00	-.1375	-.0829	.2150	-.1284	.0244	.2033	-.1167	.0310	.1871	-.0117	-.0066	.0161
.599	3.51	.01	-.1145	-.0906	.1912	-.1111	.0173	.1794	-.1016	.0236	.1653	-.0096	-.0063	.0140
.600	3.51	3.01	-.0889	-.0966	.1629	-.0912	.0111	.1511	-.0833	.0176	.1389	-.0079	-.0064	.0123
.597	3.50	6.00	-.0584	.1004	.1267	-.0664	.0077	.1148	-.0608	.0132	.1055	-.0056	-.0055	.0093
.599	3.51	9.00	-.0255	-.1009	.0848	-.0392	.0064	.0730	-.0349	.0114	.0655	-.0043	-.0050	.0075

TABLE 8. AERODYNAMIC CHARACTERISTICS FOR HORIZONTAL TAILS AFT, VERTICAL TAILS MID,
 $\phi_t = 0^\circ$, AND $\delta_h = 0^\circ$

MACH	NPR	ALPHA	CLT	C(D-F)	CMT	CL	CD	CM	CLAFT	COAFT	CMAFT	CLN	CDN	CMN
1.203	.89	.06	-.0147	.0276	.0158	-.0147	.0272	.0158	-.0116	.0169	.0110	-.0031	.0103	.0048
1.199	3.01	.07	-.0153	.0056	.0167	-.0146	.0269	.0142	-.0107	.0169	.0096	-.0039	.0100	.0046
1.201	5.02	.07	-.0120	-.0159	.0115	-.0109	.0267	.0071	-.009A	.0167	.0085	-.0011	.0100	.0014
1.201	7.02	.09	-.0086	-.0375	.0077	-.0073	.0262	.0014	-.0077	.0168	.0059	.0004	.0094	.0044
1.199	9.02	.06	-.0084	-.0605	.0092	-.0067	.0247	.0010	-.007A	.0167	.0061	.0011	.0080	.0052
1.197	.90	-2.93	-.0547	.0312	.0690	-.0507	.0308	.0690	-.0476	.0192	.0615	-.0071	.0116	.0075
1.201	.89	.07	-.0129	.0283	.0111	-.0129	.0279	.0111	-.0079	.0166	.0059	-.0049	.0112	.0052
1.196	.87	3.07	.0366	.0320	-.0481	-.0366	.0316	-.0481	.0340	.0189	-.0532	.0027	.0127	.0051
1.204	.86	6.08	.0779	.0406	.1009	.0779	.0402	-.1009	.0638	.0256	-.0951	.0141	.0146	.0058
1.195	.82	9.06	.1091	.0535	-.1452	.1091	.0531	-.1452	.0903	.0338	-.1375	.0188	.0193	.0077
1.202	6.99	-2.93	-.0565	-.0343	.0681	-.0518	.0289	.0618	-.0479	.0191	.0620	-.0039	.0099	.0002
1.202	7.04	.08	-.0068	-.0378	.0051	-.0054	.0260	-.0012	-.0058	.0167	.0032	.0004	.0094	.0045
1.202	7.00	3.09	.0520	-.0330	-.0621	.0500	.0304	-.0684	.0359	.0190	-.0558	.0141	.0115	.0126
1.203	7.01	6.06	.0914	-.0237	.1074	.0860	.0395	-.1137	.0647	.0255	-.0963	.0213	.0140	.0173
1.201	7.00	9.06	.1296	-.0106	-.1581	.1210	.0523	-.1644	.0927	.0340	-.1409	.0282	.0182	.0235
.901	1.09	.04	.0125	.0129	-.0226	.0125	.0125	-.0226	.0136	.0149	-.0260	-.0011	-.0025	.0034
.896	1.99	-.03	.0091	-.0079	-.0170	.0102	.0119	-.0197	.0126	.0142	-.0241	-.0024	-.0023	.0044
.900	3.00	-.05	.0095	.0257	-.0169	.0109	.0121	-.0212	.0128	.0143	-.0246	-.0020	-.0023	.0034
.902	5.03	-.03	.0095	.0633	-.0142	.0115	.0127	-.0220	.0132	.0144	-.0253	-.0017	.0017	.0033
.897	7.01	-.04	.0094	-.1025	-.0111	.0121	.0120	-.0224	.0130	.0139	-.0249	-.0010	.0018	.0025
.899	1.10	-3.02	.0010	.0114	-.0085	.0010	.0110	-.0085	.0058	.0135	-.0130	-.0048	.0024	.0045
.901	1.09	.04	.0114	.0128	-.0224	.0114	.0124	-.0224	.0138	.0148	-.0263	-.0024	.0024	.0039
.897	1.09	2.96	.0200	.0143	-.0335	.0200	.0139	-.0335	.0220	.0161	-.0396	-.0021	.0023	.0061
.898	1.08	5.95	.0315	.0170	-.0500	.0315	.0166	-.0500	.0325	.0180	-.0574	-.0010	.0014	.0073
.900	1.10	8.96	.0702	.0253	.1013	.0702	.0249	-.1013	.0620	.0242	-.1042	.0082	.0006	.0029
.899	5.00	-3.03	-.0064	-.0646	.0004	-.0004	.0111	-.0074	.0053	.0128	-.0122	-.0057	.0017	.0047
.901	5.00	-.03	.0085	-.0633	-.0137	.0105	.0123	-.0215	.0130	.0142	-.0251	-.0025	-.0020	.0036
.901	5.01	2.97	.0260	-.0617	-.0307	.0240	.0141	-.0385	.0224	.0157	-.0410	.0015	.0016	.0025
.899	5.00	5.97	.0461	.0587	-.0557	.0401	.0171	-.0636	.0376	.0180	-.0657	.0025	.0010	.0021
.900	5.02	8.93	.0866	-.0494	.1051	.0787	.0260	-.1129	.0661	.0245	-.1108	.0126	.0015	.0021
.601	1.05	-.03	.0080	.0073	-.0154	.0080	.0069	-.0154	.0115	.0091	-.0177	-.0035	.0022	.0024
.600	2.01	-.05	.0060	-.0389	-.0092	.0089	.0066	-.0152	.0113	.0090	-.0174	-.0023	.0024	.0022
.598	3.02	-.04	.0096	-.0805	-.0104	.0127	.0066	-.0204	.0127	.0092	-.0194	.0001	.0026	.0010
.601	3.51	-.04	.0088	-.1003	-.0091	.0133	.0075	-.0209	.0128	.0092	-.0197	.0005	.0017	.0012
.600	5.02	-.04	.0087	-.1634	-.0029	.0132	.0082	-.0205	.0125	.0093	-.0193	.0007	.0010	.0018
.600	1.04	-3.03	-.0072	.0077	.0066	-.0072	.0073	.0066	-.0046	.0090	.0056	-.0026	.0017	.0010
.601	1.05	-.03	.0104	.0088	-.0158	.0104	.0084	-.0158	.0114	.0095	-.0176	.0010	.0011	.0018
.601	1.04	2.98	.0291	.0119	-.0394	.0291	.0115	-.0394	.0285	.0114	-.0425	.0006	.0001	.0031
.602	1.04	5.97	.0592	.0160	-.0763	.0592	.0160	-.0763	.0501	.0152	-.0757	.0091	.0008	.0005
.599	1.05	8.97	.0866	.0264	-.1183	.0866	.0260	-.1183	.0747	.0217	-.1151	.0139	.0043	.0032
.602	3.49	-3.04	-.0180	-.0986	.0202	-.0091	.0071	.0085	-.0064	.0089	.0083	-.0026	.0018	.0002
.603	3.51	.03	.0110	-.0970	-.0100	.0144	.0087	-.0217	.0126	.0094	-.0194	.0017	.0006	.0022
.601	3.52	2.96	.0414	-.0455	-.0411	.0391	.0124	-.0529	.0322	.0115	-.0484	.0069	.0009	.0045
.598	3.51	5.95	.0791	-.0895	-.0808	.0711	.0187	-.0926	.0552	.0157	-.0838	.0159	.0030	.0089
.600	3.52	8.97	.1136	-.0798	-.1227	.1000	.0277	-.1346	.0792	.0222	-.1223	.0208	.0055	.0123

ORIGINAL PAGE IS
OF POOR QUALITY

TABLE 9. AERODYNAMIC CHARACTERISTICS FOR HORIZONTAL TAILS AFT, VERTICAL TAILS MID,
 $\phi_t = 0^\circ$, AND $\delta_h = -5^\circ$

MACH	NPR	ALPHA	CLT	C(D=EF)	CMT	CL	CO	CM	CLIFT	COAFT	CMOFT	CLN	CON	CMN
.901	1.08	.00	.0411	.0137	.0614	.0411	.0133	.0614	.0369	.0182	.0580	.0042	.0049	.0034
.899	2.01	.01	.0454	.0074	.0664	.0444	.0126	.0637	.0379	.0172	.0597	.0064	.0046	.0040
.898	3.02	.01	.0495	.0257	.0728	.0461	.0126	.0684	.0389	.0172	.0613	.0093	.0046	.0070
.901	4.99	.00	.0530	.0628	.0801	.0510	.0127	.0723	.0411	.0173	.0647	.0099	.0046	.0076
.901	7.01	.02	.0556	.1018	.0859	.0531	.0117	.0747	.0424	.0171	.0666	.0107	.0054	.0081
.898	1.08	-2.98	.0514	.0162	.0751	.0514	.0158	.0751	.0413	.0197	.0710	.0071	.0040	.0041
.900	1.08	.01	.0453	.0137	.0631	.0453	.0133	.0631	.0363	.0176	.0574	.0090	.0043	.0058
.898	1.08	2.99	.0345	.0114	.0487	.0345	.0110	.0487	.0277	.0157	.0433	.0068	.0048	.0054
.897	1.08	6.03	.0242	.0096	.0304	.0242	.0092	.0304	.0154	.0144	.0224	.0088	.0052	.0080
.897	1.09	9.03	.0082	.0119	.0171	.0082	.0115	.0171	.0101	.0163	.0186	.0019	.0047	.0015
.899	5.01	-2.99	.0656	.0607	.0948	.0597	.0154	.0870	.0496	.0194	.0793	.0101	.0040	.0076
.901	5.00	.03	.0541	.0633	.0805	.0522	.0123	.0727	.0407	.0170	.0642	.0115	.0048	.0085
.901	5.02	3.01	.0379	.0665	.0642	.0400	.0096	.0564	.0319	.0150	.0497	.0081	.0054	.0067
.898	5.02	6.01	.0213	.0683	.0417	.0274	.0078	.0339	.0182	.0134	.0264	.0093	.0056	.0075
.899	5.01	9.00	.0121	.0658	.0011	.0021	.0098	.0090	.0072	.0151	.0136	.0051	.0053	.0046
.597	1.04	.00	.0505	.0086	.0696	.0505	.0082	.0696	.0378	.0122	.0629	.0127	.0041	.0067
.600	1.99	.01	.0543	.0375	.0803	.0520	.0073	.0744	.0414	.0124	.0679	.0106	.0050	.0064
.601	3.00	.02	.0544	.0789	.0836	.0514	.0065	.0738	.0416	.0125	.0682	.0098	.0060	.0055
.601	3.51	.01	.0546	.1001	.0855	.0512	.0072	.0738	.0422	.0125	.0690	.0091	.0053	.0047
.601	5.00	.00	.0558	.1635	.0914	.0515	.0071	.0739	.0429	.0124	.0699	.0086	.0054	.0040
.601	1.04	-3.01	.0631	.0121	.0928	.0631	.0117	.0928	.0544	.0157	.0877	.0087	.0040	.0051
.597	1.04	.01	.0451	.0093	.0679	.0451	.0089	.0679	.0378	.0126	.0629	.0074	.0037	.0050
.598	1.04	3.00	.0268	.0077	.0449	.0268	.0073	.0449	.0211	.0110	.0380	.0077	.0037	.0058
.603	1.04	5.98	.0070	.0083	.0118	.0070	.0079	.0118	.0001	.0111	.0058	.0069	.0032	.0059
.601	1.05	9.01	.0185	.0115	.0259	.0185	.0111	.0259	.0217	.0128	.0285	.0031	.0017	.0026
.601	3.50	-2.99	.0784	.0953	.1143	.0695	.0113	.1025	.0606	.0161	.0967	.0089	.0048	.0058
.601	3.51	.00	.0517	.0996	.0844	.0484	.0077	.0727	.0423	.0126	.0693	.0061	.0049	.0034
.602	3.51	2.99	.0250	.1011	.0534	.0273	.0058	.0417	.0227	.0107	.0398	.0046	.0040	.0019
.601	3.50	6.00	.0028	.1010	.0192	.0051	.0060	.0075	.0008	.0100	.0066	.0043	.0040	.0009
.597	3.52	9.00	.0364	.0979	.0197	.0226	.0105	.0317	.0226	.0127	.0300	.0000	.0022	.0016

TABLE 10. AERODYNAMIC CHARACTERISTICS FOR HORIZONTAL TAILS AFT, VERTICAL TAILS MID,
 $\phi_t = 0^\circ$, AND $\delta_h = -10^\circ$

MACH	NPR	ALPHA	C.L.T	C(D=F)	C.M.T	CL	CD	CM	CLAFT	COAFT	CHAFT	CLN	CDN	CMN
.599	1.04	-.00	-.0927	.0176	.1603	-.0927	.0172	.1603	-.0917	.0248	.1502	-.0010	-.0076	.0100
.600	1.99	.01	-.0983	-.0289	.1704	-.0960	.0161	.1644	-.0945	.0242	.1541	-.0015	-.0081	.0104
.599	2.99	.01	-.1026	-.0702	.1784	-.0996	.0155	.1686	-.0965	.0244	.1571	-.0031	-.0089	.0115
.598	3.50	.01	-.1043	-.0918	.1813	-.1009	.0165	.1694	-.0971	.0244	.1578	-.0038	-.0079	.0116
.600	5.01	-.00	-.1070	-.1547	.1877	-.1026	.0167	.1701	-.0983	.0243	.1593	-.0043	-.0076	.0108
.599	1.03	-3.00	-.1082	.0256	.1804	-.1082	.0252	.1804	-.1053	.0310	.1705	-.0029	-.0058	.0099
.601	1.04	.01	-.0928	.0193	.1593	-.0928	.0189	.1593	-.0912	.0242	.1496	-.0017	-.0053	.0097
.601	1.04	3.01	-.0763	.0141	.1363	-.0763	.0137	.1363	-.0757	.0187	.1268	-.0007	-.0050	.0096
.599	1.04	6.01	-.0510	.0115	.0986	-.0510	.0111	.0986	-.0532	.0144	.0927	-.0022	-.0033	.0059
.599	1.04	9.00	-.0292	.0101	.0634	-.0292	.0097	.0634	-.0301	.0129	.0564	-.0008	-.0031	.0070
.600	3.50	-3.00	-.1282	-.0821	.2056	-.1192	.0249	.1939	-.1121	.0314	.1802	-.0072	-.0065	.0136
.598	3.49	.01	-.1061	-.0901	.1816	-.1027	.0177	.1697	-.0973	.0241	.1582	-.0054	-.0064	.0115
.599	3.50	3.01	-.0811	-.0961	.1542	-.0834	.0119	.1424	-.0801	.0182	.1328	-.0034	-.0063	.0096
.601	3.50	6.00	-.0507	-.0985	.1177	-.0586	.0084	.1060	-.0575	.0139	.0987	-.0011	-.0054	.0073
.598	3.50	9.00	-.0184	-.0997	.0757	-.0320	.0072	.0639	-.0323	.0120	.0592	-.0003	-.0048	.0047

TABLE 11. AERODYNAMIC CHARACTERISTICS FOR HORIZONTAL TAILS AFT, VERTICAL TAILS AFT,
 $\phi_t = 0^\circ$, AND $\delta_h = 0^\circ$

MACH	NPR	ALPHA	CLY	C(D _{REF})	CMT	CL	CD	CM	CI AFT	CO AFT	CM AFT	CLN	CDN	CMN
1.201	86	0.3	0.167	0.285	0.255	0.167	0.281	0.255	0.144	0.171	0.213	0.018	0.111	0.041
1.201	2.97	0.4	0.183	0.059	0.258	0.176	0.267	0.234	0.149	0.168	0.214	0.026	0.099	0.019
1.200	5.02	0.2	0.151	0.162	0.202	0.140	0.263	0.158	0.149	0.168	0.214	0.009	0.095	0.056
1.199	7.03	0.2	0.131	0.386	0.174	0.116	0.255	0.111	0.146	0.167	0.210	0.029	0.088	0.099
1.201	9.03	0.3	0.143	0.611	0.200	0.125	0.240	0.118	0.152	0.165	0.219	0.027	0.075	0.102
1.199	7.01	3.05	0.594	0.357	0.755	0.545	0.281	0.691	0.517	0.192	0.732	0.028	0.089	0.041
1.202	6.99	0.2	0.136	0.378	0.173	0.121	0.256	0.110	0.143	0.165	0.206	0.022	0.091	0.095
1.200	7.01	2.97	0.383	0.346	0.418	0.344	0.291	0.482	0.230	0.175	0.316	0.134	0.116	0.166
1.200	7.03	5.96	0.770	0.271	0.862	0.717	0.367	0.926	0.505	0.220	0.710	0.212	0.146	0.216
1.200	7.01	8.95	1.161	0.149	1.377	1.075	0.483	1.440	0.798	0.298	1.171	0.278	0.185	0.269
0.900	1.06	0.4	0.081	0.102	0.018	0.081	0.098	0.018	0.000	0.109	0.056	0.081	0.011	0.075
0.899	2.01	0.4	0.067	0.114	0.021	0.057	0.087	0.006	0.015	0.105	0.081	0.072	0.018	0.075
0.899	2.99	0.5	0.034	0.285	0.020	0.020	0.092	0.063	0.025	0.108	0.099	0.045	0.016	0.035
0.900	5.01	0.5	0.011	0.650	0.026	0.009	0.100	0.104	0.035	0.107	0.118	0.026	0.007	0.014
0.901	7.00	0.3	0.024	1.035	0.046	0.050	0.099	0.158	0.053	0.107	0.147	0.063	0.007	0.011
0.900	5.01	3.03	0.137	0.664	0.101	0.077	0.093	0.023	0.037	0.108	0.031	0.040	0.015	0.012
0.898	5.00	0.5	0.002	0.669	0.034	0.019	0.100	0.113	0.039	0.107	0.123	0.020	0.007	0.010
0.899	5.00	2.95	0.183	0.643	0.228	0.163	0.117	0.306	0.140	0.113	0.295	0.023	0.004	0.011
0.898	5.03	5.95	0.393	0.620	0.469	0.333	0.144	0.548	0.284	0.132	0.536	0.049	0.012	0.012
0.898	5.03	8.95	0.778	0.537	0.934	0.678	0.223	1.012	0.551	0.183	0.949	0.127	0.040	0.063
0.598	1.04	0.5	0.017	0.070	0.063	0.017	0.066	0.063	0.056	0.082	0.106	0.073	0.015	0.043
0.599	2.01	0.4	0.039	0.191	0.098	0.062	0.066	0.158	0.091	0.082	0.161	0.029	0.016	0.003
0.600	3.02	0.3	0.076	0.800	0.119	0.107	0.064	0.218	0.108	0.085	0.188	0.001	0.021	0.030
0.602	3.52	0.5	0.082	1.002	0.111	0.116	0.072	0.229	0.115	0.085	0.200	0.001	0.013	0.029
0.601	5.01	0.2	0.078	1.633	0.055	0.122	0.076	0.231	0.113	0.086	0.196	0.009	0.009	0.035
0.601	3.52	3.03	0.194	1.016	0.177	0.103	0.058	0.059	0.072	0.091	0.081	0.031	0.033	0.022
0.602	3.52	0.6	0.090	0.997	0.115	0.125	0.076	0.232	0.113	0.088	0.196	0.012	0.012	0.036
0.602	3.50	2.97	0.380	0.960	0.412	0.358	0.113	0.530	0.299	0.102	0.475	0.059	0.012	0.055
0.601	3.50	5.94	0.748	0.893	0.803	0.670	0.176	0.920	0.523	0.133	0.825	0.148	0.042	0.095
0.598	3.50	8.96	1.089	0.811	1.218	0.954	0.261	1.336	0.764	0.192	1.211	0.190	0.069	0.125

ORIGINAL PAGE IS
OF POOR QUALITY

TABLE 12. AERODYNAMIC CHARACTERISTICS FOR HORIZONTAL TAILS AFT, VERTICAL TAILS AFT,
 $\phi_t = 0^\circ$, AND $\delta_h = -5^\circ$

MACH	NPR	ALPHA	CLT	C(D=AF)	CMT	CL	CD	CM	CLAFT	CMRAFT	CLN	CDN	CMN
.900	1.06	.03	.0543	.0144	.0851	.0543	.0140	.0851	.0501	.0164	.0042	.0023	.0065
.898	2.03	.02	.0556	.0073	.0854	.0546	.0132	.0827	.0497	.0158	.0048	.0026	.0052
.898	3.01	.02	.0574	.0250	.0880	.0561	.0132	.0836	.0503	.0158	.0057	.0026	.0052
.899	5.02	.03	.0594	.0629	.0918	.0574	.0134	.0839	.0504	.0157	.0070	.0022	.0057
.901	7.01	.03	.0602	.1006	.0938	.0576	.0128	.0826	.0510	.0156	.0066	.0028	.0038
.899	4.99	.04	.0696	.0588	.1043	.0636	.0167	.0965	.0577	.0191	.0059	.0024	.0046
.899	4.99	.03	.0597	.0620	.0919	.0577	.0137	.0842	.0513	.0158	.0064	.0021	.0046
.899	4.99	2.98	.0432	.0650	.0744	.0452	.0107	.0666	.0411	.0130	.0041	.0023	.0039
.898	5.02	5.98	.0261	.0681	.0506	.0322	.0082	.0427	.0261	.0110	.0061	.0028	.0054
.901	5.01	9.00	.0030	.0664	.0133	.0070	.0088	.0055	.0023	.0117	.0047	.0029	.0046
.600	1.04	.02	.0533	.0118	.0780	.0533	.0114	.0780	.0438	.0130	.0095	.0016	.0072
.602	2.00	.02	.0526	.0346	.0804	.0502	.0101	.0745	.0437	.0127	.0065	.0026	.0045
.601	3.02	.03	.0504	.0766	.0800	.0474	.0095	.0701	.0434	.0128	.0040	.0033	.0008
.601	3.51	.03	.0508	.0975	.0818	.0474	.0097	.0700	.0433	.0128	.0040	.0030	.0009
.600	5.02	.03	.0526	.1618	.0881	.0482	.0098	.0705	.0442	.0126	.0039	.0028	.0004
.601	3.52	.01	.0747	.0945	.1099	.0657	.0130	.0981	.0610	.0165	.0047	.0035	.0018
.601	3.51	.03	.0491	.0972	.0807	.0457	.0100	.0689	.0432	.0127	.0025	.0026	.0001
.601	3.51	2.96	.0237	.0989	.0518	.0260	.0083	.0401	.0248	.0106	.0012	.0023	.0006
.599	3.50	5.98	.0043	.0986	.0172	.0036	.0091	.0053	.0021	.0099	.0015	.0008	.0006
.597	3.50	8.97	.0374	.0939	.0215	.0238	.0135	.0334	.0202	.0124	.0037	.0011	.0044

TABLE 13. AERODYNAMIC CHARACTERISTICS FOR HORIZONTAL TAILS AFT, VERTICAL TAILS MID,
 $\phi_t = -10^\circ$, AND $\delta_h = 0^\circ$

MACH	NPR	ALPHA	CLT	C(D=F)	CMT	CL	CD	CM	CLAFT	CAFT	CMFT	CLN	CDN	CMN
1.199	.94	.01	-.0136	.0240	.0146	-.0136	.0276	.0146	-.0096	.0177	.0090	-.0040	.0099	.0056
1.200	3.02	.02	-.0163	.0056	.0186	-.0155	.0270	.0161	-.0102	.0175	.0098	-.0053	.0095	.0064
1.198	5.00	.01	-.0135	.0160	.0145	-.0124	.0266	.0101	-.0101	.0175	.0097	-.0023	.0090	.0004
1.199	7.01	.01	-.0119	.0381	.0121	-.0105	.0258	.0057	-.0104	.0175	.0101	-.0001	.0083	.0044
1.198	8.96	.01	-.0115	.0602	.0130	-.0098	.0246	.0047	-.0090	.0174	.0084	-.0008	.0071	.0037
1.199	.89	3.00	-.0556	.0311	.0704	-.0556	.0307	.0704	-.0468	.0202	.0613	-.0088	.0105	.0091
1.200	.88	.00	-.0145	.0284	.0139	-.0145	.0280	.0139	-.0085	.0174	.0075	-.0060	.0106	.0063
1.200	.88	2.96	.0322	.0311	.0437	.0322	.0307	.0437	.0295	.0191	-.0463	.0027	.0117	.0026
1.202	.86	5.97	.0703	.0393	.0915	.0703	.0389	.0915	.0585	.0248	-.0872	.0118	.0142	-.0043
1.199	.83	8.99	.1026	.0517	.1379	.1026	.0513	.1379	.0865	.0325	-.1314	.0161	.0188	-.0065
1.200	7.03	3.02	-.0576	.0350	.0694	-.0527	.0289	.0631	-.0480	.0200	.0629	-.0048	.0089	.0022
1.201	7.01	.02	-.0116	.0380	.0112	-.0101	.0257	.0049	-.0084	.0172	.0075	-.0018	.0085	.0026
1.202	7.02	3.00	.0439	.0340	.0518	.0420	.0297	.0581	.0315	.0189	-.0488	.0105	.0108	-.0093
1.200	6.99	5.98	.0827	.0252	.0963	.0774	.0383	.1026	.0591	.0248	-.0880	.0184	.0134	-.0147
1.201	7.04	8.96	.1211	.0129	.1477	.1125	.0505	.1541	.0880	.0328	-.1334	.0245	.0177	-.0207
.899	1.09	.03	.0043	.0136	.0149	.0043	.0132	.0149	.0109	.0152	-.0206	-.0060	.0020	.0057
.902	2.03	.02	.0019	.0078	.0100	.0029	.0126	.0127	.0093	.0147	-.0191	-.0064	.0021	.0064
.900	3.02	.02	.0038	.0254	.0109	.0051	.0127	.0153	.0103	.0149	-.0207	-.0052	.0022	.0054
.899	5.01	.03	.0046	.0631	.0088	.0066	.0130	.0167	.0107	.0148	-.0214	-.0041	.0018	.0048
.900	7.03	.02	.0048	.1013	.0060	.0073	.0126	.0173	.0109	.0145	-.0217	-.0035	.0020	.0045
.899	1.09	3.02	-.0028	.0122	.0031	-.0028	.0118	.0031	.0031	.0147	-.0083	-.0060	.0029	.0051
.902	1.09	.05	.0056	.0135	.0153	.0056	.0131	.0153	.0103	.0156	-.0208	-.0047	.0024	.0055
.898	1.08	2.99	.0133	.0144	.0254	.0133	.0140	.0254	.0175	.0160	-.0328	-.0042	.0020	.0074
.900	1.08	5.99	.0263	.0170	.0432	.0263	.0166	.0432	.0274	.0172	-.0503	-.0011	.0006	.0071
.900	1.09	8.98	.0630	.0245	.0928	.0630	.0241	.0928	.0562	.0228	-.0961	.0068	.0013	.0034
.903	5.01	3.03	-.0082	.0635	.0038	-.0023	.0118	.0039	.0037	.0143	-.0093	-.0060	.0026	.0053
.899	5.01	.01	.0058	.0635	.0093	.0078	.0127	.0171	.0104	.0150	-.0211	-.0027	.0023	.0040
.899	5.01	2.97	.0220	.0618	.0253	.0200	.0144	.0332	.0194	.0158	-.0364	.0006	.0023	.0032
.898	5.00	5.99	.0410	.0587	.0476	.0350	.0172	.0554	.0318	.0175	-.0575	.0032	.0003	.0021
.898	5.03	8.99	.0806	.0508	.0952	.0705	.0252	.1030	.0594	.0230	-.1012	.0111	.0022	.0018
.602	1.04	.04	.0068	.0084	.0124	.0068	.0080	.0124	.0098	.0097	-.0148	-.0030	.0018	.0024
.598	2.04	.01	.0073	.0378	.0093	.0093	.0091	.0154	.0108	.0097	-.0163	-.0011	.0006	.0008
.599	3.03	.02	.0083	.0787	.0079	.0113	.0084	.0179	.0112	.0098	-.0170	.0002	.0014	.0010
.599	3.49	.03	.0082	.0988	.0061	.0116	.0088	.0179	.0112	.0099	-.0169	.0004	.0011	.0010
.599	5.01	.02	.0072	.1625	.0001	.0117	.0092	.0175	.0111	.0099	-.0169	.0006	.0007	.0007
.599	1.04	3.02	-.0076	.0089	.0074	-.0076	.0085	.0074	-.0053	.0104	.0076	-.0023	.0019	.0002
.601	1.06	.00	.0088	.0102	.0137	.0088	.0088	.0137	.0102	.0103	-.0154	.0014	.0004	.0017
.602	1.04	2.99	.0261	.0131	.0357	.0261	.0127	.0357	.0261	.0115	-.0389	.0001	.0013	.0032
.600	1.04	5.99	.0539	.0181	.0714	.0539	.0177	.0714	.0476	.0146	-.0721	.0063	.0032	.0007
.597	1.04	8.97	.0838	.0266	.1126	.0838	.0262	.1126	.0711	.0202	-.1097	.0127	.0060	.0030
.599	3.50	3.03	-.0191	.1000	.0225	-.0100	.0075	.0107	-.0071	.0103	.0102	-.0029	.0028	.0005
.601	3.50	.03	.0087	.0981	.0063	.0121	.0091	.0181	.0110	.0102	-.0167	.0011	.0014	.0014
.599	3.49	2.99	.0376	.0951	.0362	.0354	.0122	.0480	.0300	.0115	-.0452	.0053	.0007	.0028
.598	3.49	5.97	.0738	.0890	.0740	.0659	.0186	.0858	.0519	.0149	-.0790	.0140	.0037	.0068
.603	3.50	8.98	.1073	.0787	.1150	.0939	.0268	.1267	.0752	.0206	-.1164	.0187	.0062	.0103

ORIGINAL PAGE IS
OF POOR QUALITY

TABLE 14. AERODYNAMIC CHARACTERISTICS FOR HORIZONTAL TAILS AFT, VERTICAL TAILS MID,
 $\phi_t = 10^\circ$, AND $\delta_h = 0^\circ$

MACH	NPR	ALPHA	CLT	C(D-F)	CMT	CL	CD	CM	CLAFT	CDRAFT	CMAFT	CLN	CDN	CMN
1.199	89	.01	.0116	.0269	.0124	.0116	.0265	.0124	.0098	.0171	.0081	.0018	.0094	.0043
1.200	3.00	.03	.0147	.0045	.0165	.0140	.0257	.0140	.0099	.0170	.0081	.0041	.0087	.0058
1.201	5.00	.01	.0119	.0170	.0122	.0109	.0255	.0078	.0097	.0169	.0079	.0012	.0086	.0001
1.201	6.99	.01	.0098	.0385	.0093	.0084	.0249	.0030	.0087	.0169	.0067	.0003	.0080	.0037
1.202	9.01	.02	.0100	.0612	.0111	.0083	.0236	.0029	.0087	.0168	.0069	.0004	.0068	.0040
1.899	1.09	.01	.0136	.0125	.0263	.0136	.0121	.0263	.0168	.0142	.0308	.0032	.0020	.0045
1.900	2.00	.01	.0109	.0087	.0210	.0119	.0113	.0237	.0155	.0133	.0287	.0036	.0021	.0050
1.899	3.00	.00	.0119	.0267	.0207	.0133	.0112	.0251	.0160	.0137	.0294	.0027	.0025	.0043
1.899	4.98	.02	.0125	.0641	.0182	.0144	.0115	.0260	.0165	.0136	.0301	.0021	.0021	.0041
1.899	7.01	.01	.0119	.1028	.0145	.0144	.0110	.0257	.0161	.0134	.0295	.0017	.0024	.0038
1.600	1.04	.02	.0093	.0077	.0174	.0093	.0073	.0174	.0128	.0089	.0196	.0035	.0016	.0022
1.601	1.99	.01	.0099	.0378	.0136	.0122	.0069	.0195	.0135	.0089	.0205	.0013	.0020	.0010
1.602	3.00	.00	.0107	.0787	.0116	.0137	.0066	.0214	.0140	.0091	.0214	.0003	.0026	.0000
1.602	3.51	.00	.0104	.0995	.0095	.0137	.0074	.0212	.0138	.0092	.0210	.0001	.0017	.0002
1.596	4.98	.02	.0090	.1645	.0025	.0133	.0077	.0202	.0139	.0091	.0211	.0005	.0014	.0010

TABLE 15. AERODYNAMIC CHARACTERISTICS FOR HORIZONTAL TAILS AFT, VERTICAL TAILS MID,
 $\phi_t = 20^\circ$, AND $\delta_h = 0^\circ$

MACH	NPR	ALPHA	CLT	C(D-F)	CMT	CL	CD	CM	CLIFT	CDIFT	CMIFT	CLN	CDN	CMN
1.202	.90	.03	-.0140	.0268	.0135	-.0140	.0264	.0135	-.0103	.0166	.0090	-.0037	.0094	.0045
1.200	3.02	.04	.0169	.0045	.0172	-.0162	.0258	.0148	-.0107	.0165	.0095	-.0054	.0093	.0052
1.201	5.02	.02	-.0149	-.0169	.0140	-.0134	.0256	.0096	-.0109	.0164	.0099	-.0029	.0092	.0003
1.202	7.00	.03	-.0136	-.0387	.0124	-.0122	.0248	.0061	-.0113	.0164	.0105	-.0009	.0084	.0004
1.201	9.03	.04	.0129	.0615	.0130	-.0112	.0235	.0048	-.0092	.0165	.0078	-.0020	.0071	.0030
1.198	.91	-2.97	-.0613	.0301	.0753	-.0613	.0297	.0753	-.0539	.0194	.0695	-.0074	.0103	.0058
1.201	.89	.04	-.0162	.0274	.0136	-.0162	.0270	.0136	-.0096	.0164	.0081	-.0066	.0105	.0055
1.200	.89	3.05	.0368	.0310	-.0510	.0368	.0308	-.0510	.0341	.0187	-.0529	.0027	.0119	.0019
1.198	.86	6.04	.0769	.0393	.0105	.0769	.0389	-.0105	.0657	.0249	-.0975	.0112	.0141	-.0040
1.201	.82	9.01	.1119	.0519	.1497	.1119	.0515	-.1497	.0953	.0331	-.1431	.0166	.0184	-.0066
1.199	7.01	-2.95	-.0648	-.0357	.0770	-.0600	.0280	.0707	-.0545	.0193	.0702	-.0055	.0087	.0004
1.200	7.01	.03	-.0135	.0394	.0119	-.0121	.0244	.0055	-.0095	.0165	.0079	-.0026	.0079	.0024
1.199	7.00	3.04	.0464	-.0349	.0564	.0444	.0288	-.0627	.0341	.0184	-.0527	.0103	.0104	-.0100
1.201	6.04	.04	.0907	.0254	.1082	.0854	.0380	-.0617	.0668	.0244	-.0989	.0186	.0131	-.0156
1.201	7.02	9.00	.1299	-.0124	.1597	.1213	.0507	-.1660	.0952	.0332	-.1444	.0251	.0175	-.0217
.900	1.10	.04	.0122	.0108	-.0252	.0122	.0104	-.0252	.0156	.0135	-.0285	-.0034	-.0031	.0033
.901	2.02	.03	.0099	-.0103	.0201	.0109	.0098	-.0228	.0145	.0128	-.0266	-.0036	-.0030	.0038
.900	2.98	.03	.0106	-.0276	-.0194	.0119	.0099	-.0242	.0149	.0129	-.0271	-.0030	.0030	.0027
.898	5.07	.01	.0109	-.0663	.0169	.0128	.0101	-.0248	.0152	.0126	-.0275	-.0024	-.0026	.0027
.902	6.99	.04	.0099	-.1027	-.0128	.0123	.0099	-.0239	.0144	.0125	-.0266	-.0021	-.0026	.0027
.897	1.10	-2.98	-.0011	.0093	-.0072	-.0011	.0089	-.0072	.0032	.0121	-.0095	-.0043	-.0032	.0023
.902	1.10	.02	.0134	.0111	-.0256	.0134	.0107	-.0256	.0155	.0135	-.0283	-.0021	-.0028	.0027
.900	1.09	3.04	.0271	.0135	.0423	.0271	.0131	-.0423	.0269	.0149	-.0462	.0003	.0018	.0040
.902	1.09	6.02	.0402	.0166	-.0402	.0402	.0162	-.0610	.0393	.0172	-.0669	.0009	.0010	.0059
.900	1.10	9.00	.0791	.0253	-.1145	.0791	.0249	-.1145	.0691	.0235	-.1151	.0100	.0014	.0006
.905	5.02	-2.97	-.0092	-.0663	.0031	-.0033	.0090	-.0047	.0026	.0119	-.0084	-.0059	.0029	.0037
.900	5.01	.03	.0121	-.0656	-.0177	.0140	.0104	-.0255	.0149	.0126	-.0273	-.0009	-.0023	.0018
.901	5.04	6.04	.0535	-.0596	.0647	.0474	.0164	-.0725	.0435	.0173	-.0740	.0038	-.0009	.0015
.898	4.99	9.03	.0956	.0497	-.1156	.0856	.0255	-.1234	.0729	.0236	-.1209	.0127	.0019	-.0025
.599	1.05	.03	.0059	.0067	-.0143	.0059	.0063	-.0143	.0104	.0088	-.0161	-.0045	-.0024	.0018
.599	2.01	.03	.0034	-.0394	-.0075	.0062	.0063	-.0136	.0097	.0086	-.0150	-.0035	-.0023	.0014
.601	3.01	.04	.0064	-.0799	-.0077	.0094	.0059	-.0176	.0109	.0088	-.0168	-.0015	-.0029	-.0008
.601	3.52	.03	.0067	-.1011	-.0064	.0100	.0067	-.0182	.0109	.0088	-.0169	-.0009	-.0020	.0013
.602	4.99	.03	.0061	-.1624	-.0005	.0103	.0072	-.0179	.0113	.0087	-.0174	-.0010	-.0015	-.0005
.600	1.05	-2.98	-.0119	.0068	.0108	-.0119	.0064	.0108	-.0090	.0092	.0113	-.0029	-.0028	-.0005
.601	1.05	.04	.0089	.0081	-.0155	.0089	.0077	-.0155	.0106	.0091	-.0163	-.0017	-.0014	.0008
.600	1.04	3.04	.0316	.0112	-.0434	.0316	.0108	-.0434	.0309	.0104	-.0454	.0007	.0004	.0019
.599	1.04	6.02	.0641	.0175	-.0840	.0641	.0171	-.0840	.0561	.0141	-.0832	.0080	.0029	-.0008
.599	1.05	9.02	.0949	.0264	-.1282	.0949	.0260	-.1282	.0826	.0206	-.1251	.0123	.0054	-.0031
.602	3.53	-2.95	-.0233	-.1018	.0265	-.0144	.0058	.0146	-.0132	.0095	.0171	-.0012	-.0037	-.0025
.602	3.52	.06	.0089	-.1002	-.0075	.0121	.0072	-.0193	.0110	.0090	-.0170	.0011	-.0018	.0023
.601	3.52	3.03	.0428	-.0965	-.0433	.0405	.0112	-.0551	.0343	.0105	-.0506	.0062	.0007	-.0045
.598	3.51	6.04	.0834	-.0904	-.0868	.0753	.0178	-.0987	.0605	.0145	-.0901	.0148	.0034	-.0085
.601	3.52	9.04	.1184	-.0799	-.1298	.1047	.0270	-.1416	.0853	.0208	-.1298	.0194	.0062	-.0118

TABLE 16. AERODYNAMIC CHARACTERISTICS FOR HORIZONTAL TAILS AFT, VERTICAL TAILS MID,
 $\phi_t = 20^\circ$, AND $\delta_h = -5^\circ$

MACH	NPR	ALPHA	CLT	C(D+F)	CMT	CI	CD	CM	CL AFT	CD AFT	CM AFT	CLN	CDN	CMN
.901	1.09	.00	-.0325	.0124	.0519	-.0325	.0120	.0519	-.0309	.0168	.0501	-.0016	-.0048	.0018
.900	2.04	-.01	-.0375	-.0096	.0587	-.0365	.0109	.0559	-.0330	.0161	.0533	-.0035	-.0052	.0026
.899	3.00	.00	-.0418	-.0267	.0653	-.0405	.0112	.0609	-.0338	.0162	.0549	-.0067	-.0050	.0060
.898	5.02	.00	-.0457	-.0651	.0732	-.0438	.0114	.0653	-.0359	.0161	.0581	-.0079	-.0047	.0072
.898	7.02	.01	-.0489	-.1037	.0791	-.0464	.0105	.0678	-.0372	.0158	.0601	-.0092	-.0053	.0078
.897	1.09	-2.98	-.0486	.0145	.0726	-.0486	.0141	.0726	-.0436	.0180	.0702	-.0049	-.0038	.0024
.901	1.09	-.04	-.0376	.0129	.0545	-.0376	.0125	.0545	-.0314	.0165	.0508	-.0062	-.0040	.0037
.901	1.09	2.99	-.0238	.0111	.0348	-.0238	.0107	.0348	-.0185	.0151	.0307	-.0053	-.0044	.0042
.899	1.08	5.99	-.0108	.0102	.0118	-.0108	.0098	.0118	-.0032	.0147	.0053	-.0075	-.0049	.0065
.899	1.10	8.99	.0250	.0151	.0372	-.0250	.0147	-.0372	.0235	.0176	-.0375	-.0016	-.0029	.0003
.899	4.99	-3.01	-.0649	-.0822	.0959	-.0589	.0135	.0881	-.0501	.0179	.0805	-.0089	-.0043	.0076
.899	5.02	.00	-.0471	.0651	.0737	-.0452	.0111	.0658	-.0358	.0158	.0581	-.0093	-.0046	.0077
.900	5.00	2.99	-.0281	-.0666	.0523	-.0301	.0092	.0445	-.0229	.0144	.0380	-.0072	-.0051	.0066
.899	5.04	6.02	-.0082	-.0685	.0249	-.0143	.0079	.0171	-.0062	.0137	.0101	-.0081	-.0058	.0070
.898	5.04	9.00	.0279	.0635	.0190	.0178	.0126	-.0269	.0203	.0163	-.0315	-.0025	-.0037	.0046
.600	1.04	.00	-.0459	.0082	.0665	-.0459	.0078	.0665	-.0359	.0118	.0603	-.0100	-.0040	.0063
.601	2.00	.00	-.0505	.0382	.0780	-.0481	.0068	.0720	-.0394	.0118	.0654	-.0087	-.0050	.0067
.598	3.02	-.01	-.0518	.0810	.0830	-.0487	.0059	.0730	-.0409	.0120	.0673	-.0078	-.0061	.0057
.599	3.52	.01	-.0516	-.1016	.0844	-.0483	.0066	.0725	-.0408	.0120	.0672	-.0075	-.0054	.0054
.599	5.03	-.01	-.0535	-.1661	.0911	-.0491	.0065	.0734	-.0421	.0120	.0688	-.0070	-.0055	.0046
.600	1.04	-3.00	-.0624	.0111	.0946	-.0624	.0107	.0946	-.0566	.0154	.0903	-.0058	-.0046	.0043
.602	1.04	.02	-.0411	.0088	.0654	-.0411	.0084	.0654	-.0391	.0121	.0606	-.0050	-.0037	.0049
.600	1.04	3.01	-.0211	.0077	.0376	-.0211	.0073	.0376	-.0159	.0107	.0314	-.0052	-.0034	.0063
.600	1.04	5.99	.0040	.0090	.0001	.0040	.0086	.0001	.0088	.0113	-.0056	-.0047	-.0027	.0057
.601	1.05	8.99	.0331	.0140	-.0412	.0331	.0136	-.0412	.0330	.0138	-.0433	-.0001	-.0002	.0021
.600	3.52	-3.01	-.0792	-.0969	.1179	-.0702	.0102	.1061	-.0632	.0158	.0998	-.0070	-.0055	.0063
.601	3.52	.02	-.0495	-.1009	.0841	-.0461	.0070	.0723	-.0412	.0122	.0678	-.0049	-.0052	.0045
.601	3.52	3.00	-.0188	.1023	.0482	-.0211	.0055	.0364	-.0177	.0105	.0334	-.0034	-.0050	.0030
.599	3.52	6.00	.0103	-.1008	.0082	.0063	.0073	-.0037	.0086	.0104	-.0056	-.0024	-.0031	.0019
.601	3.51	9.00	.0507	-.0932	-.0343	.0372	.0133	-.0461	.0337	.0138	-.0445	-.0034	-.0004	-.0015

TABLE 17. AERODYNAMIC CHARACTERISTICS FOR HORIZONTAL TAILS AFT, VERTICAL TAILS MID,
 $\phi_t = 20^\circ$, AND $\delta_h = -10^\circ$

MACH	NPR	ALPHA	CLT	C(DMF)	CMT	CL	CD	CM	CLAFT	CMMAFT	CLN	CDN	CMN
.508	1.04	.00	-.0956	.0185	.1608	-.0958	.0181	.1608	.0896	.0245	-.0062	-.0064	.0136
.602	2.01	.00	-.1024	-.0273	.1709	-.1000	.0178	.1649	-.0925	.0242	-.0076	-.0064	.0137
.600	3.01	.00	-.1064	-.0687	.1789	-.1034	.0173	.1691	-.0943	.0243	-.0090	-.0070	.0152
.600	3.51	-.00	-.1081	-.0496	.1820	-.1047	.0183	.1702	-.0950	.0244	-.0097	-.0061	.0155
.599	5.01	.01	-.1101	-.1537	.1877	-.1057	.0182	.1700	-.0957	.0242	-.0101	-.0060	.0146
.598	1.03	-3.01	-.1142	.0269	.1851	-.1142	.0265	.1851	-.1061	.0308	-.0081	-.0043	.0140
.599	1.04	-.00	-.0970	.0205	.1609	-.0970	.0201	.1609	-.0898	.0243	-.0072	-.0041	.0134
.599	1.04	3.02	-.0773	.0152	.1331	-.0773	.0148	.1331	-.0701	.0191	-.0072	-.0043	.0138
.597	1.04	6.01	-.0511	.0127	.0937	-.0511	.0123	.0937	-.0456	.0153	-.0055	-.0031	.0107
.597	1.05	9.00	-.0259	.0115	.0548	-.0259	.0111	.0548	-.0210	.0141	-.0049	-.0030	.0103
.600	3.52	-2.99	-.1341	-.0423	.2098	-.1250	.0256	.1980	.1127	.0310	-.0124	-.0055	.0176
.600	3.50	-.01	-.1087	-.0444	.1817	-.1053	.0149	.1699	-.0948	.0242	-.0104	-.0053	.0153
.600	3.52	3.01	-.0812	-.0951	.1503	-.0835	.0130	.1385	-.0742	.0186	-.0093	-.0056	.0136
.598	3.50	6.01	-.0467	-.0980	.1114	-.0567	.0096	.0995	-.0496	.0148	-.0072	-.0051	.0111
.598	3.51	9.01	-.0136	-.0992	.0661	-.0275	.0085	.0542	-.0224	.0135	-.0051	-.0050	.0080

TABLE 18. TAIL DRAG COEFFICIENTS

HT	VT	ϕ_t	M	$C_{D,tails}$
Mid	Forward	0	0.6	0.0032
			.9	.0031
			1.2	.0092
	Mid	0	0.6	0.0033
			.9	.0032
			1.2	.0095
Aft	Forward	0	0.6	0.0033
			.9	.0032
			1.2	.0093
	Mid	-10, 0, 10, and 20	0.6	0.0034
			.9	.0033
			1.2	.0095
	Aft	0	0.6	0.0035
			.9	.0034
			1.2	.0097

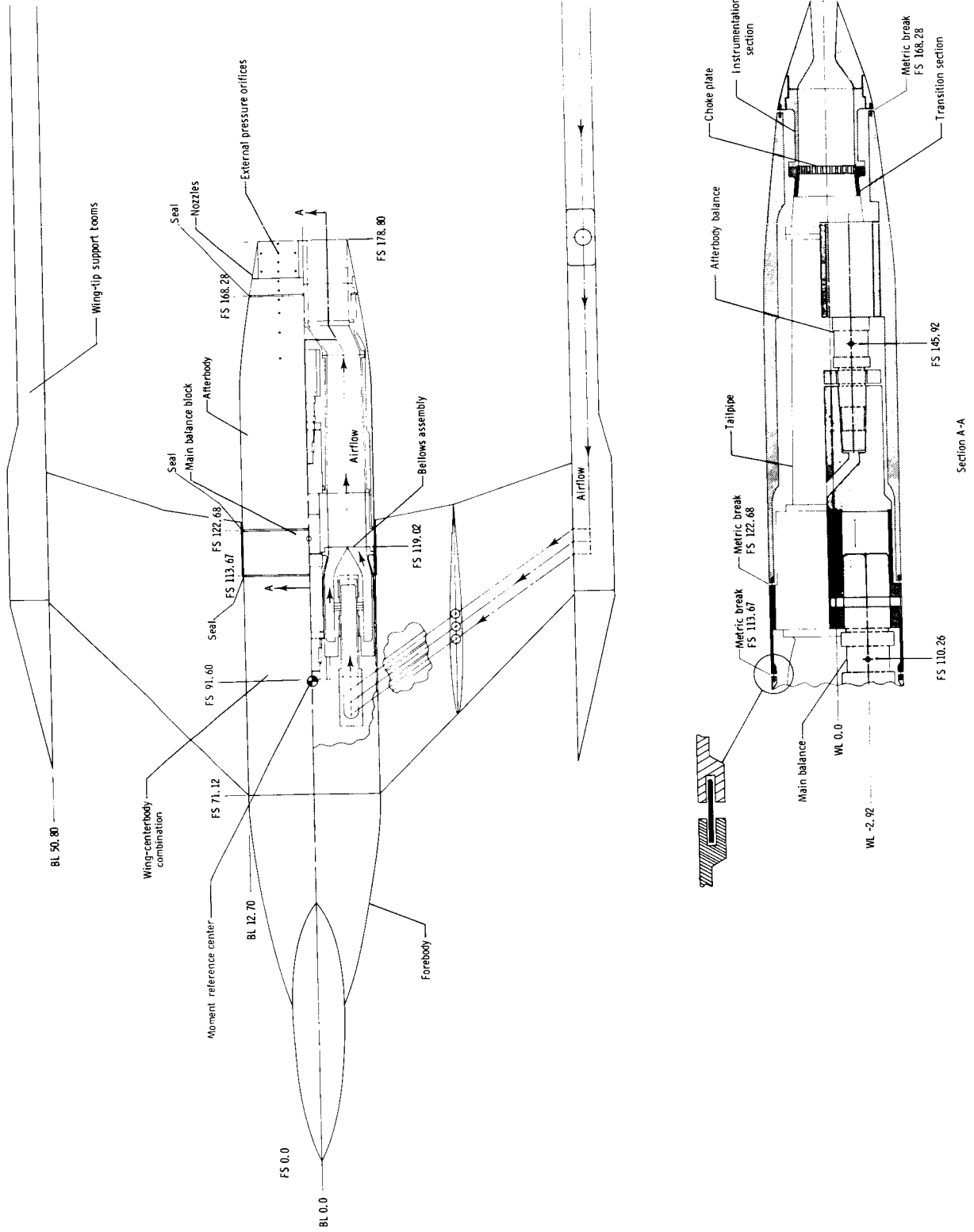


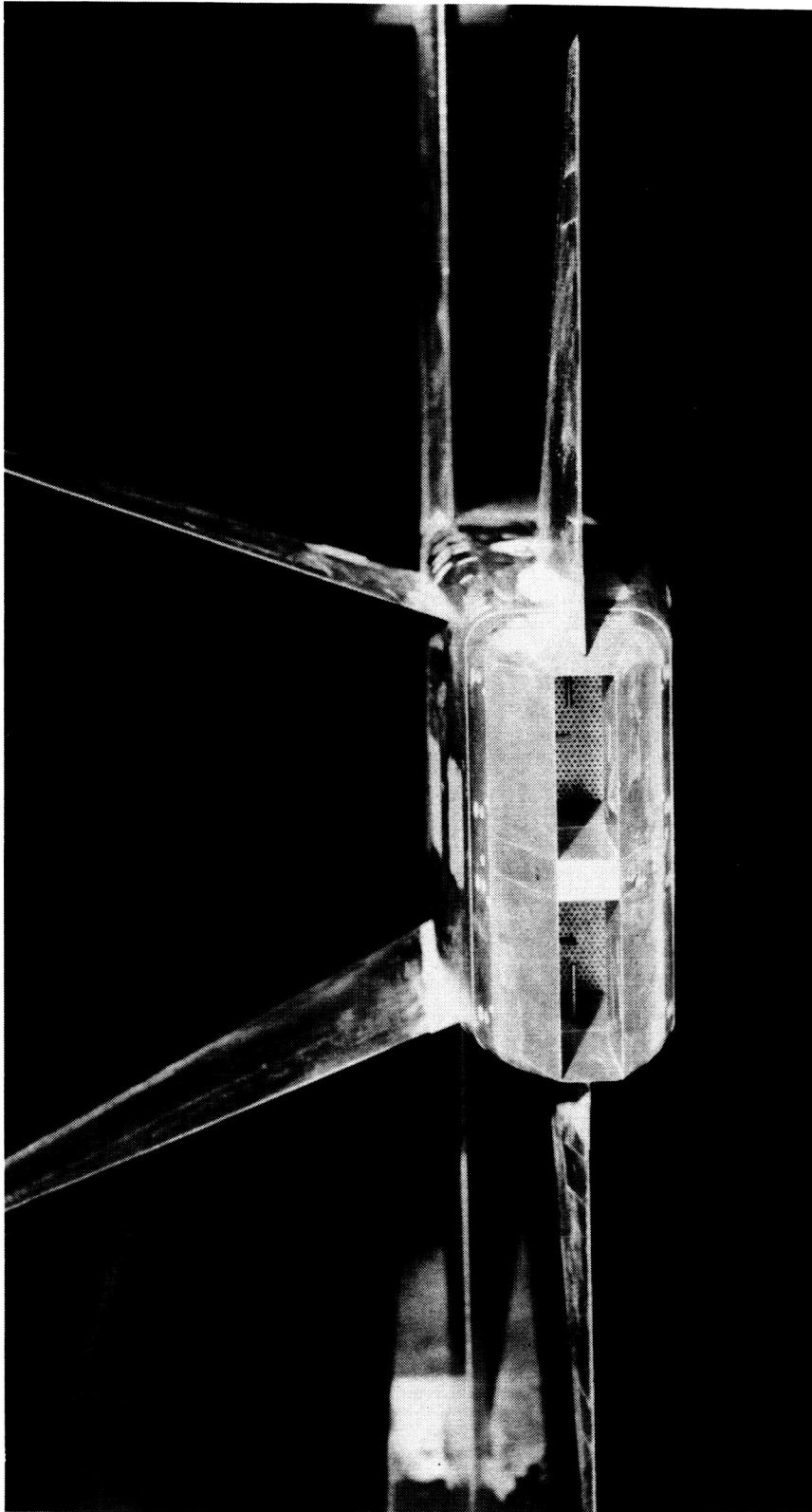
Figure 1. Air-powered, twin-engine, wing-tip-supported model with nonaxisymmetric convergent-divergent dry power nozzles showing jet simulation system and balance arrangement.



L-82-1374

(a) Overall view.

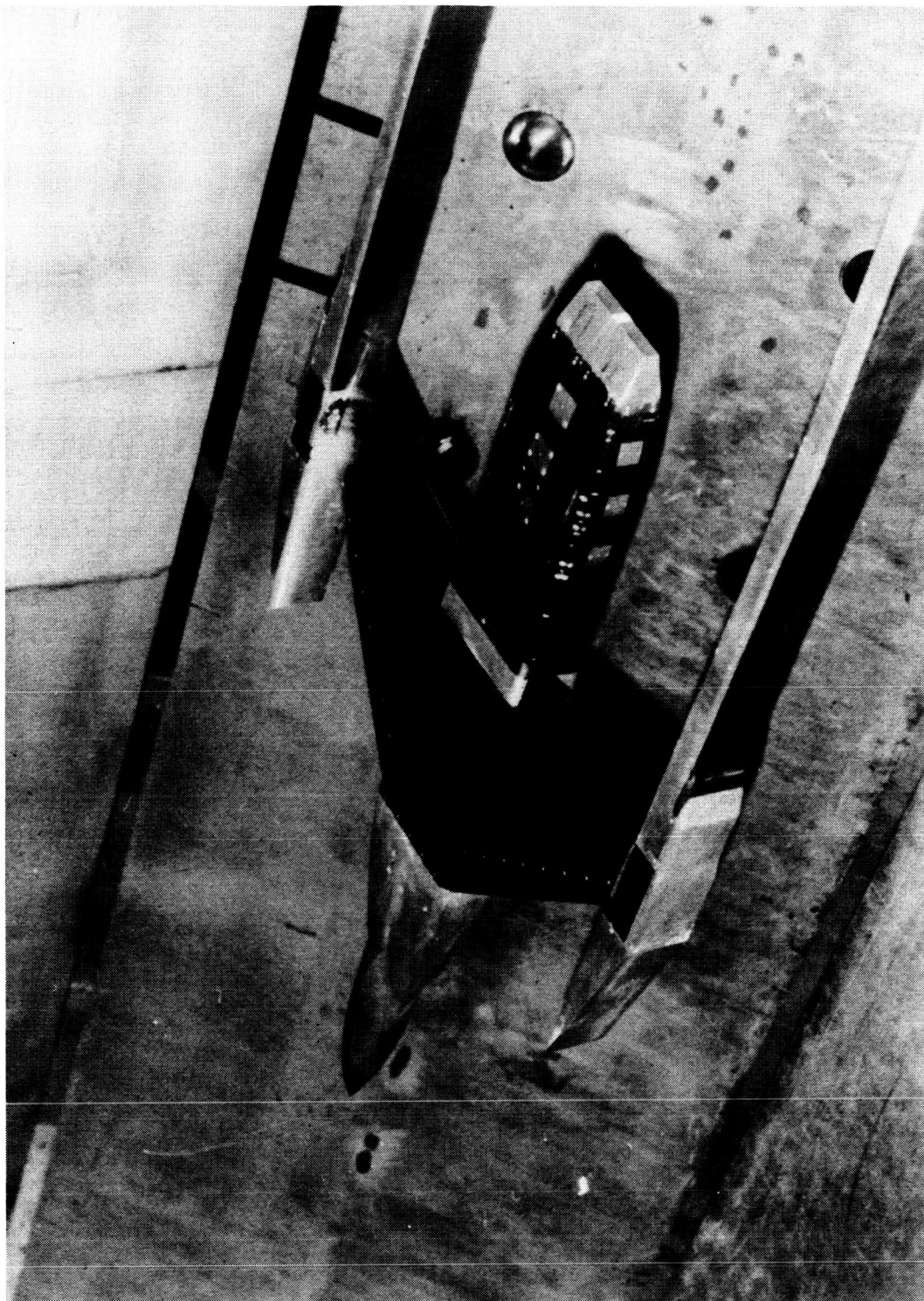
Figure 2. Aircraft model.



L-82-1375

(b) Vertical tails canted 20°.

Figure 2. Continued.



L-80-212

(c) Without tail fins.

Figure 2. Concluded.

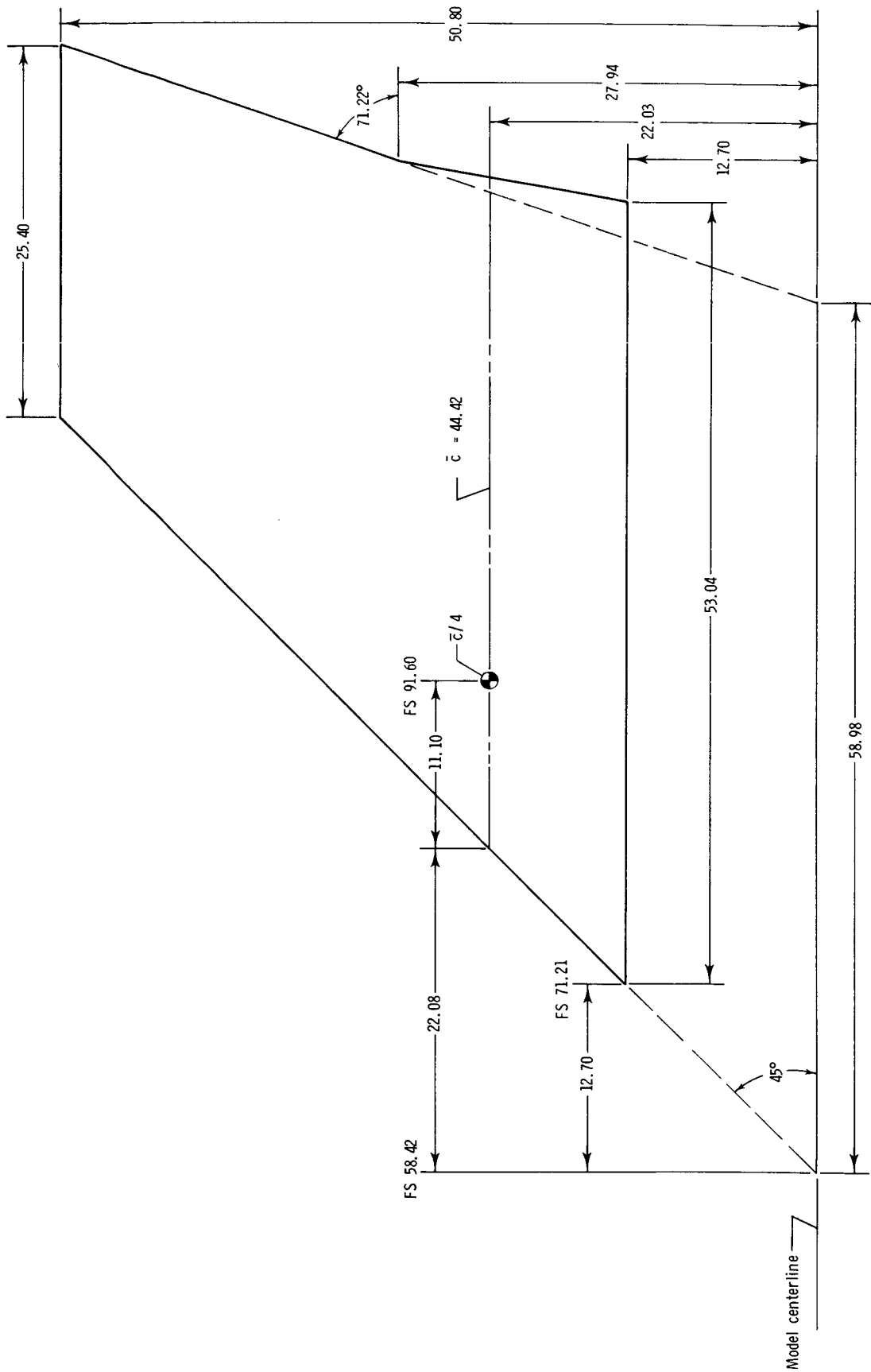


Figure 3. Wing planform geometry. All linear dimensions are in centimeters.

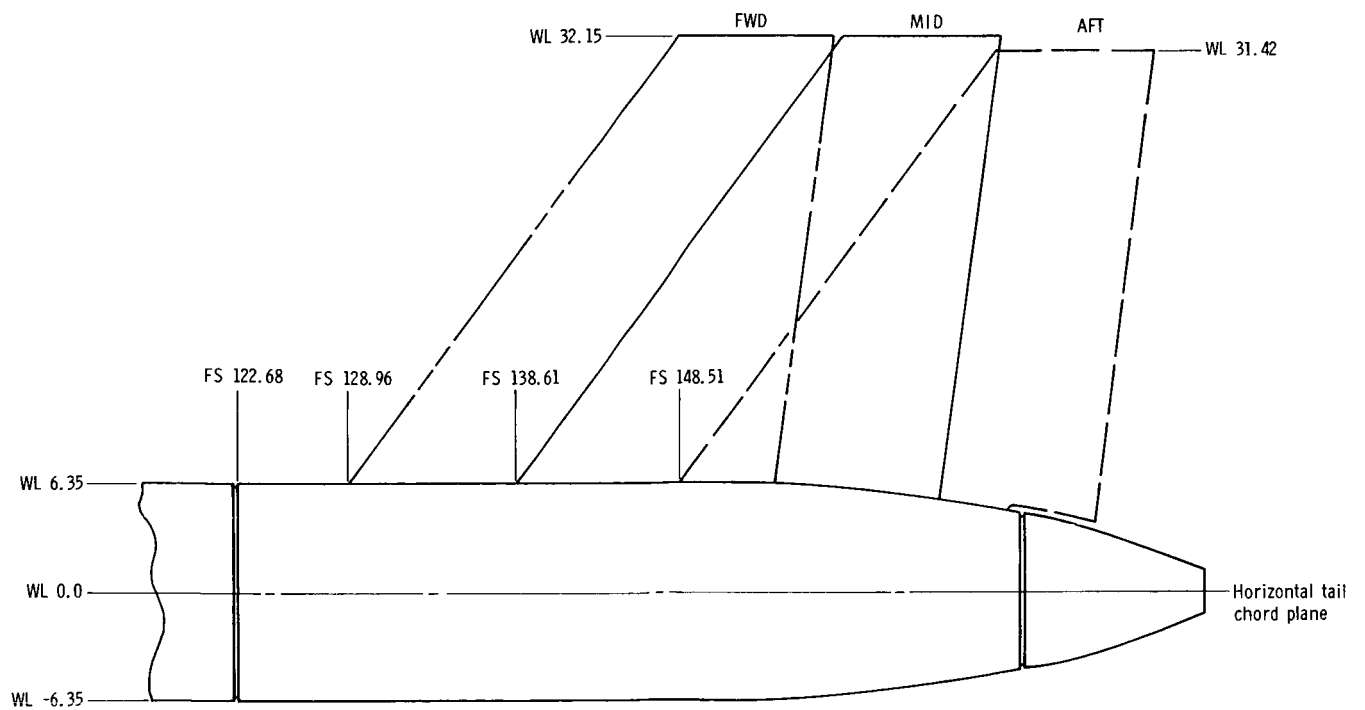
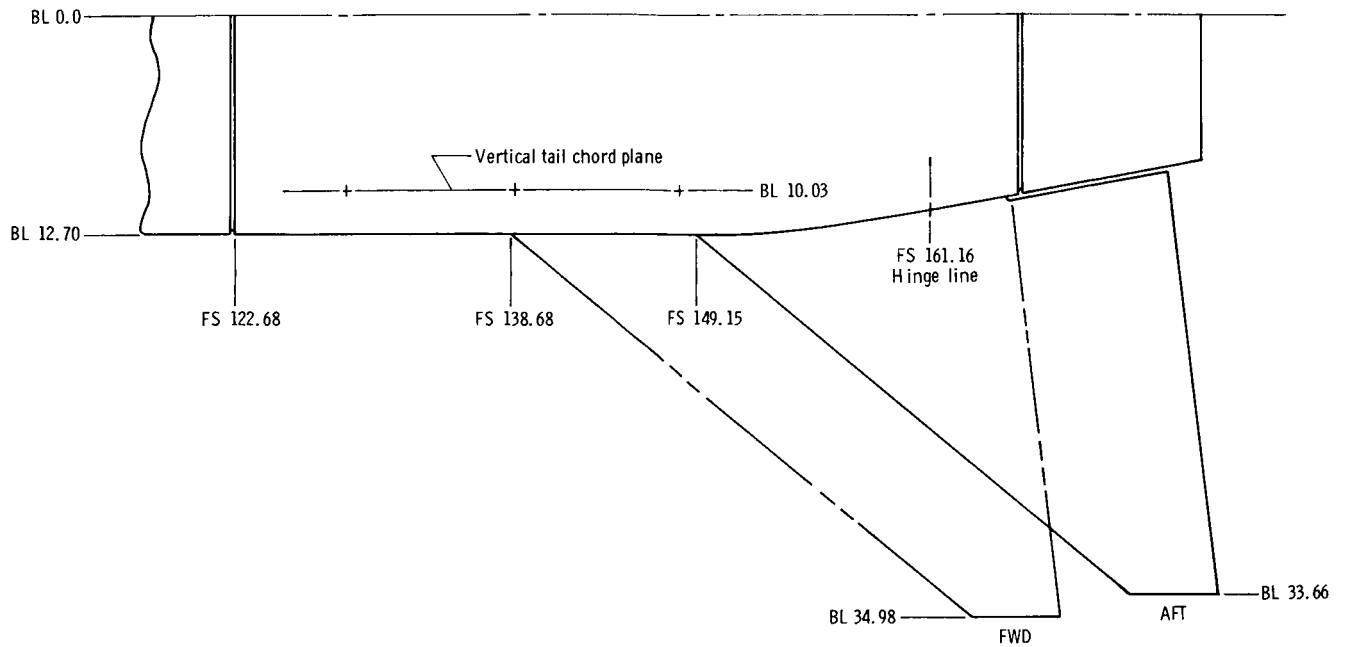


Figure 4. Location of horizontal and vertical tails.

Horizontal Tail Geometry

Airfoil sections	
Tip	NACA 64-002.5
Root	NACA 64-005.5
Tip chord, cm	5.08
Root chord, cm	28.96
Taper ratio175
Span, cm	
Mid on body	68.58
Aft on body	67.51
Planform area (one side exposed, filler excluded), m ²0372
Aspect ratio (exposed, filler excluded)	2.564
$\Lambda_{1/4}$, deg	50.0

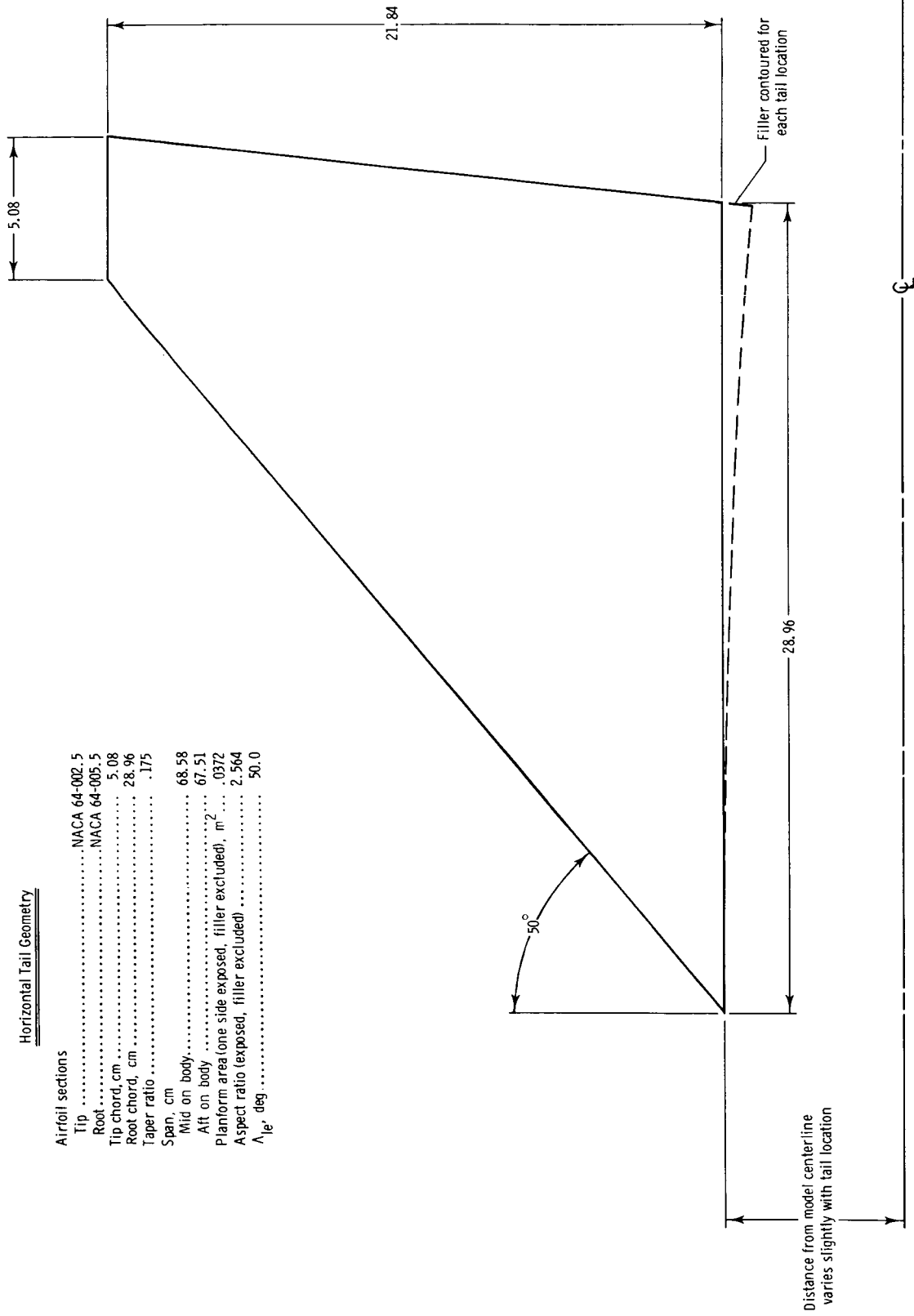


Figure 5. Horizontal tail geometry. All linear dimensions are in centimeters.

Twin Vertical Tail Geometry

Airfoil sections

Tip	NACA 64-003.5
Root	NACA 64-005
Tip chord, cm	9.14
Root chord, cm	24.38
Taper ratio375
Tail height (root to tip), cm	25.40
Planform area (one side exposed, filler excluded), m ²0426
Aspect ratio (exposed, filler excluded)	1.514
Λ_{le} , deg	36.52

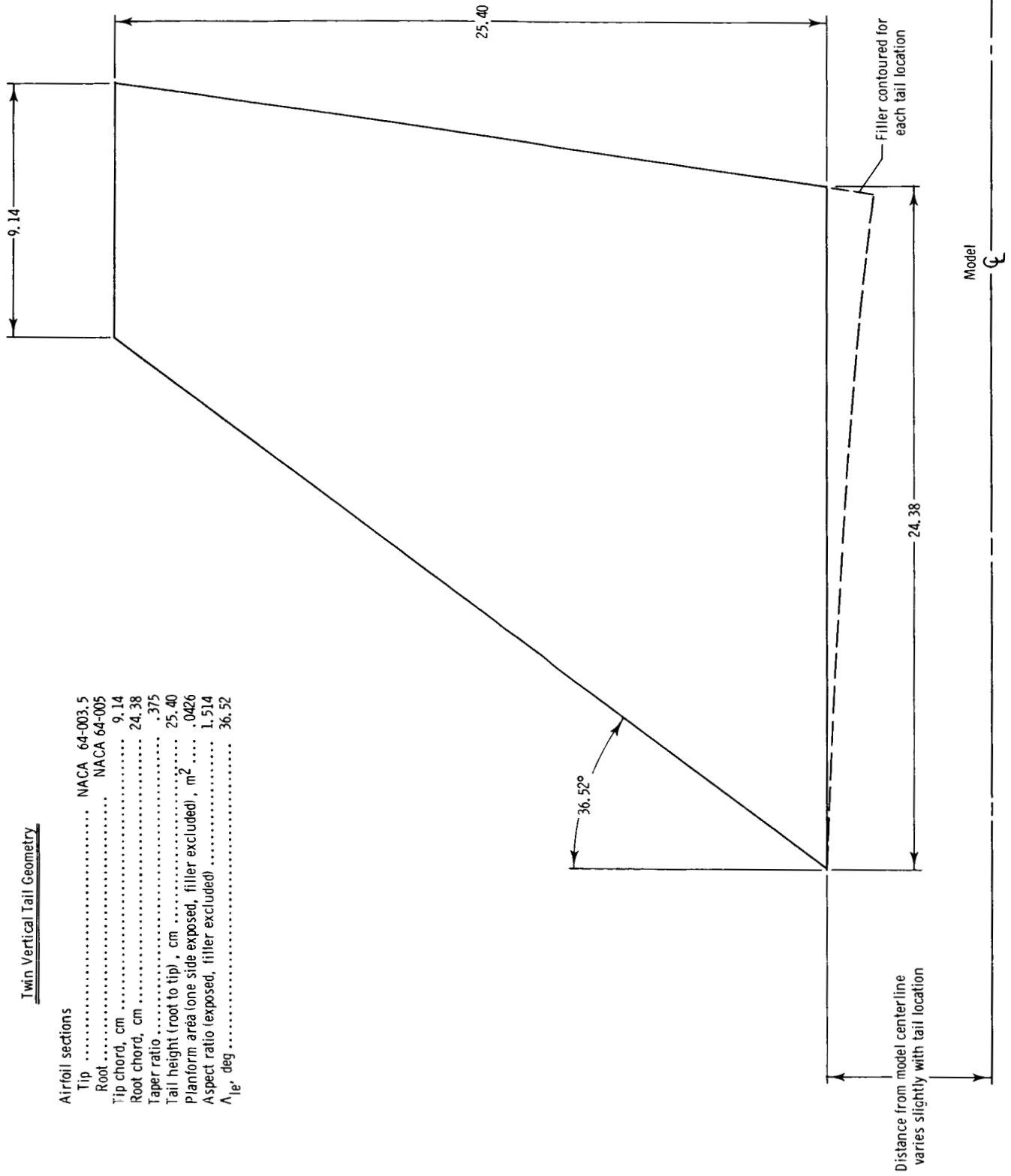


Figure 6. Vertical tail geometry. All linear dimensions are in centimeters.

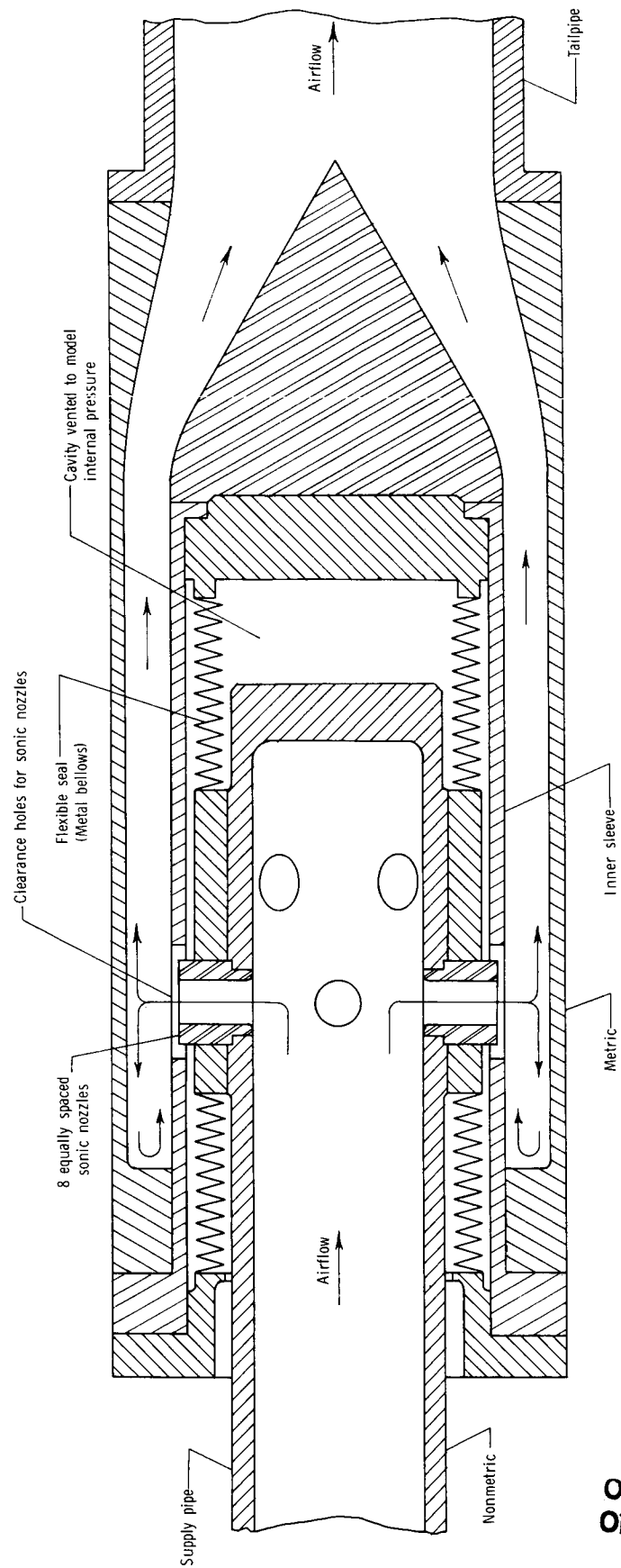


Figure 7. Details of bellows arrangement used to transfer air from nonmetric to metric portions of model.

ORIGINAL PAGE IS
OF POOR QUALITY

ORIGINAL PAGE IS
OF POOR QUALITY

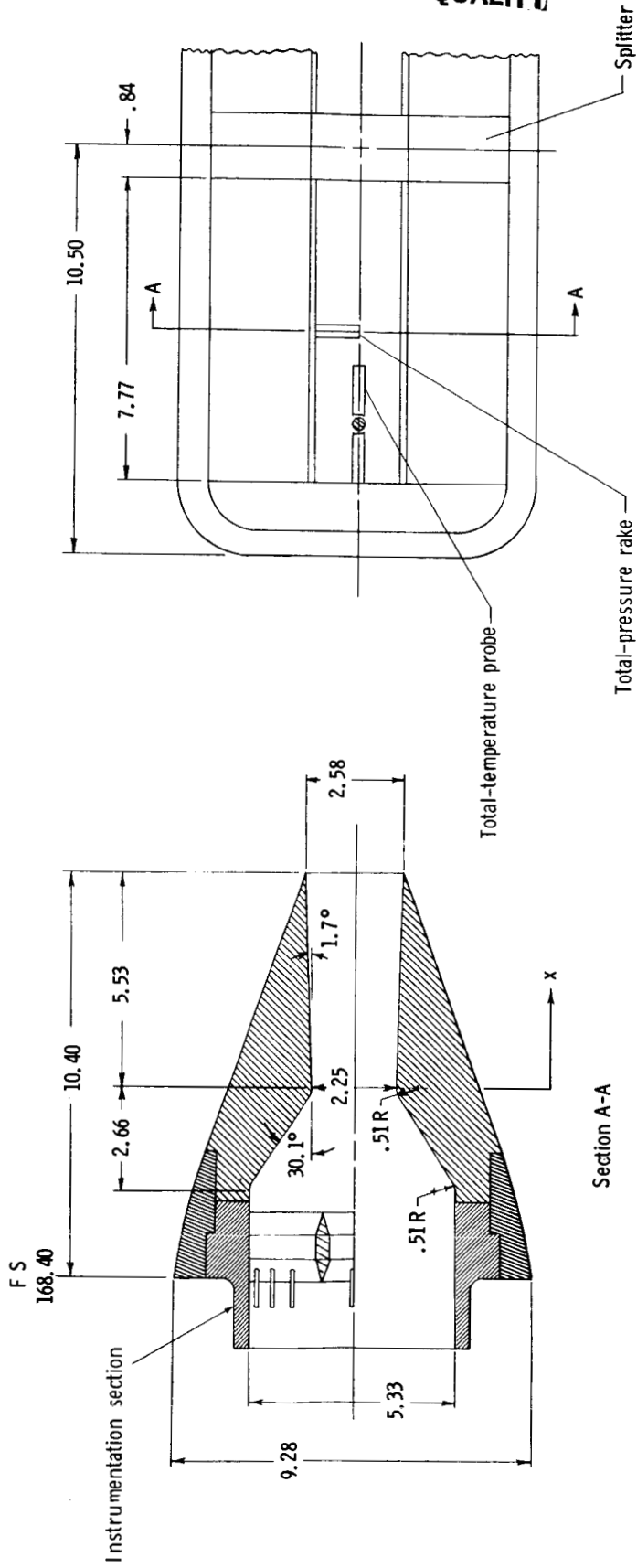
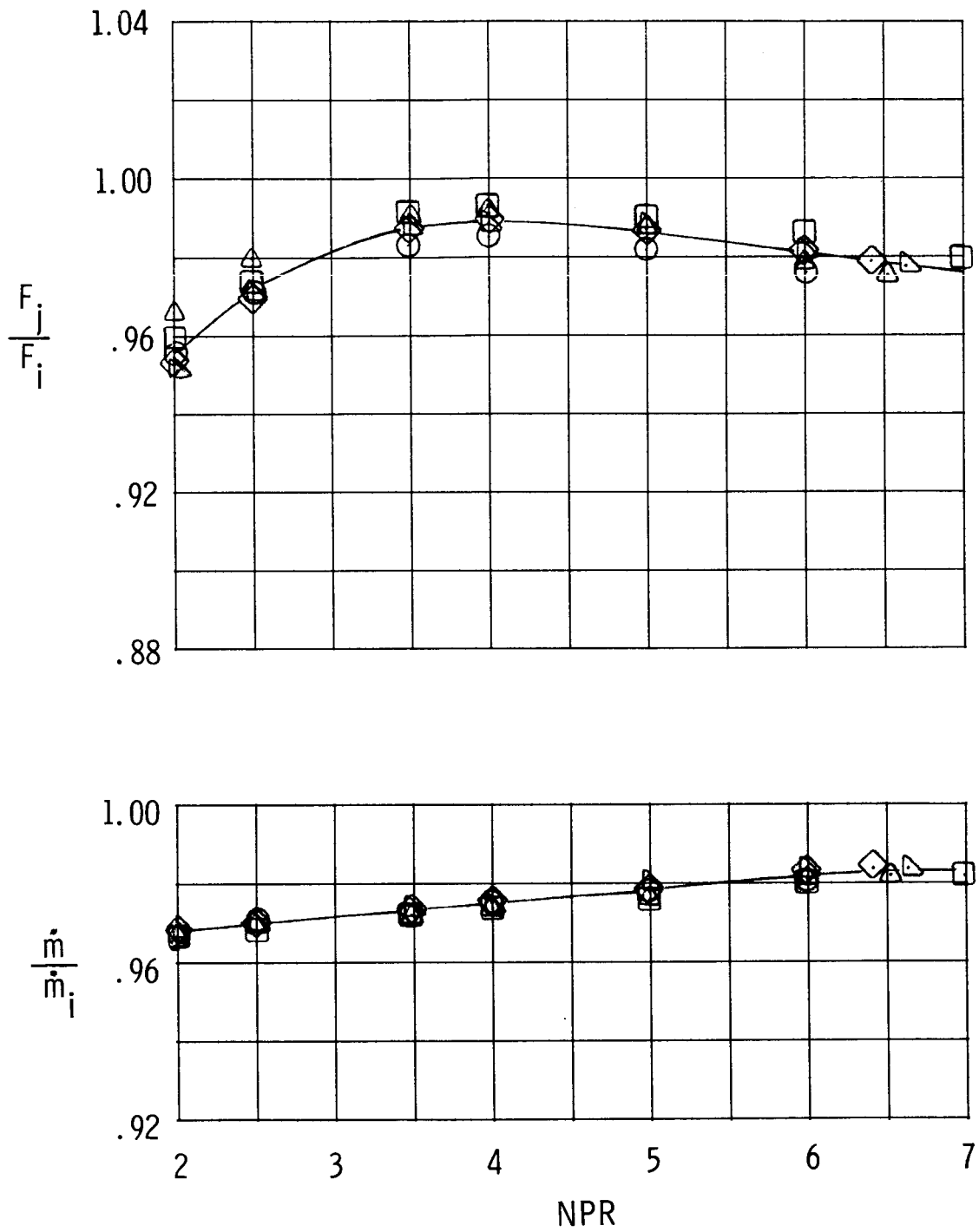
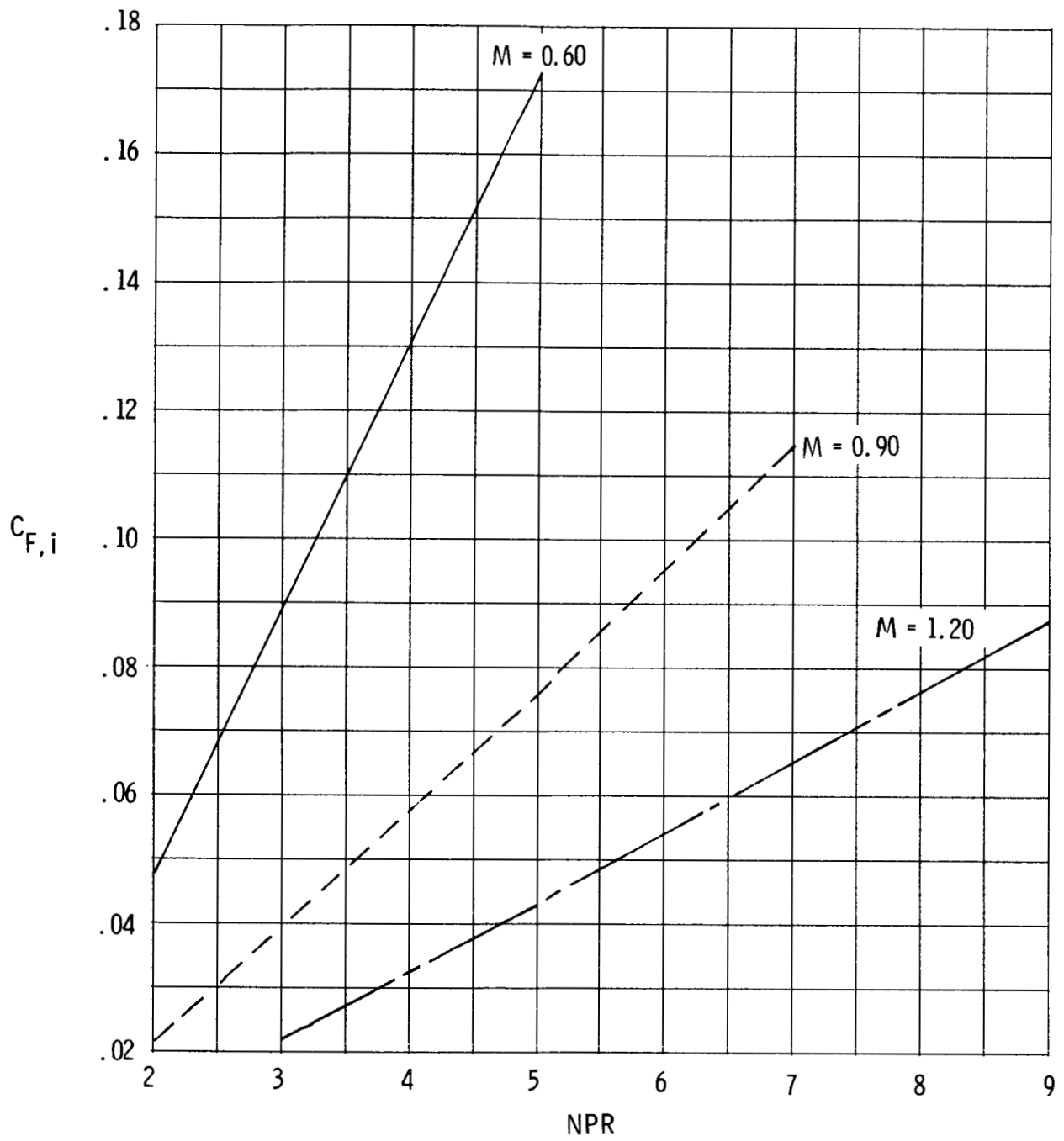


Figure 8. Nonaxisymmetric nozzle. All linear dimensions are in centimeters.



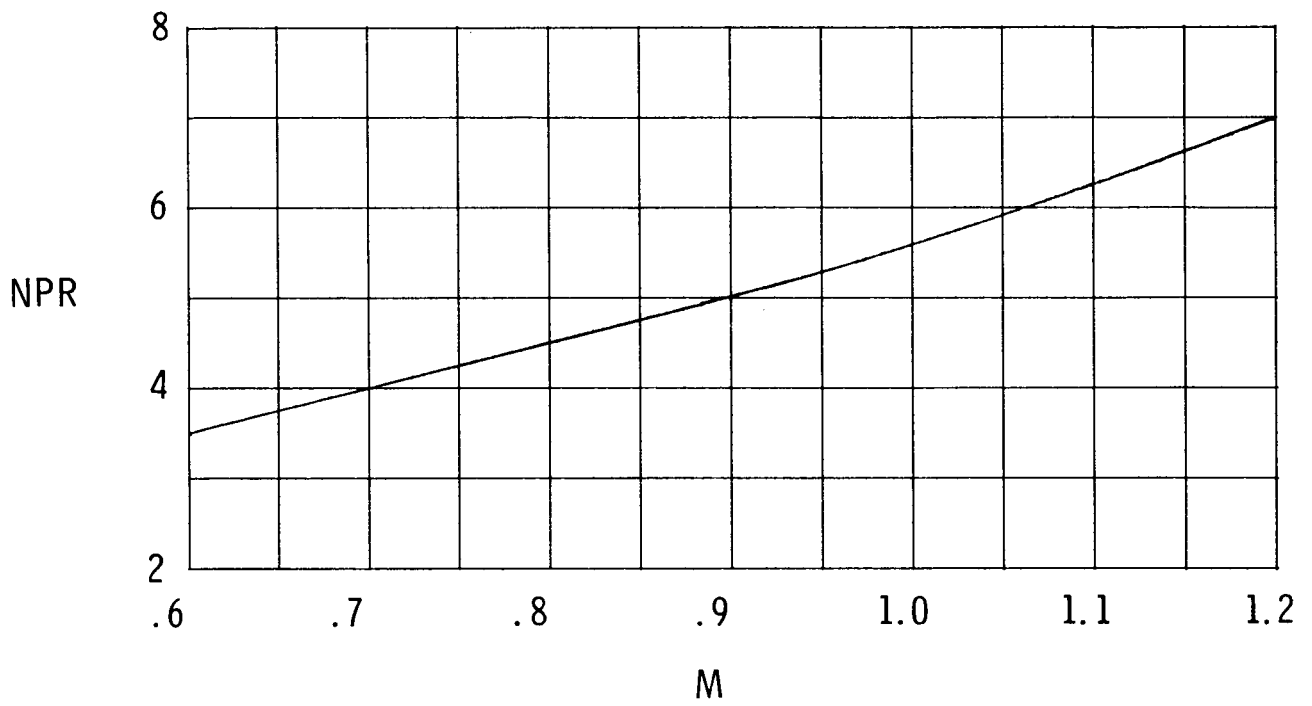
(a) Static performance.

Figure 9. Nozzle characteristics.



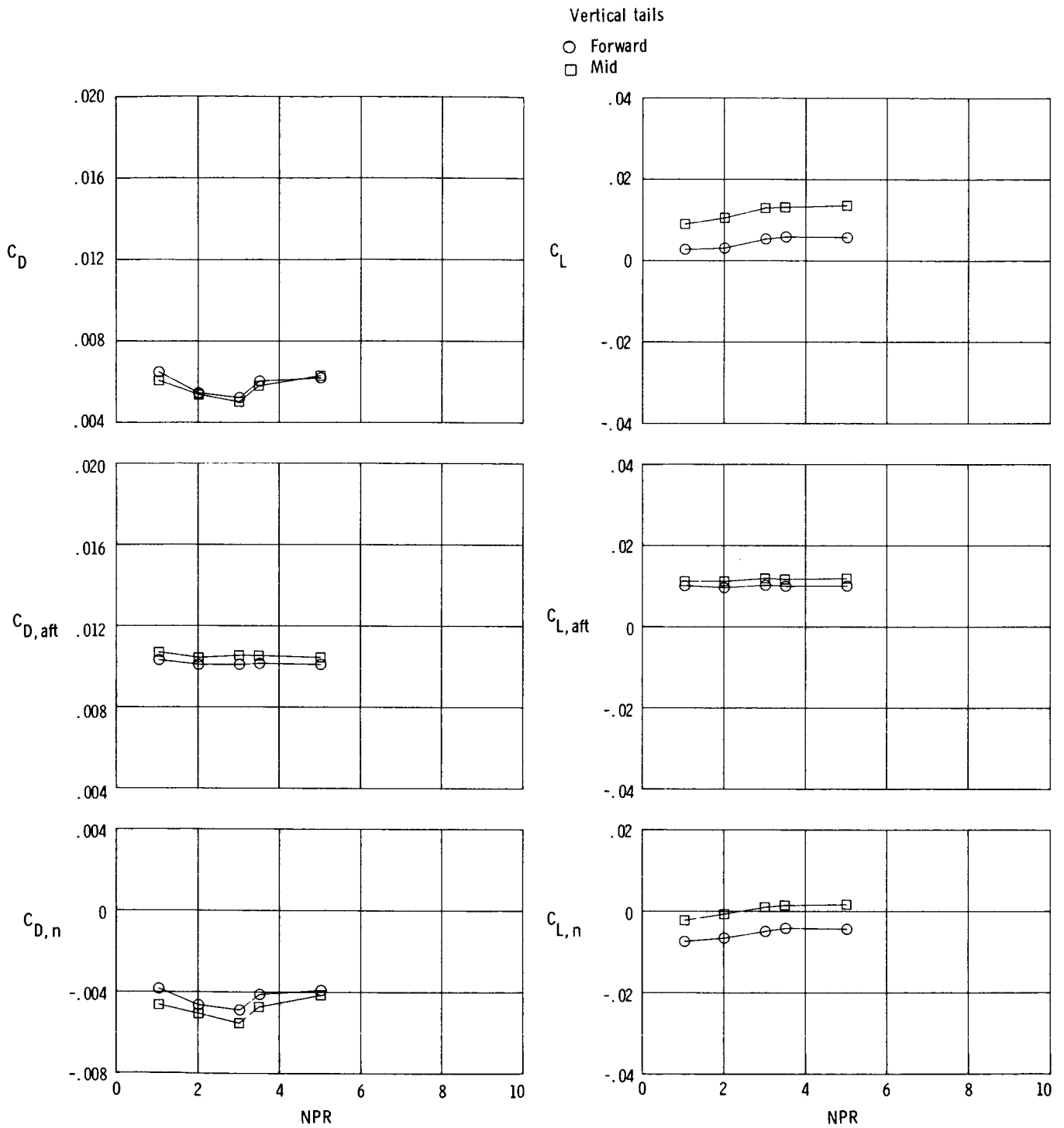
(b) Ideal thrust coefficients.

Figure 9. Continued.



(c) Scheduled nozzle pressure ratios.

Figure 9. Concluded.

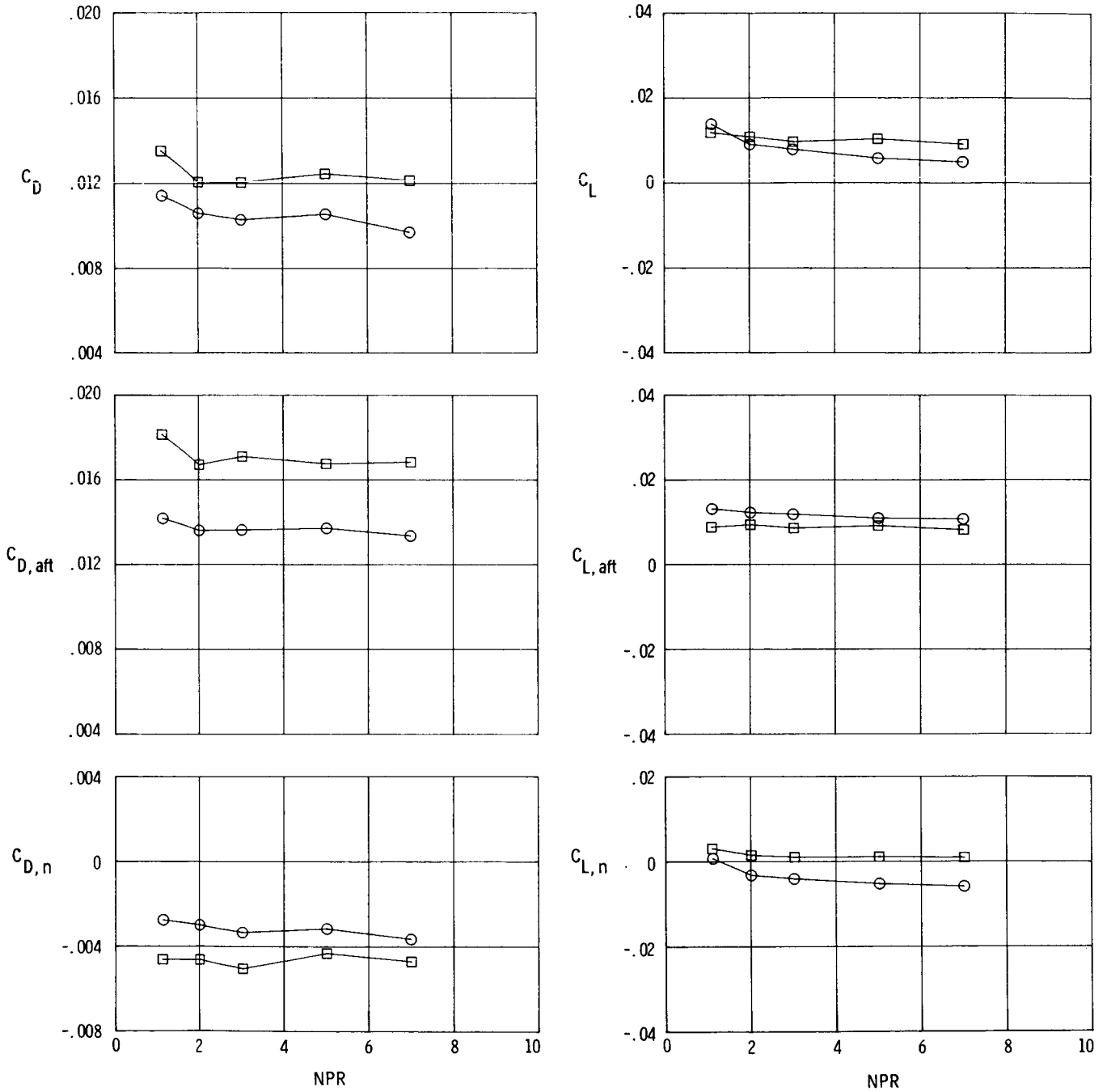


(a) $M = 0.60$.

Figure 10. Effect of vertical tail position on afterbody aerodynamic characteristics for horizontal tails mid, $\phi_t = 0^\circ$, and $\alpha = 0^\circ$.

Vertical tails

- Forward
- Mid

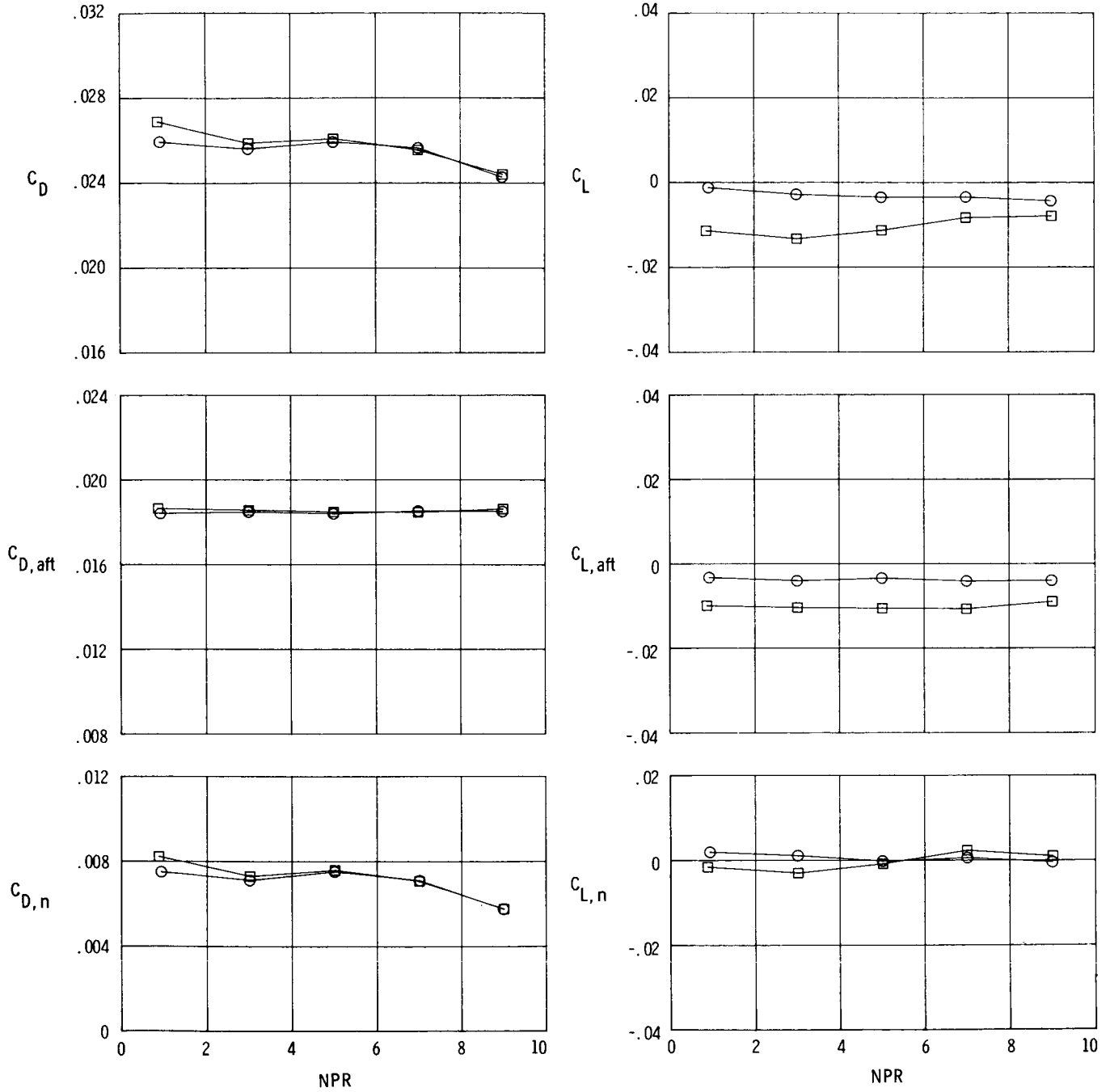


(b) $M = 0.90$.

Figure 10. Continued.

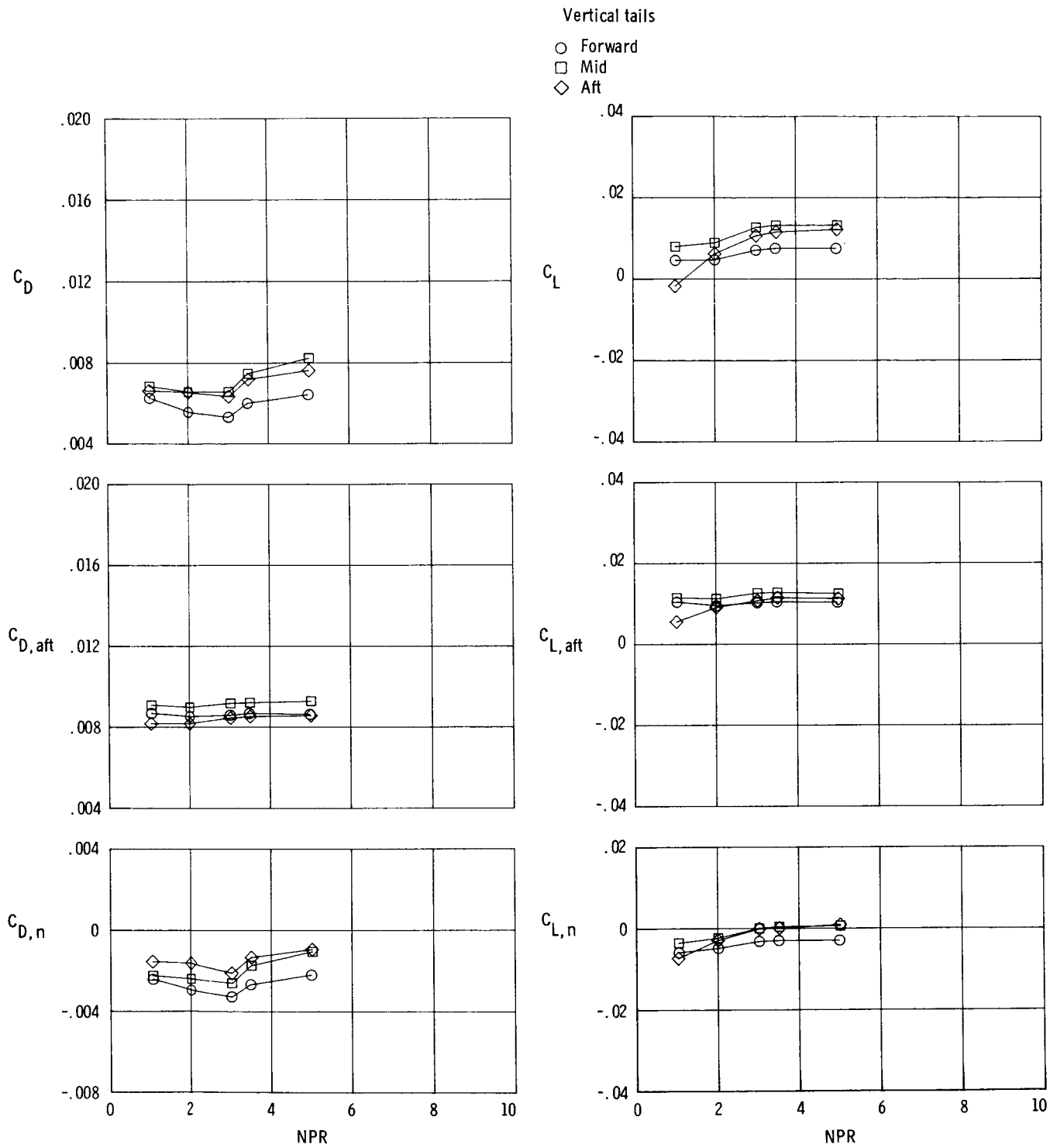
Vertical tails

○ Forward
□ Mid



(c) $M = 1.20$.

Figure 10. Concluded.

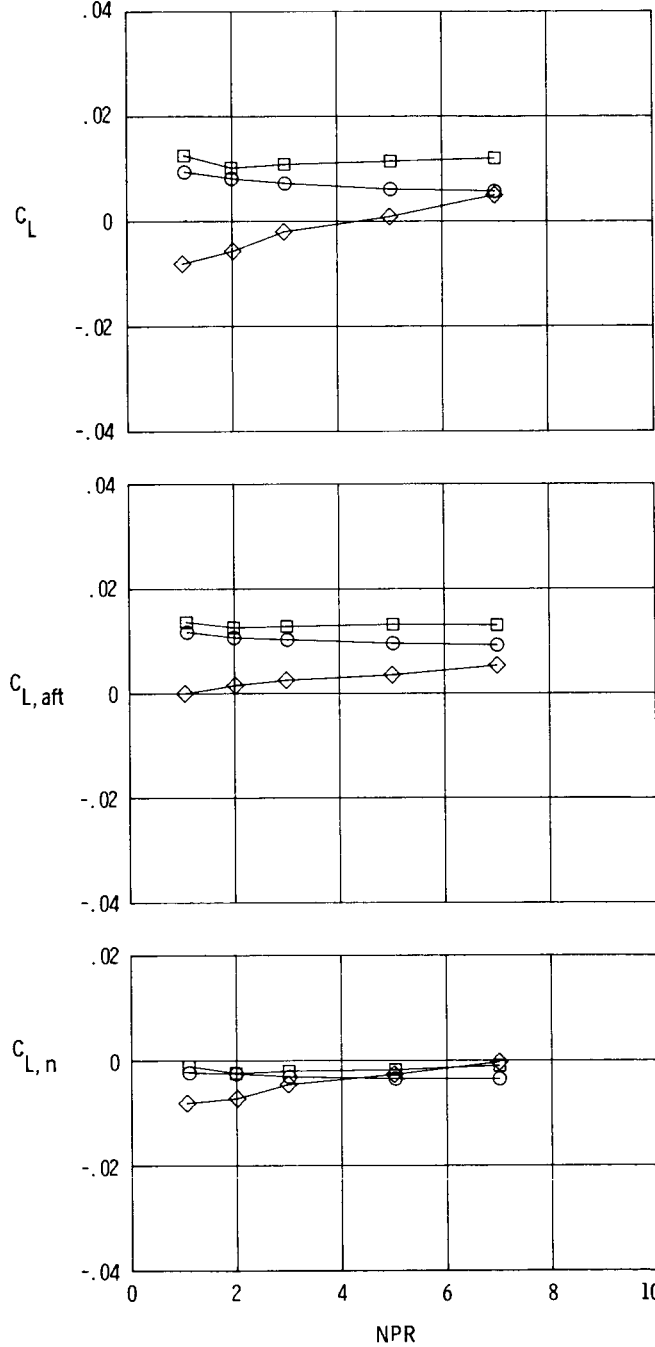
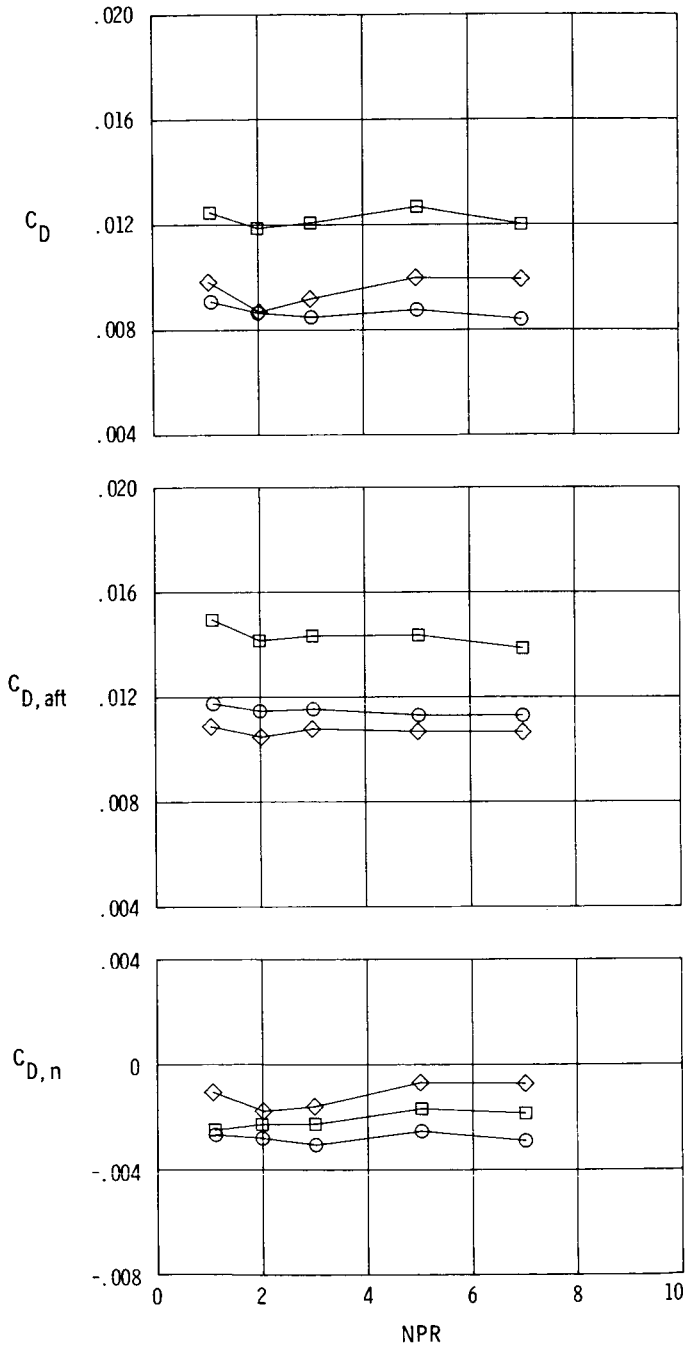


(a) $M = 0.60$.

Figure 11. Effect of vertical tail position on afterbody aerodynamic characteristics for horizontal tails aft, $\phi_t = 0^\circ$, and $\alpha = 0^\circ$.

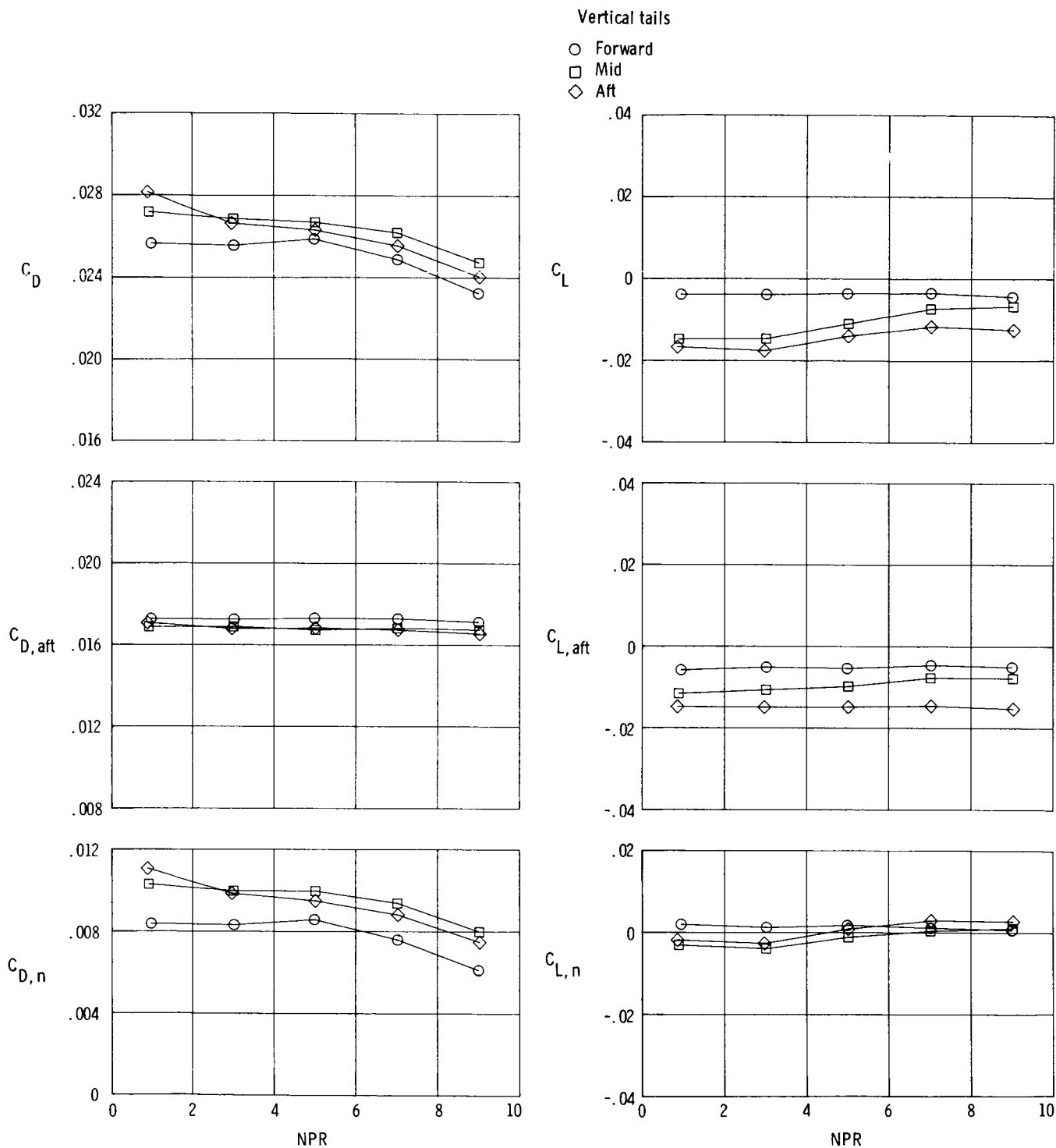
Vertical tails

- Forward
- Mid
- ◇ Aft



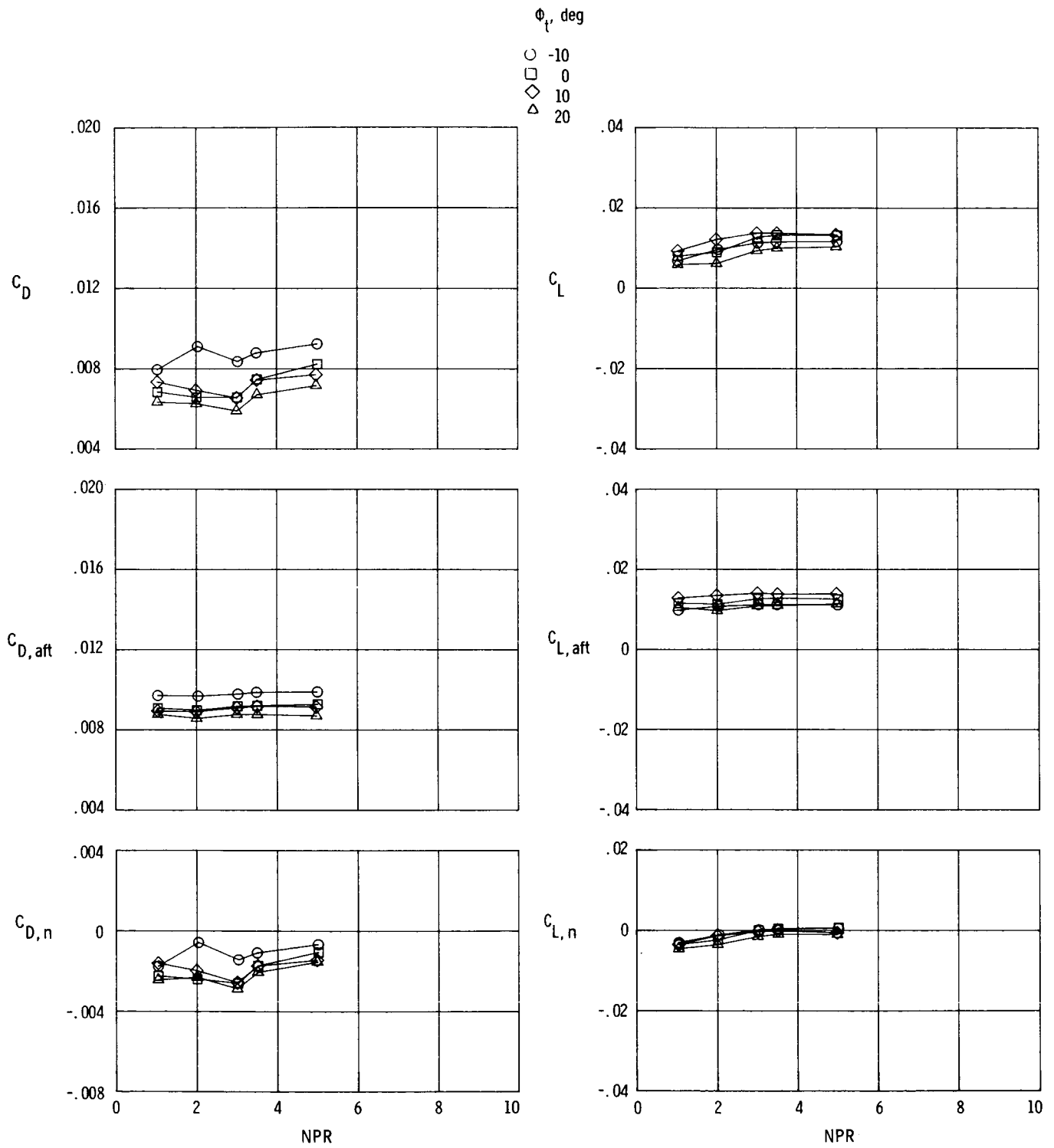
(b) $M = 0.90$.

Figure 11. Continued.



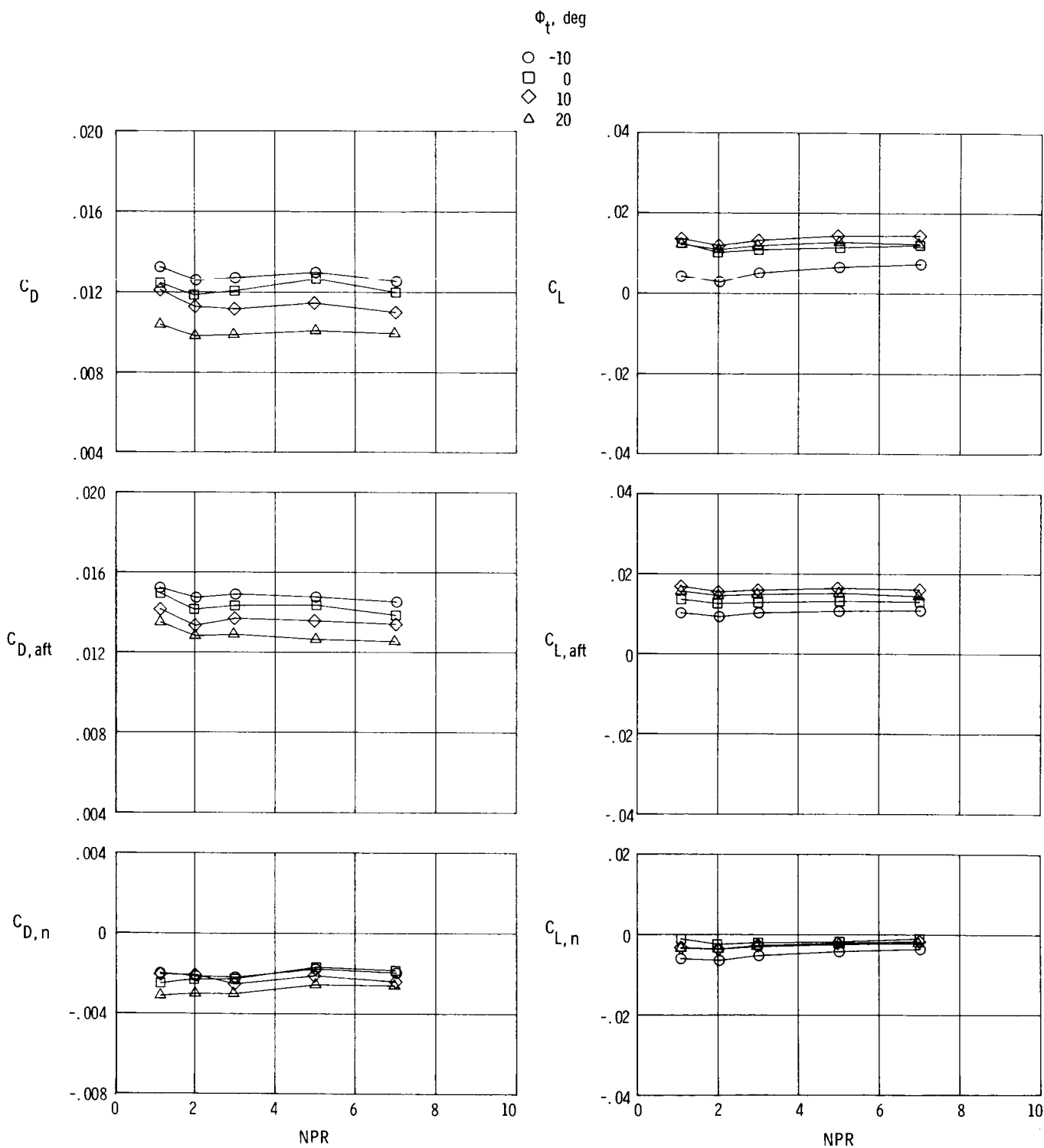
(c) $M = 1.20$.

Figure 11. Concluded.



(a) $M = 0.60$.

Figure 12. Effect of vertical tail cant angle on afterbody aerodynamic characteristics for horizontal tails aft, vertical tails mid, and $\alpha = 0^\circ$.

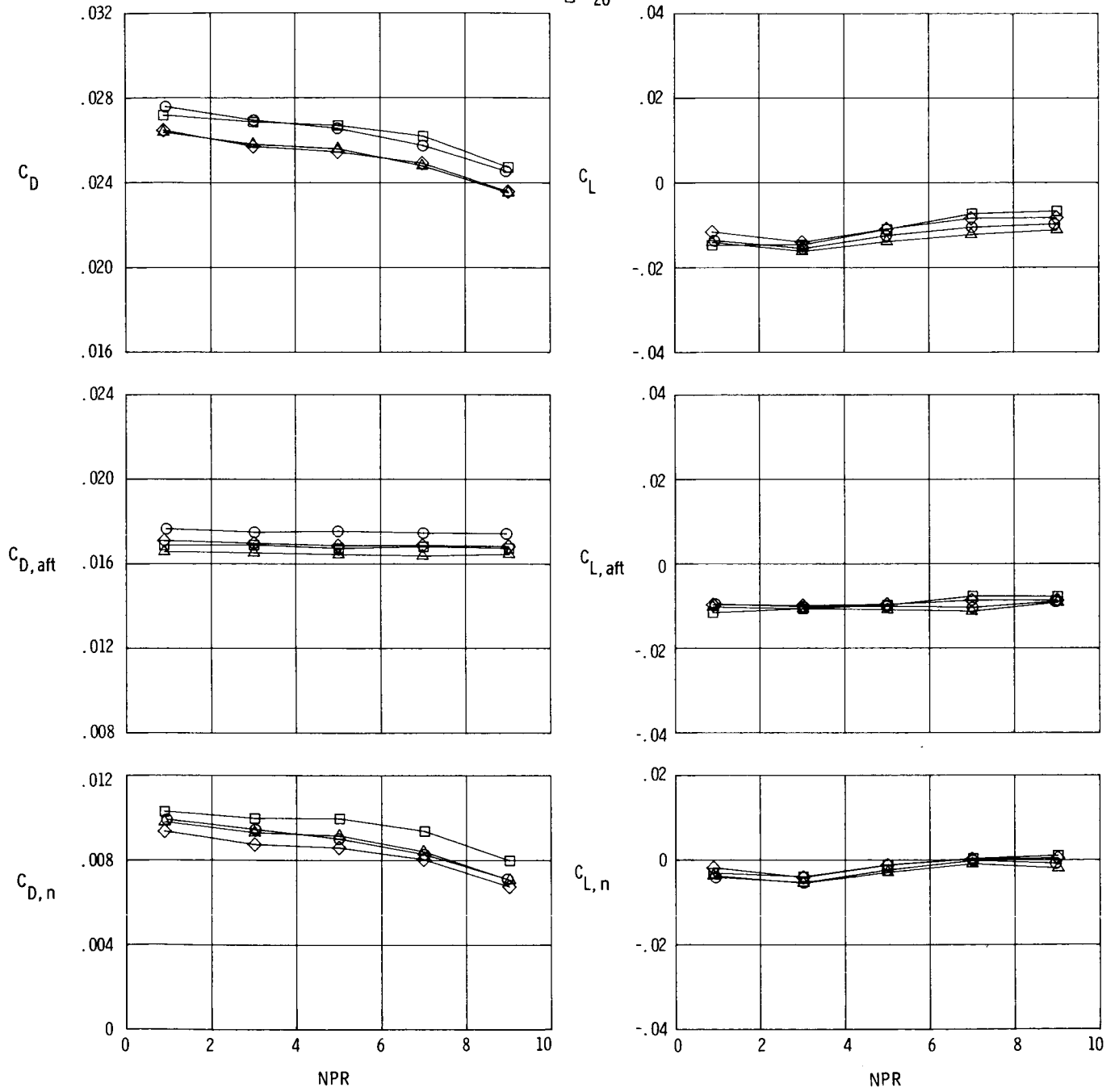


(b) $M = 0.90$.

Figure 12. Continued.

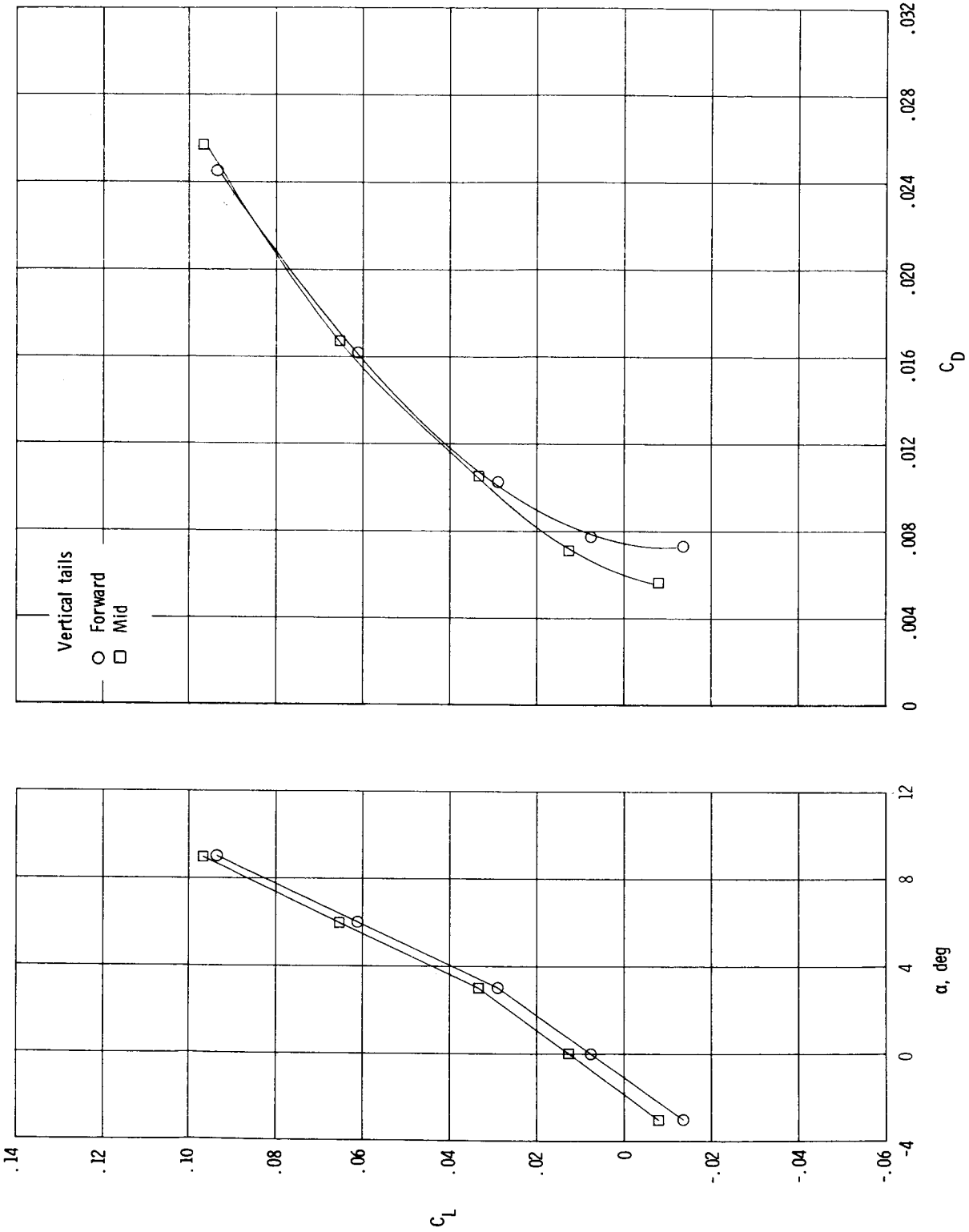
ϕ_i , deg

- -10
- 0
- ◇ 10
- △ 20



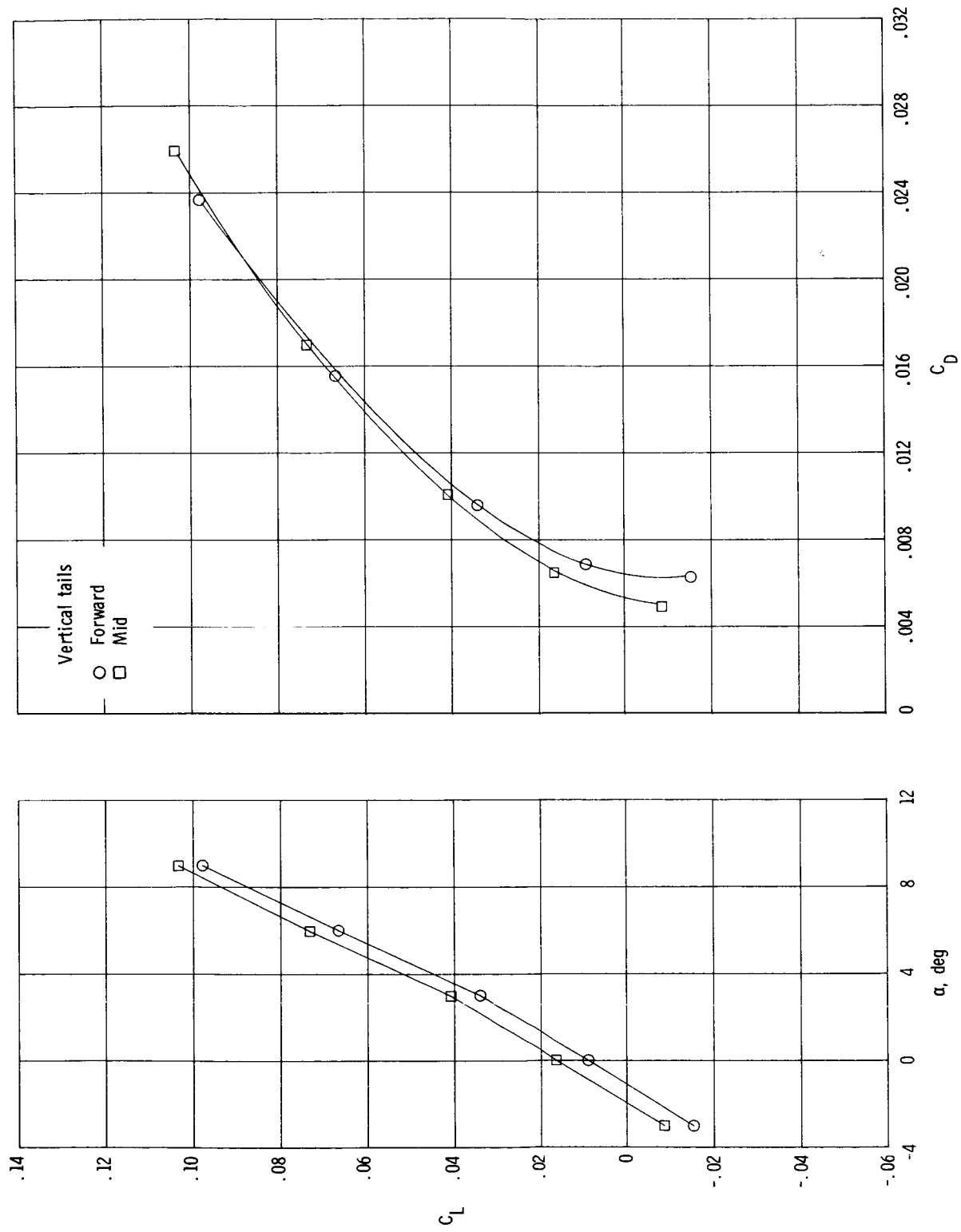
(c) $M = 1.20$.

Figure 12. Concluded.



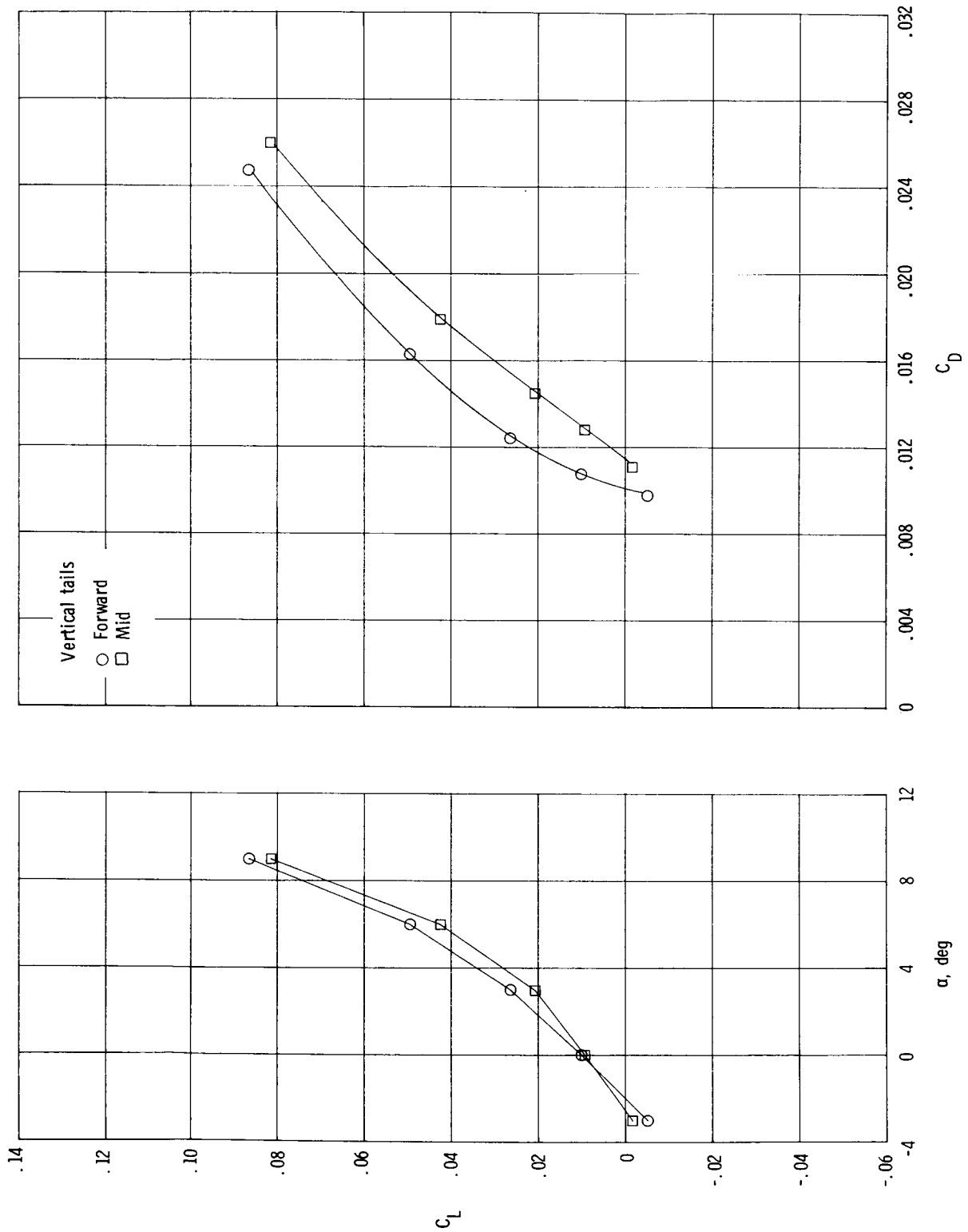
(a) $M = 0.60$; $NPR = 1.0$.

Figure 13. Effect of vertical tail position on total aft-end aerodynamic characteristics for horizontal tails mid and $\phi_t = 0^\circ$.



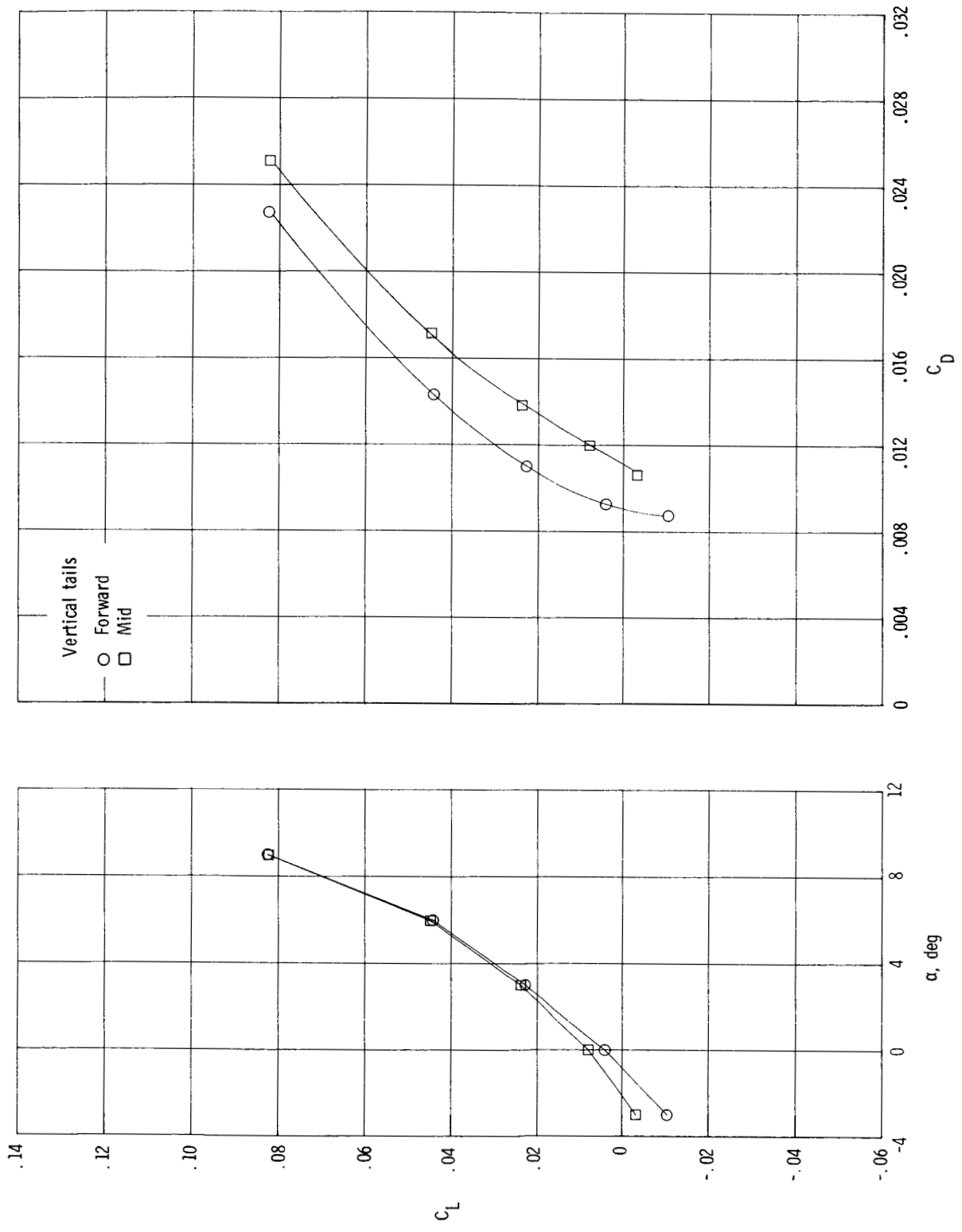
(b) $M = 0.60$; $NPR = 3.5$.

Figure 13. Continued.



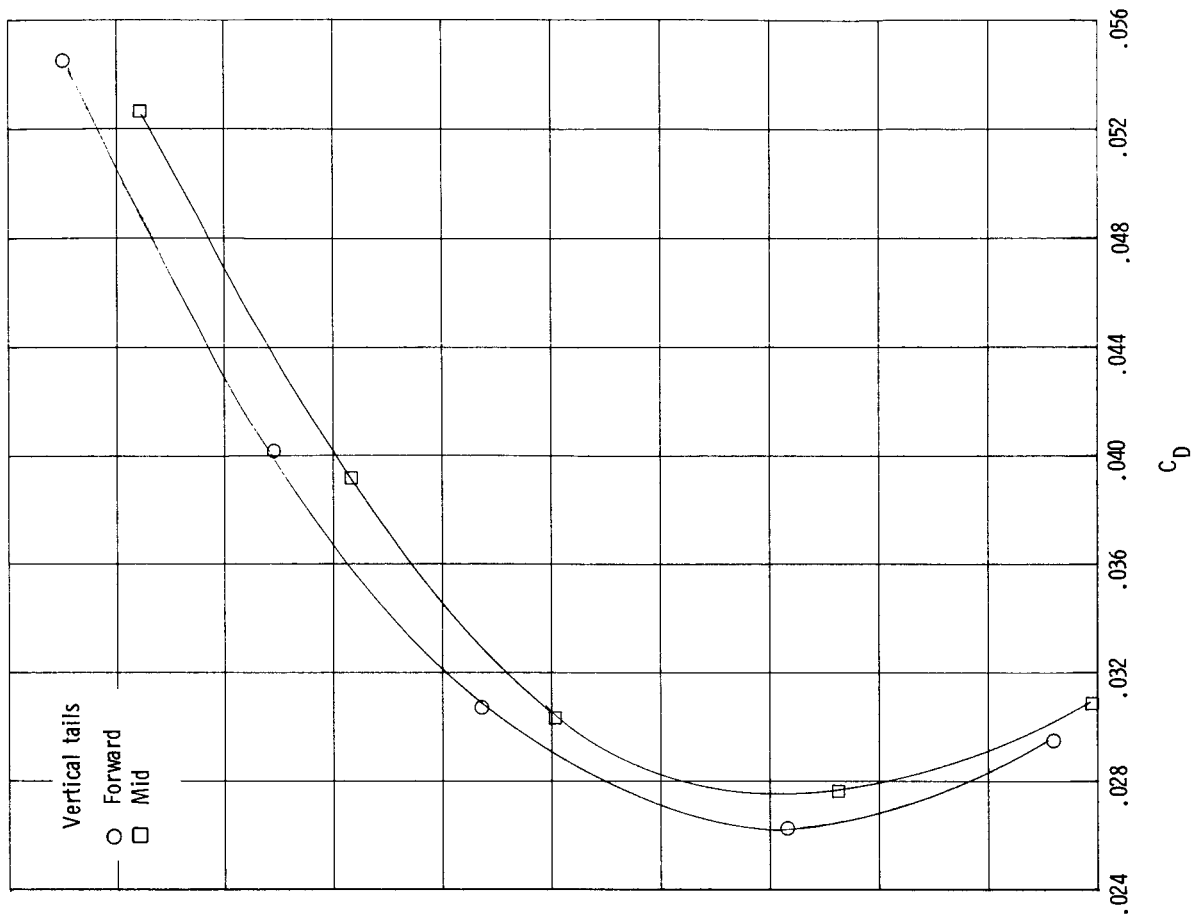
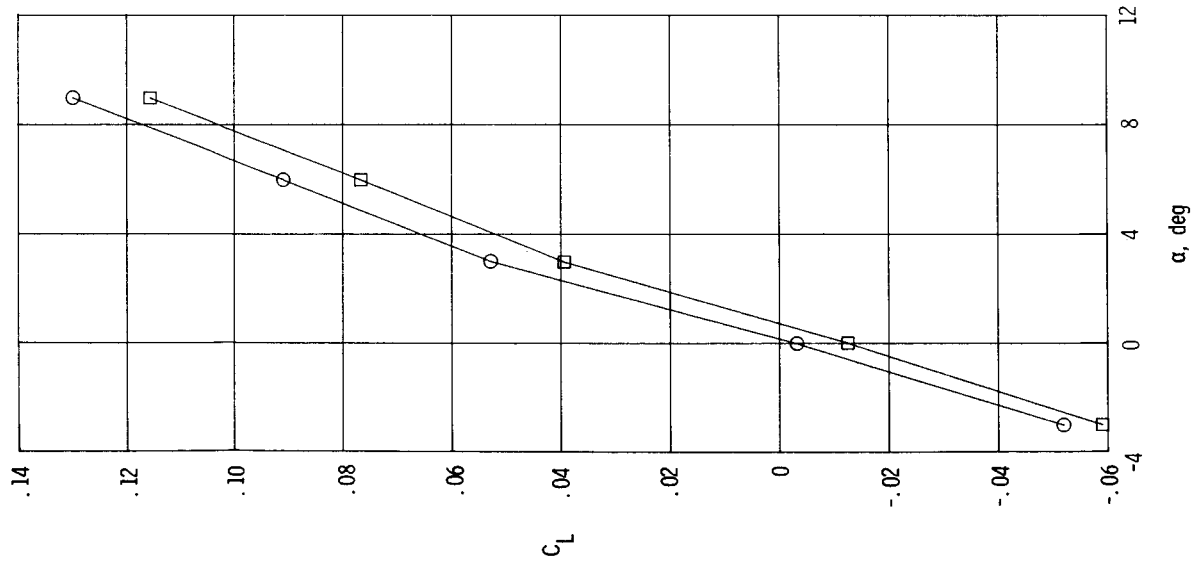
(c) $M = 0.90$; $NPR = 1.0$.

Figure 13. Continued.



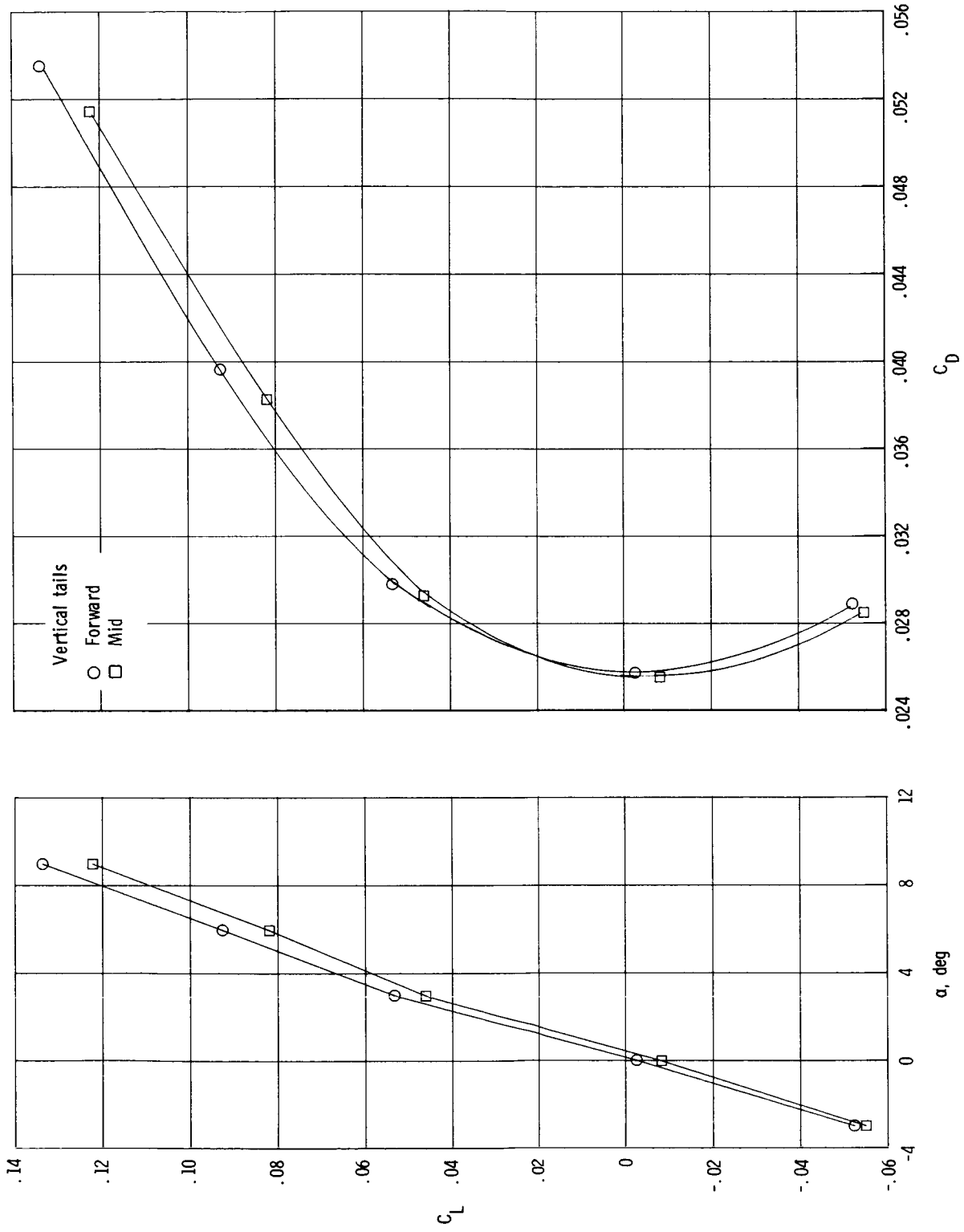
(d) $M = 0.90$; $NPR = 5.0$.

Figure 13. Continued.



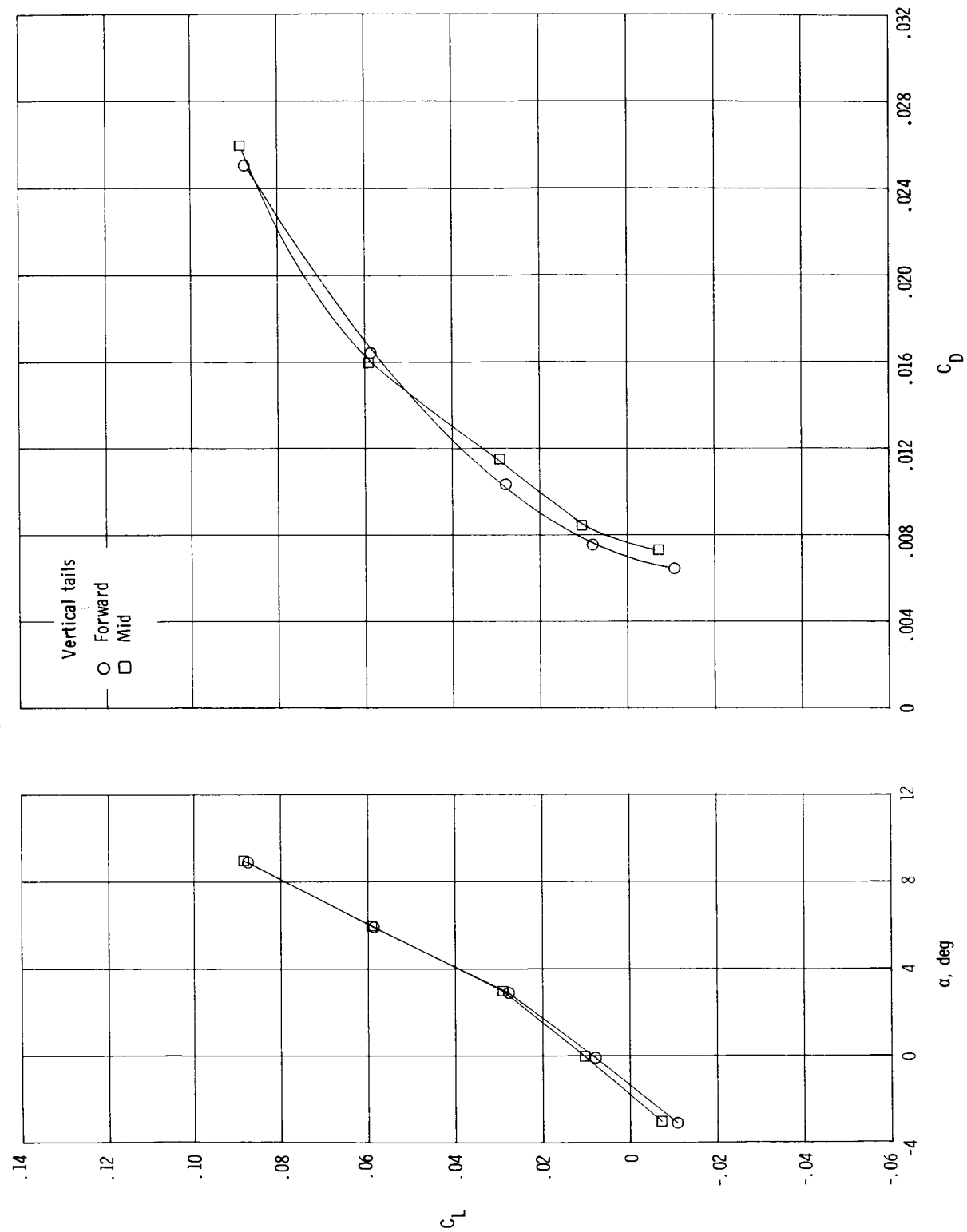
(e) $M = 1.20$; $NPR = 1.0$.

Figure 13. Continued.



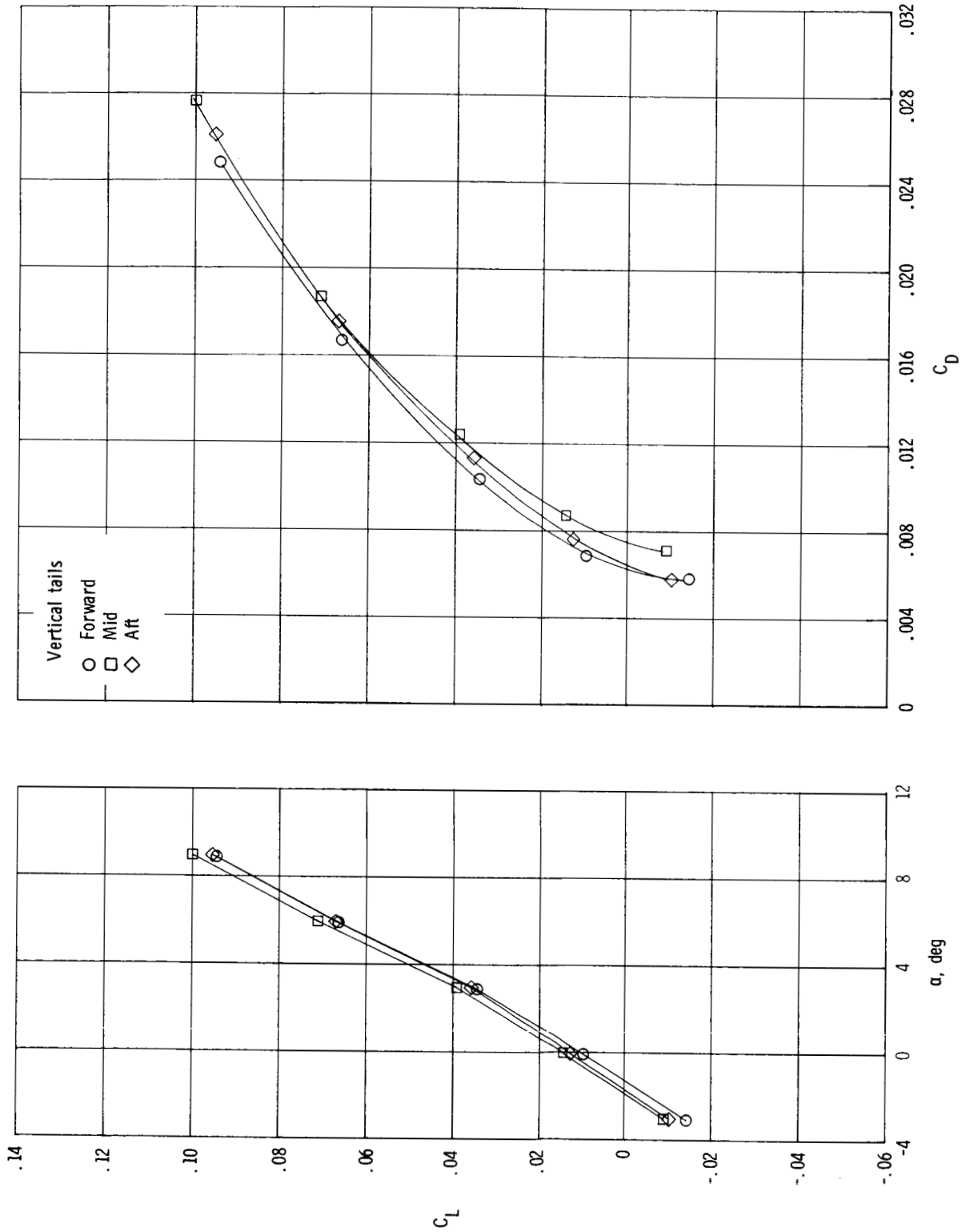
(f) $M = 1.20$; $NPR = 7.0$.

Figure 13. Concluded.



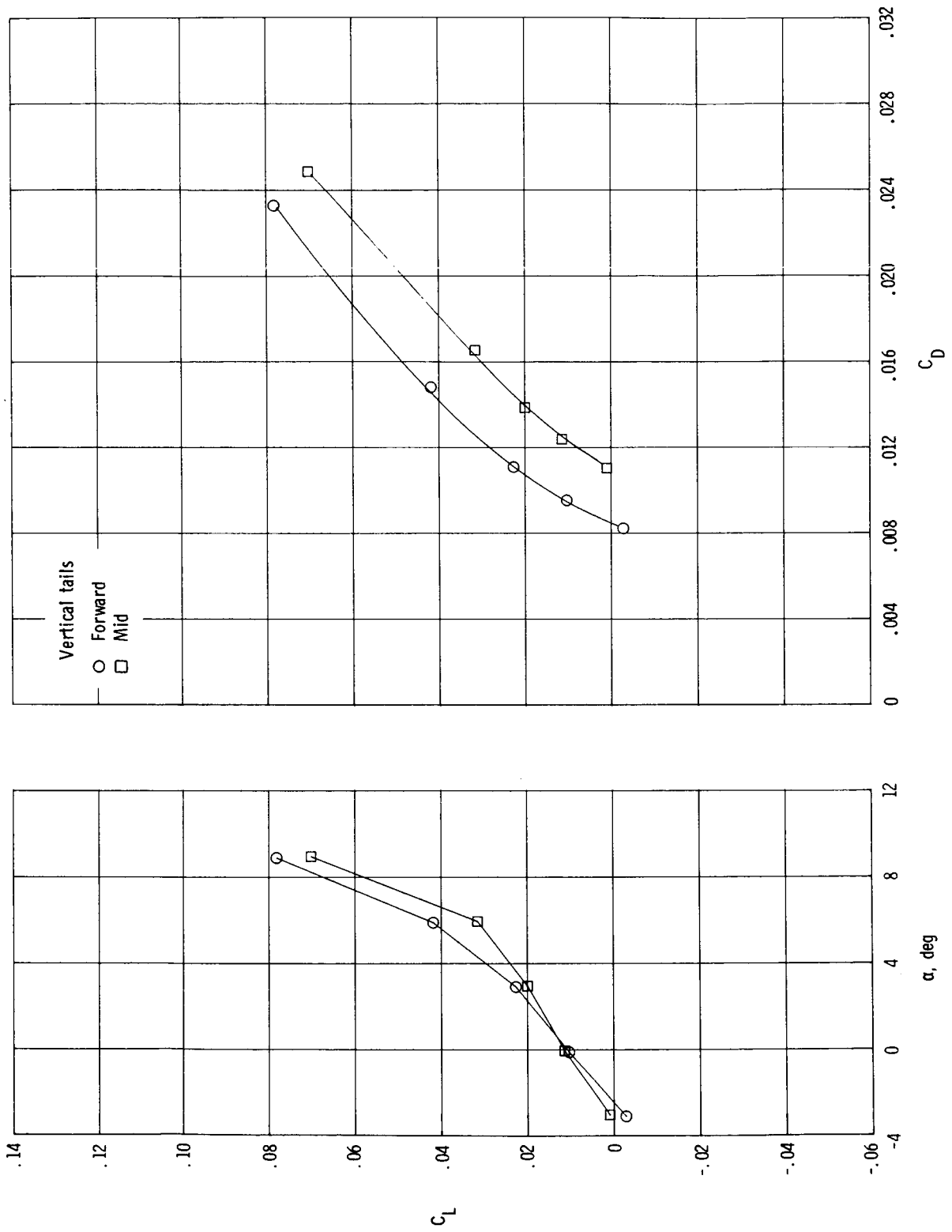
(a) $M = 0.60$; $NPR = 1.0$.

Figure 14. Effect of vertical tail position on total aft-end aerodynamic characteristics for horizontal tails aft and $\phi_t = 0^\circ$.



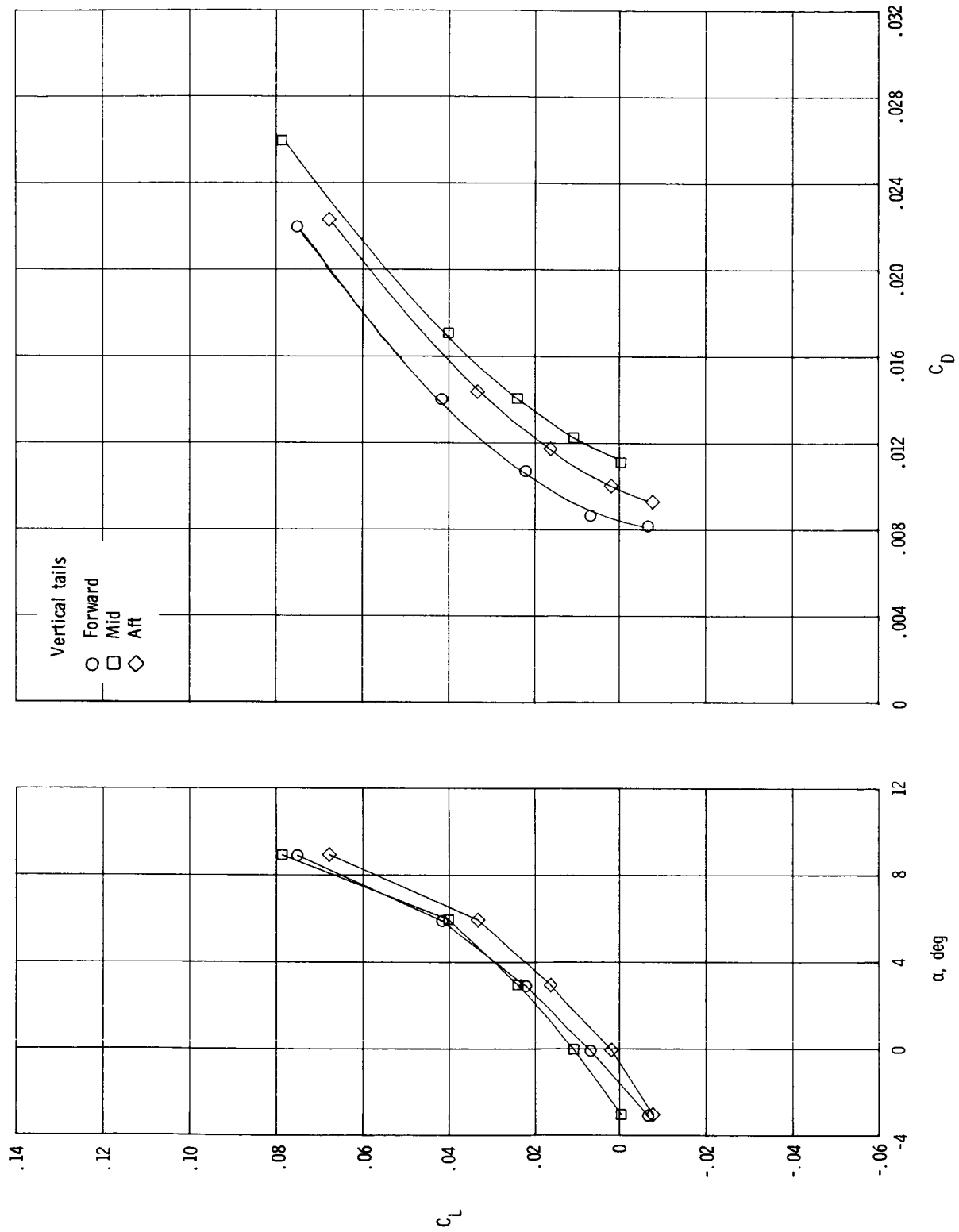
(b) $M = 0.60$; NPR = 3.5.

Figure 14. Continued.



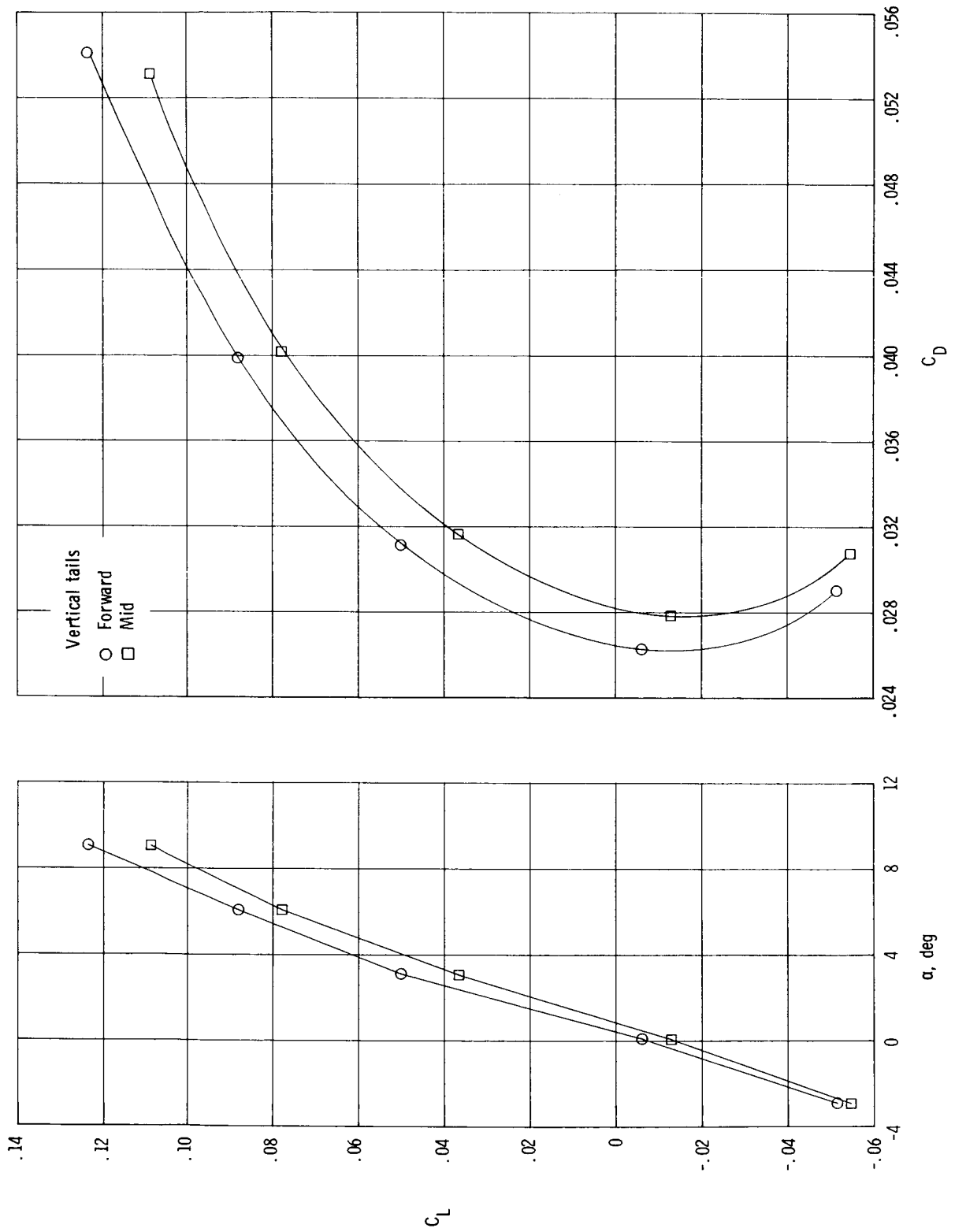
(c) $M = 0.90$; NPR = 1.0.

Figure 14. Continued.



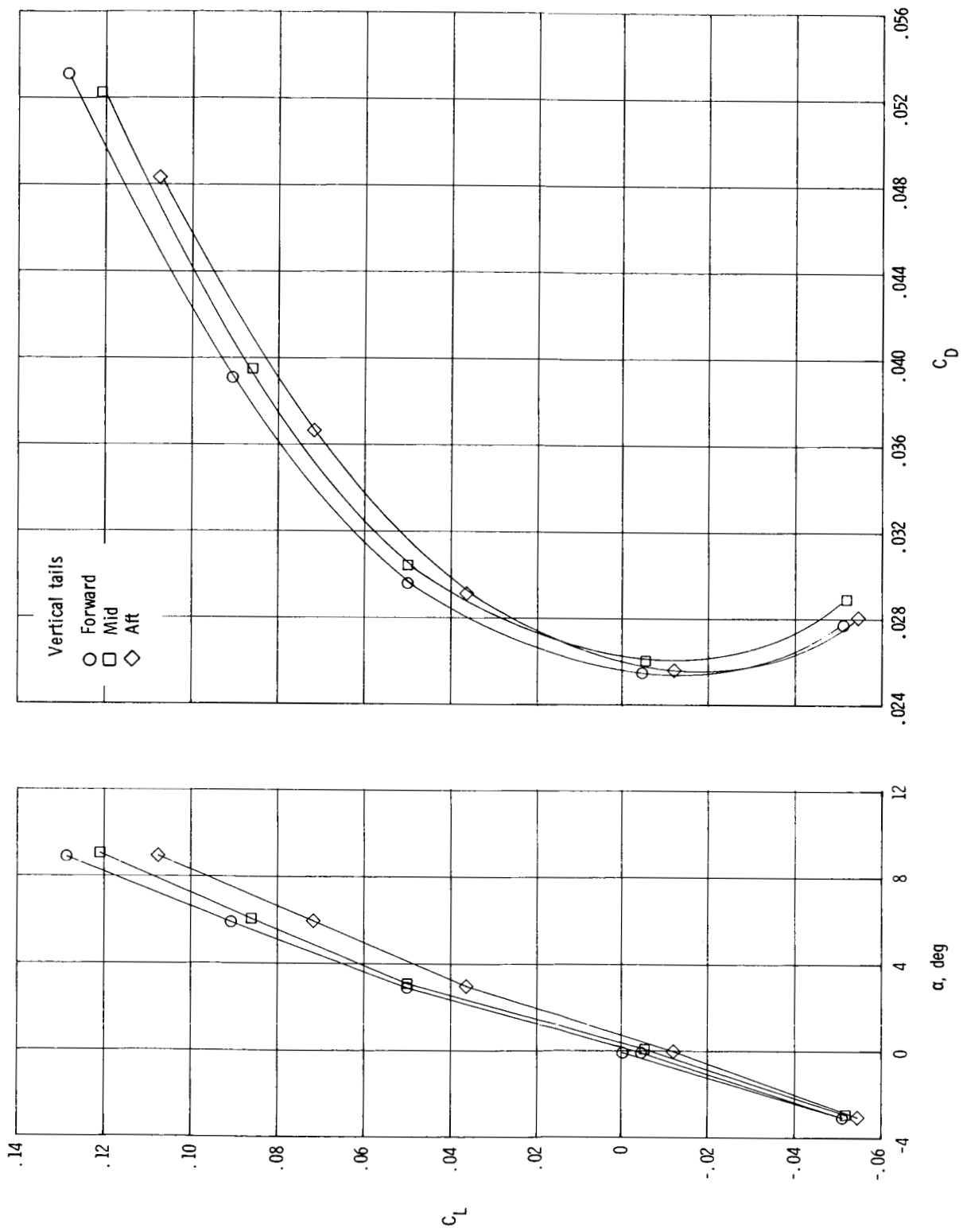
(d) $M = 0.90$; $NPR = 5.0$.

Figure 14. Continued.



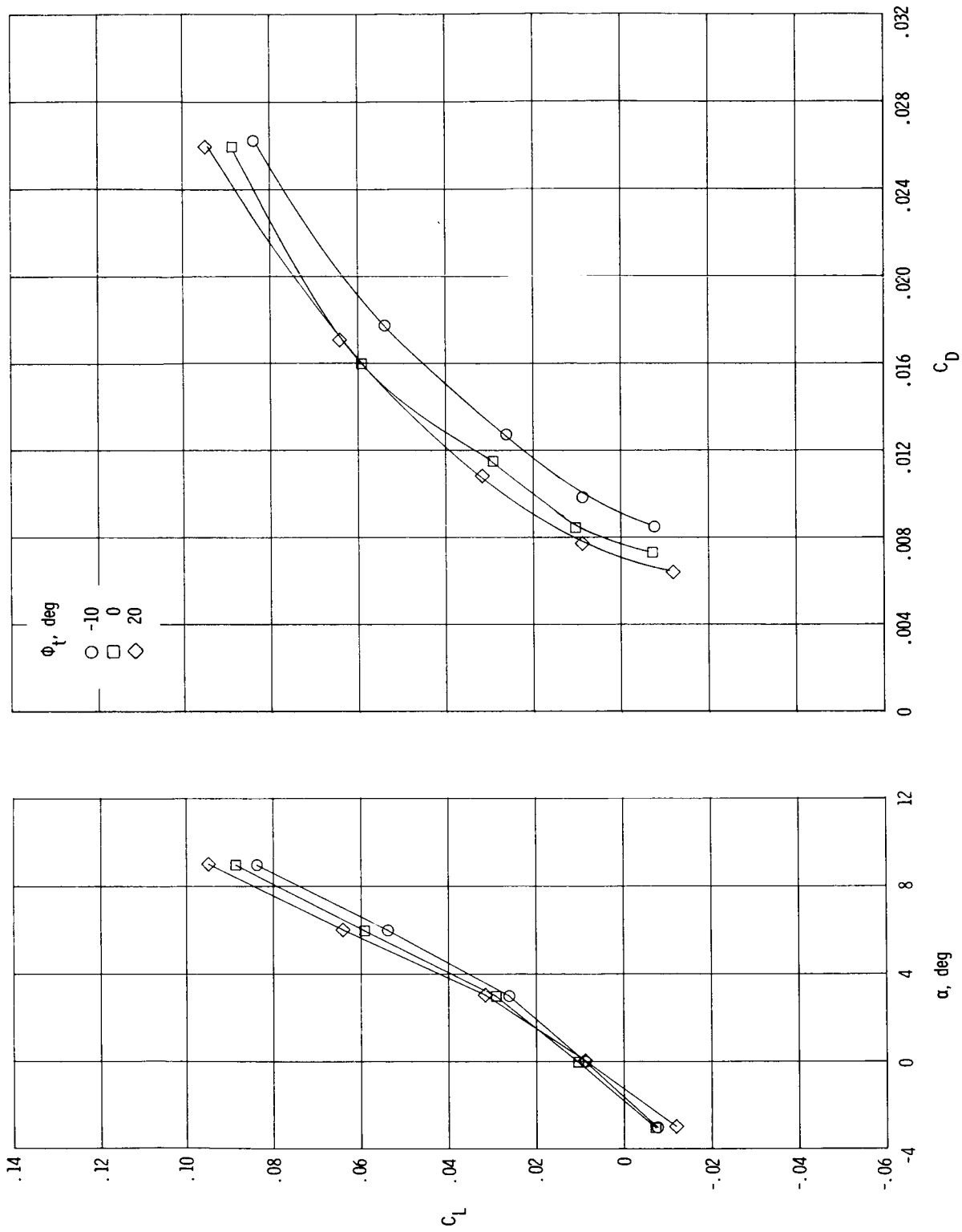
(e) $M = 1.20$; $NPR = 1.0$.

Figure 14. Continued.



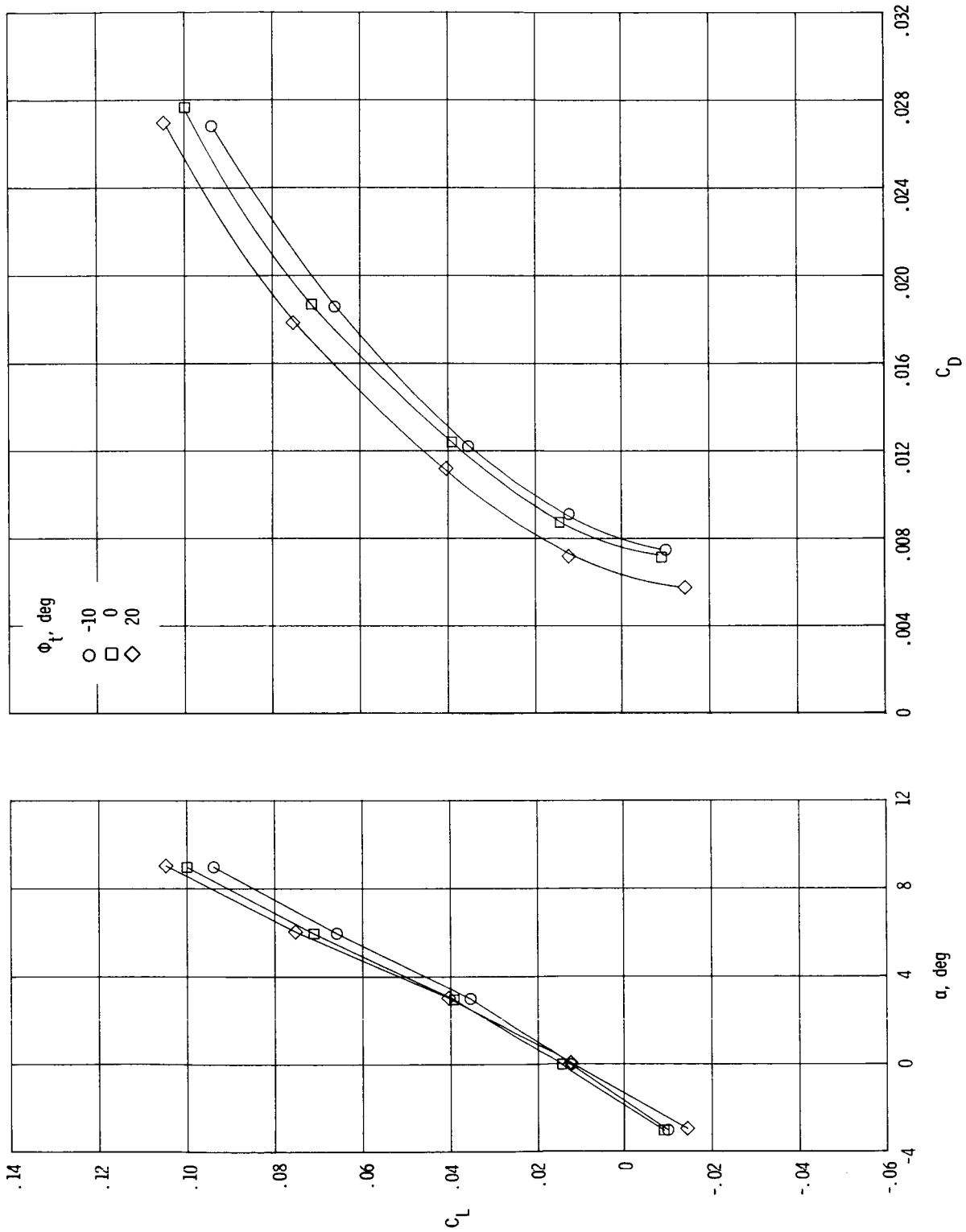
(f) $M = 1.20$; NPR = 7.0.

Figure 14. Concluded.



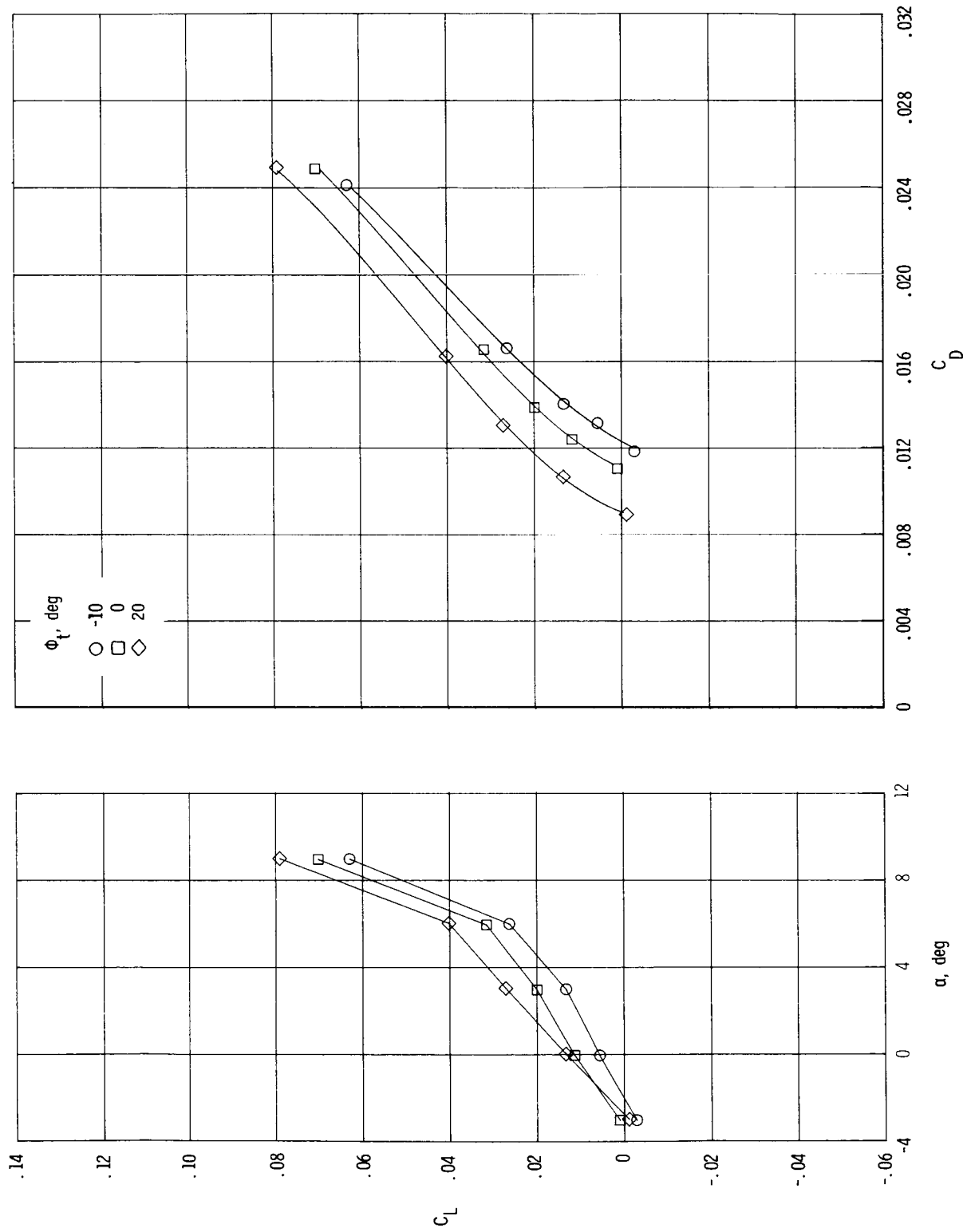
(a) $M = 0.60$; $NPR = 1.0$.

Figure 15. Effect of vertical tail cant angle on total aft-end characteristics for horizontal tails aft and vertical tails mid.



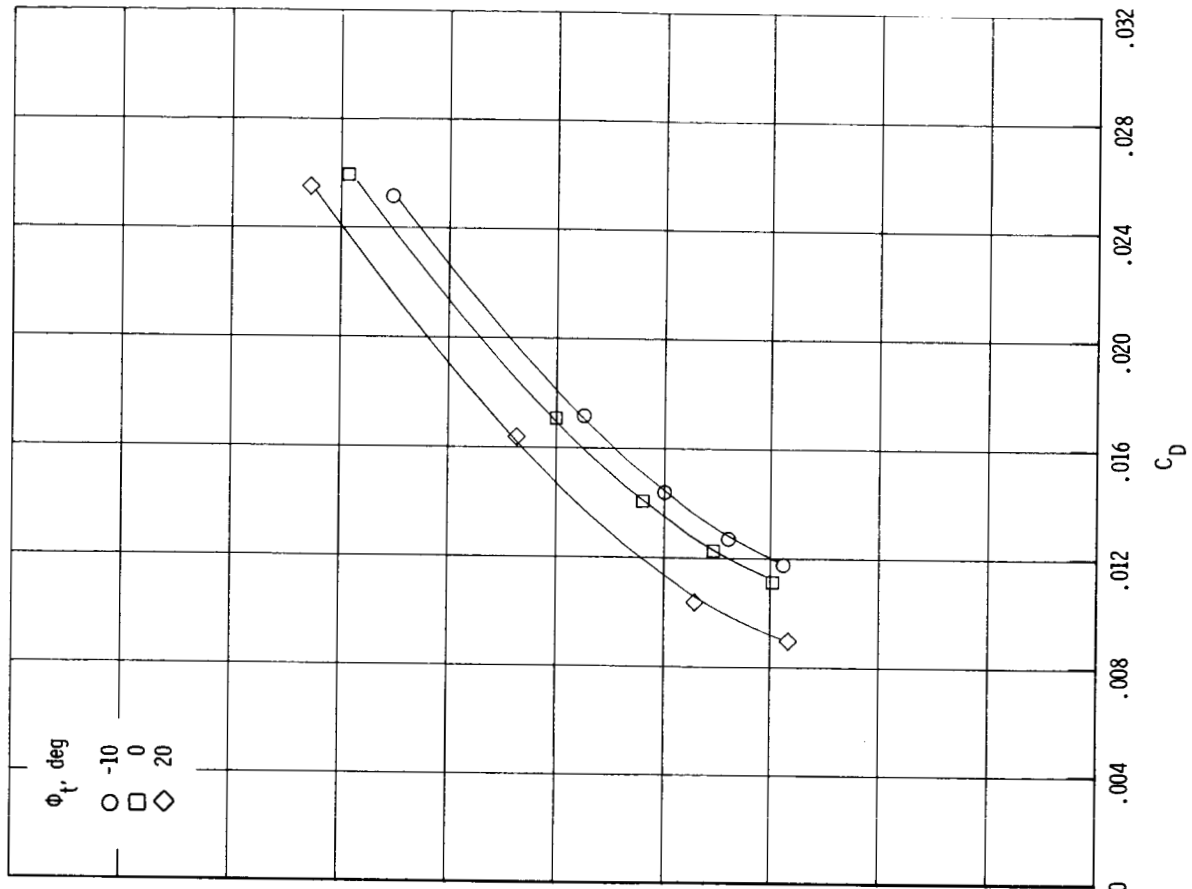
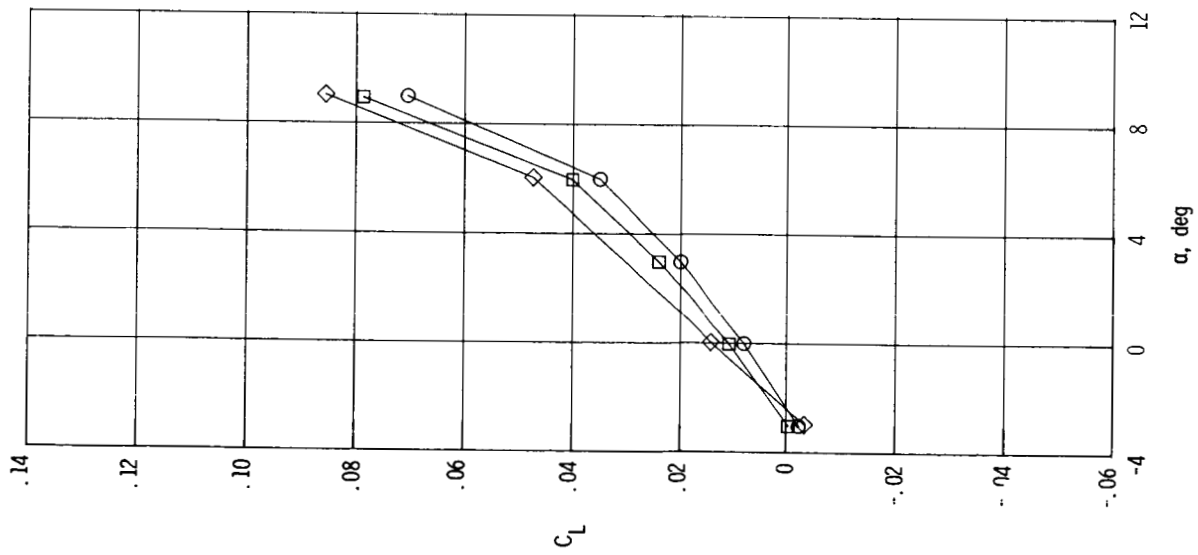
(b) $M = 0.60$; $NPR = 3.5$.

Figure 15. Continued.



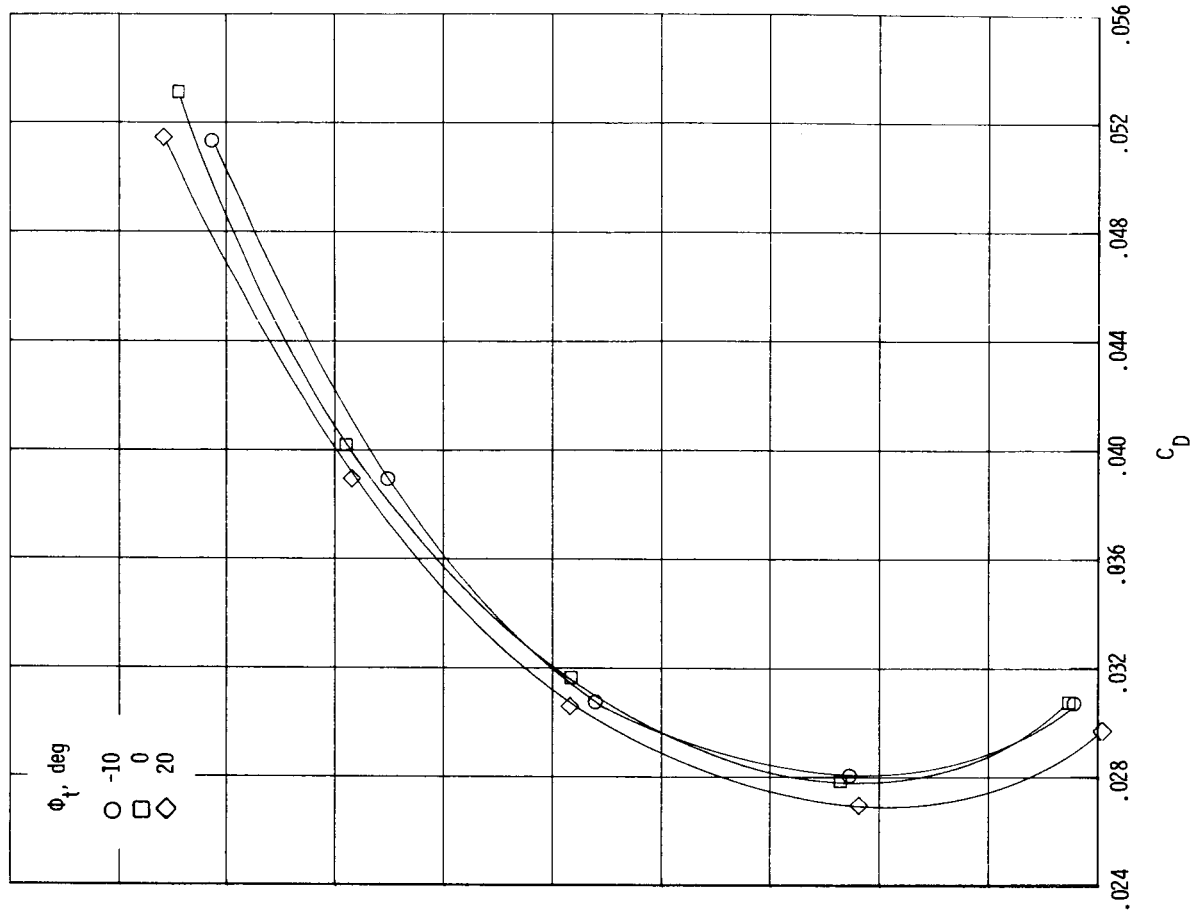
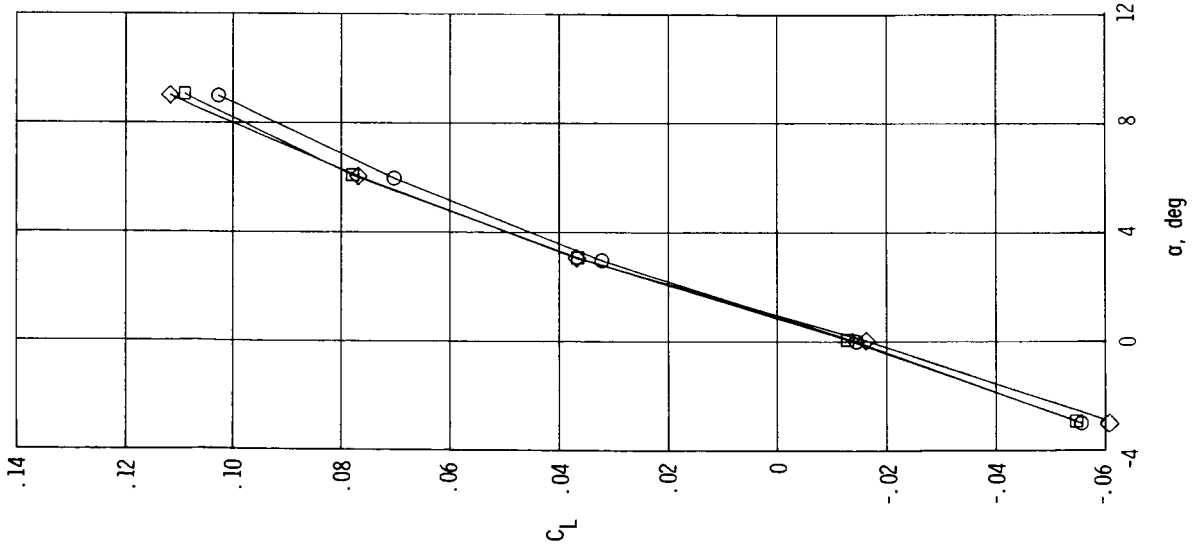
(c) $M = 0.90$; $NPR = 1.0$.

Figure 15. Continued.



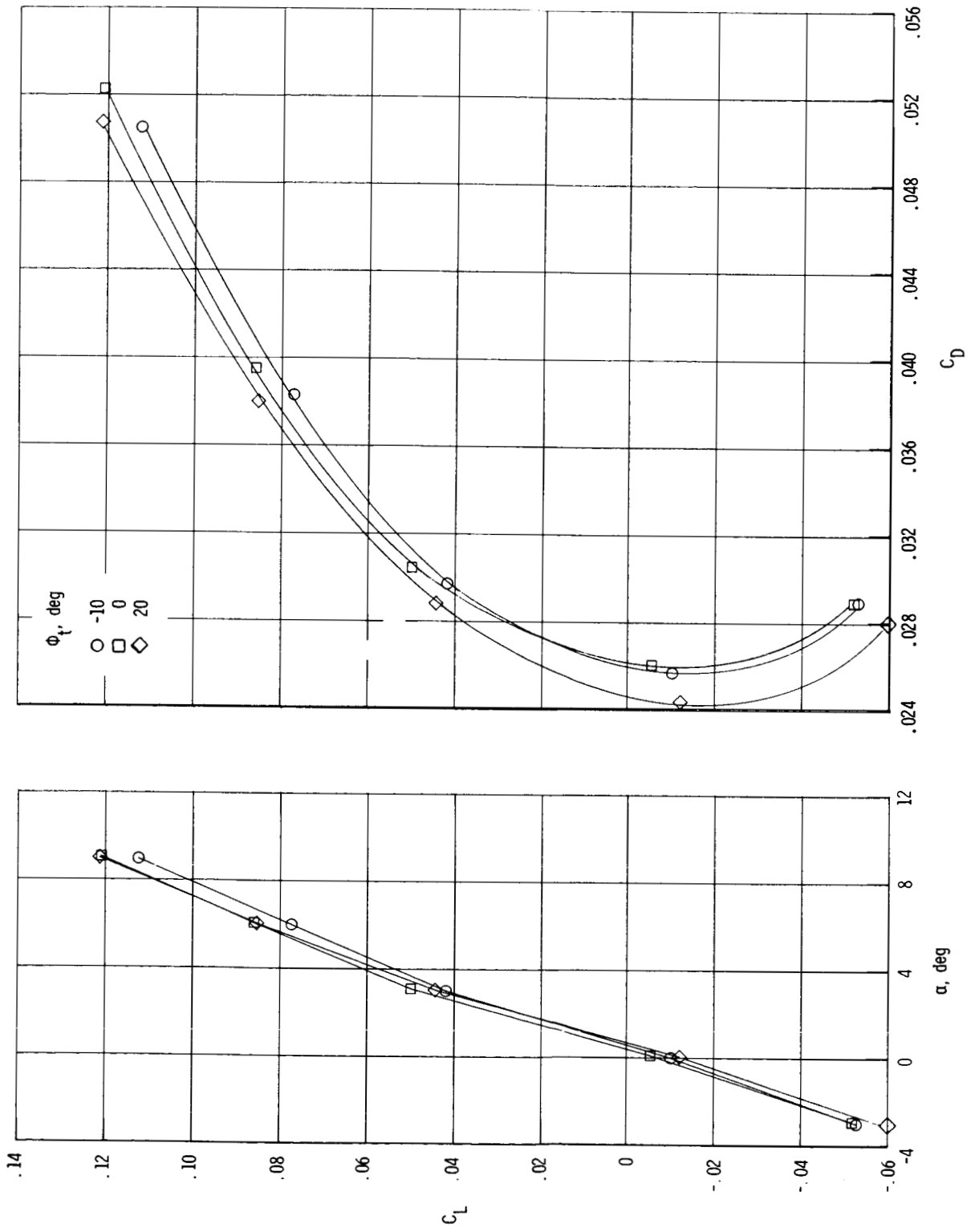
(d) $M = 0.90$; $NPR = 5.0$.

Figure 15. Continued.



(e) $M = 1.20$; NPR = 1.0.

Figure 15. Continued.



(f) $M = 1.20$; $NPR = 7.0$.

Figure 15. Concluded.

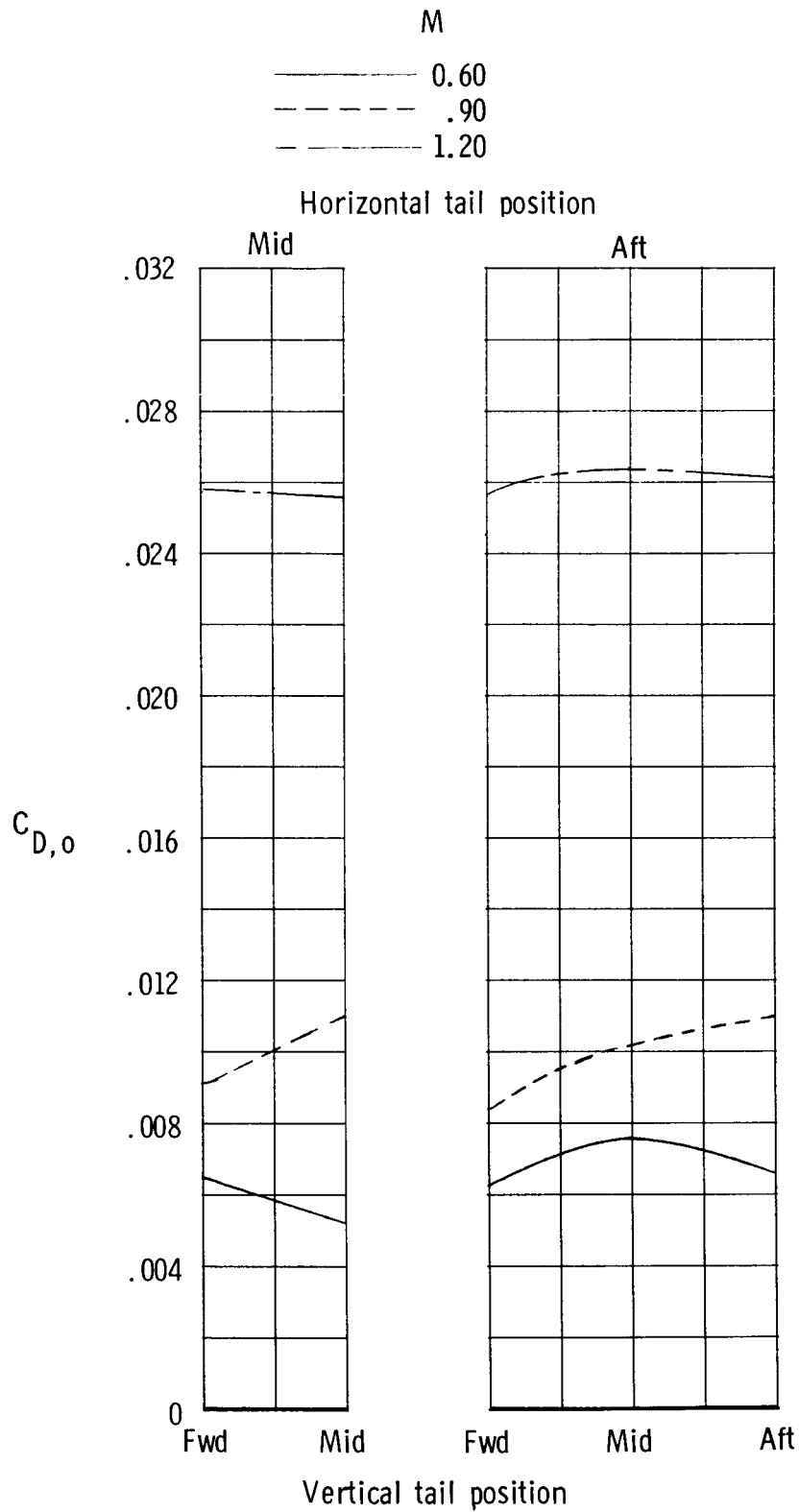


Figure 16. Summary of effect of empennage location on total aft-end drag coefficient at $C_L = 0$ for scheduled NPR. $\phi_t = 0^\circ$.

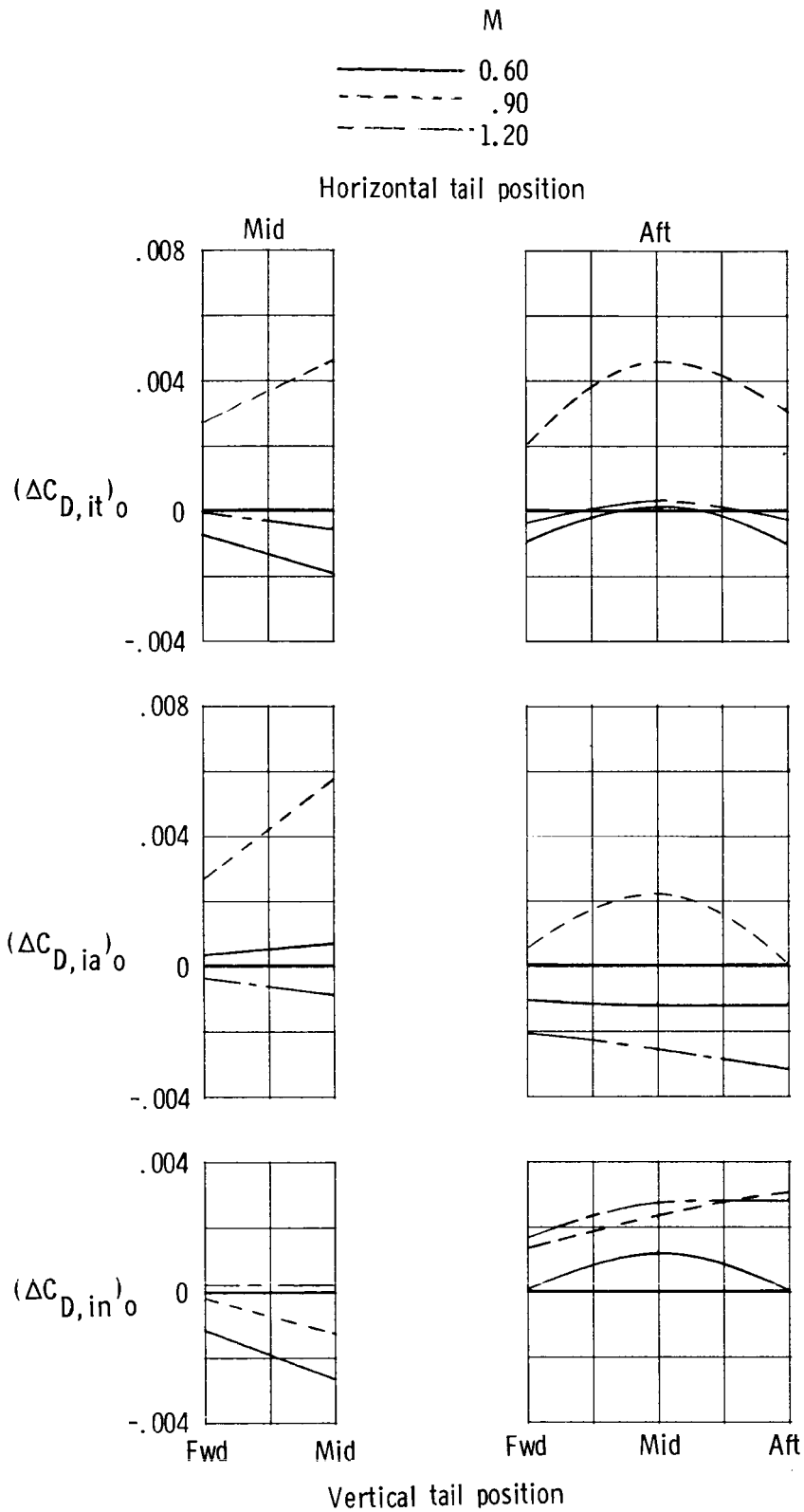


Figure 17. Summary of effect of empennage location on individual interference drag increments at $C_L = 0$ for scheduled NPR. $\phi_t = 0^\circ$.

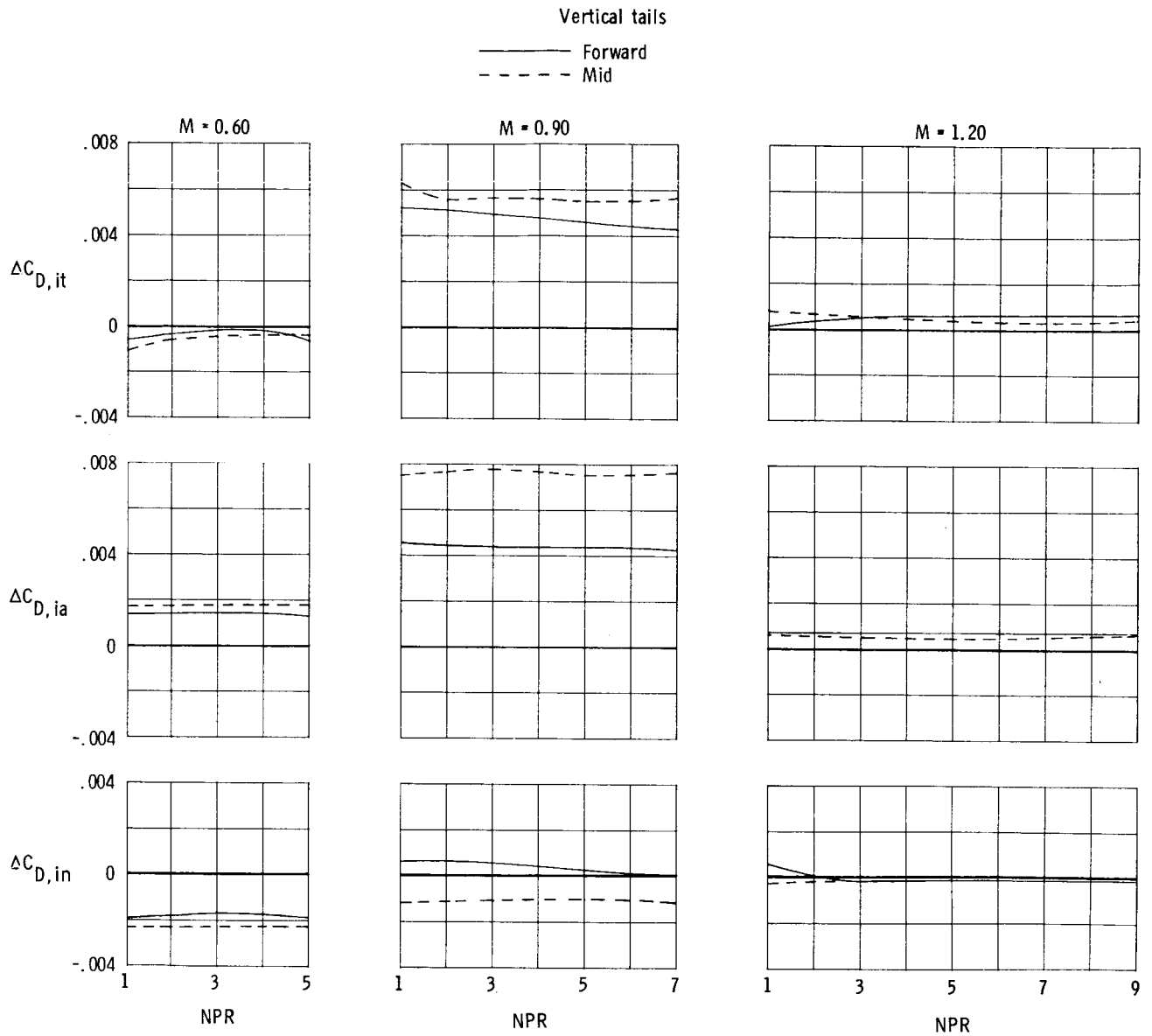


Figure 18. Effect of vertical tail position on individual interference drag increments for horizontal tails mid, $\phi_t = 0^\circ$, and $\alpha = 0^\circ$.

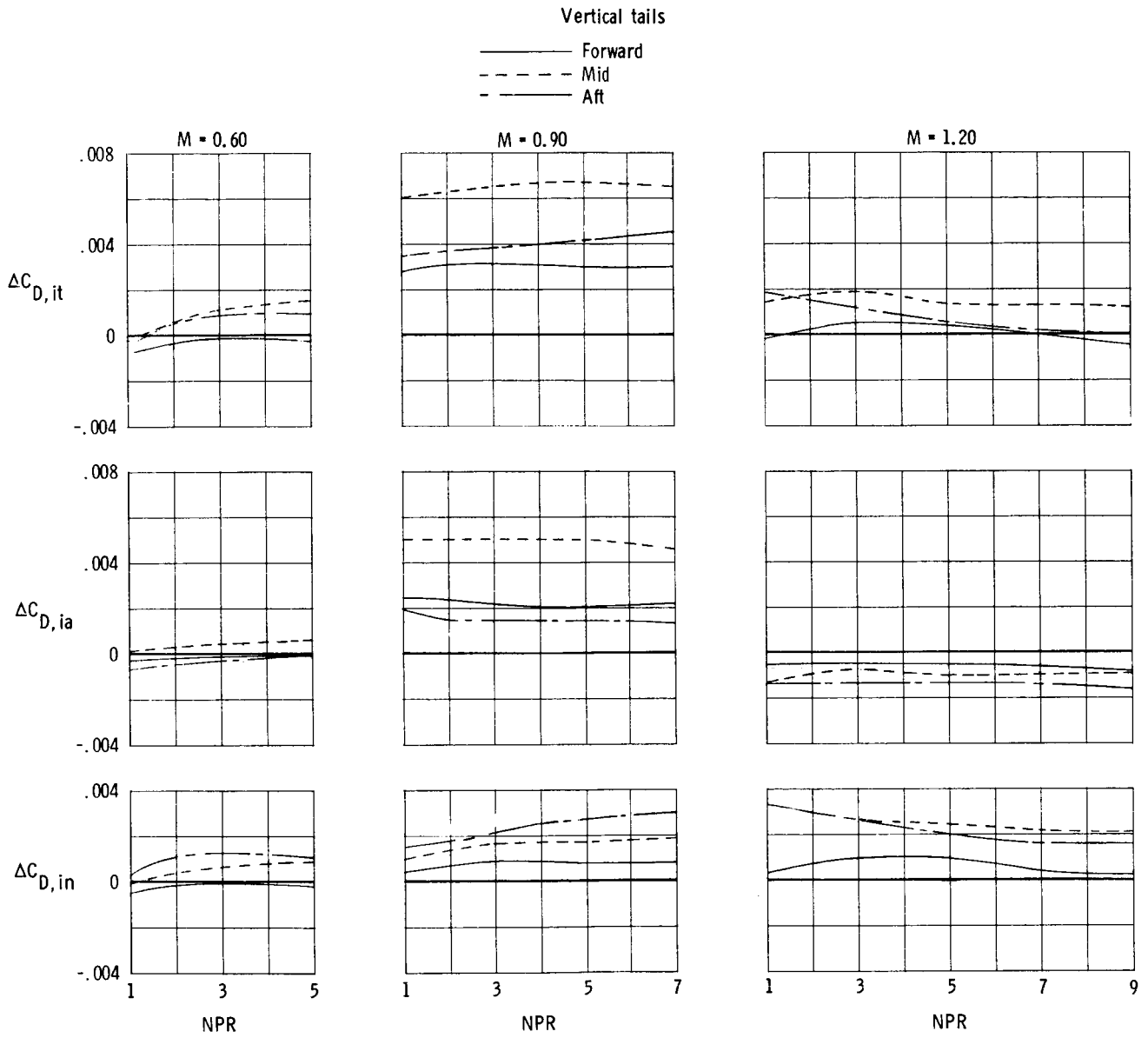


Figure 19. Effect of vertical tail position on individual interference drag increments for horizontal tails aft, $\phi_t = 0^\circ$, and $\alpha = 0^\circ$.

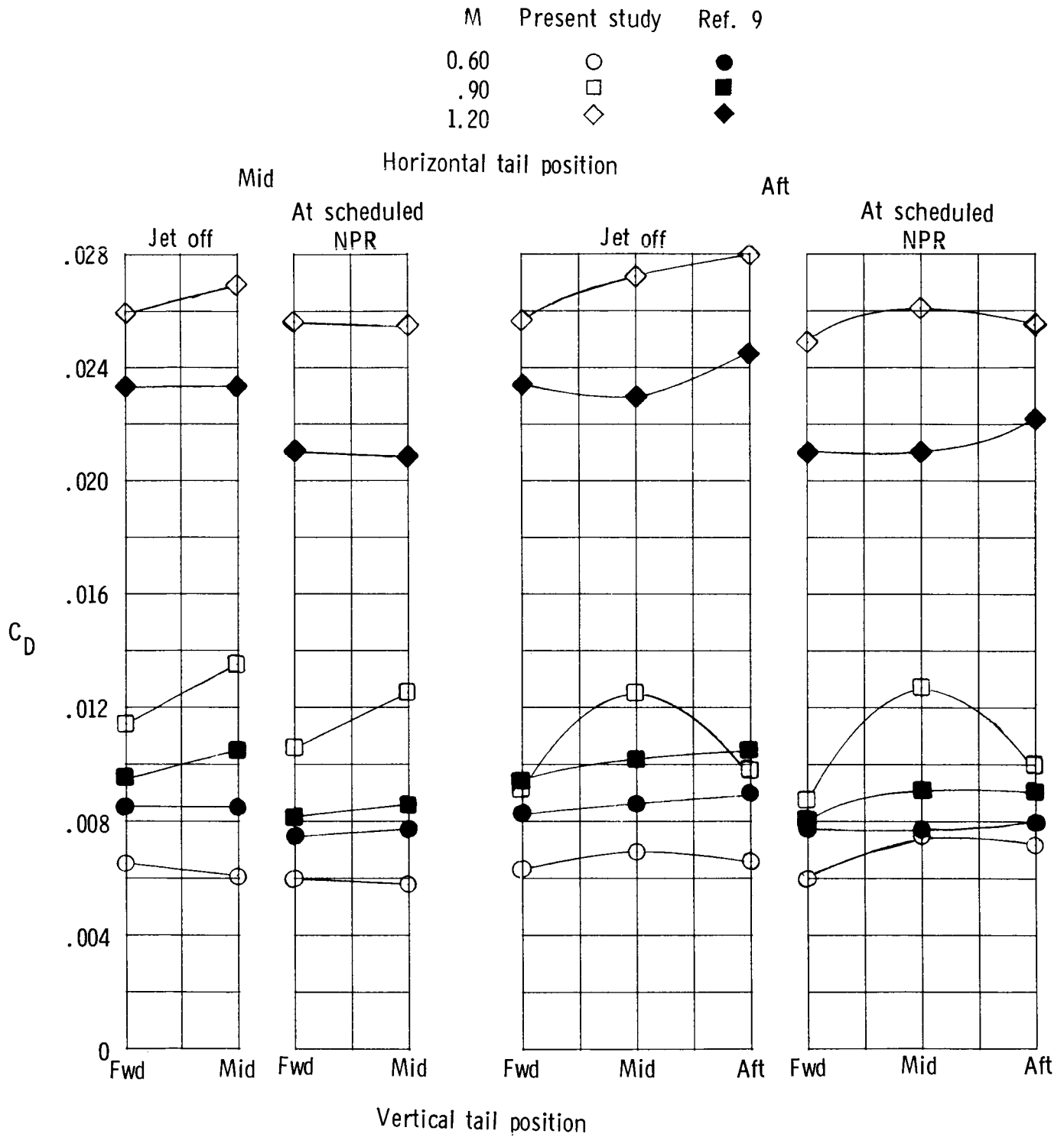


Figure 20. Comparison of total aft-end drag of present study with configuration with axisymmetric nozzles, $\alpha = 0^\circ$, and $\phi = 0^\circ$.

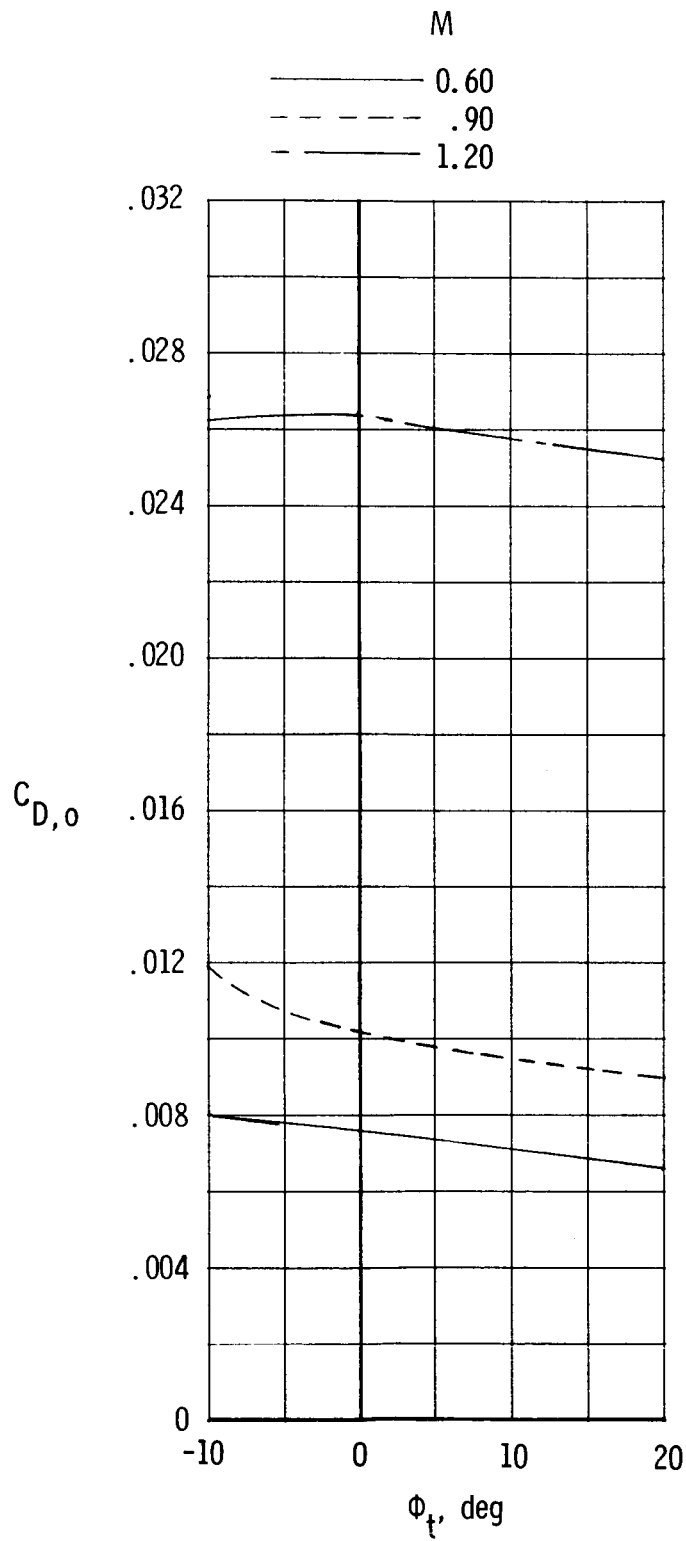


Figure 21. Summary of effect of vertical tail cant angle on total aft-end zero-lift drag coefficient for scheduled NPR, horizontal tails aft, and vertical tails mid.

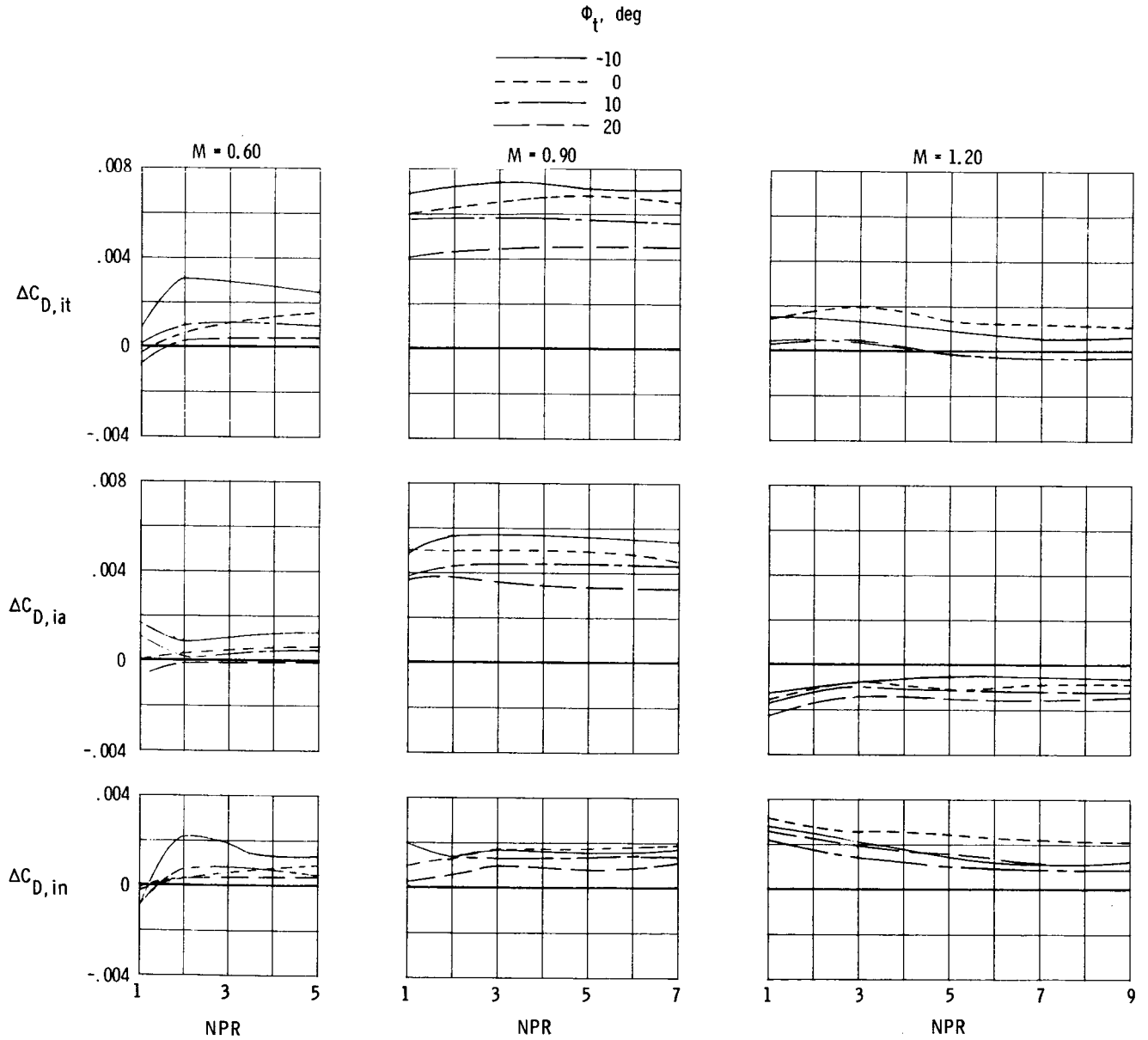
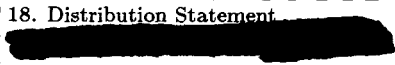


Figure 22. Effect of vertical tail cant angle on individual interference drag increments for horizontal tails aft, vertical tails mid, $\phi_t = 0^\circ$, and $\alpha = 0^\circ$.

1. Report No. NASA TP-2392	2. Government Accession No.	3. Recipient's Catalog No.	
4. Title and Subtitle EFFECTS OF EMPENNAGE SURFACE LOCATION ON AERODYNAMIC CHARACTERISTICS OF A TWIN- ENGINE AFTERBODY MODEL WITH NONAXISYMMETRIC NOZZLES		5. Report Date February 1985	6. Performing Organization Code 505-43-90-07
		8. Performing Organization Report No. L-15825	
7. Author(s) Francis J. Capone and George T. Carson, Jr.		10. Work Unit No.	
9. Performing Organization Name and Address NASA Langley Research Center Hampton, VA 23665		11. Contract or Grant No.	
		13. Type of Report and Period Covered Technical Paper	
12. Sponsoring Agency Name and Address National Aeronautics and Space Administration Washington, DC 20546		14. Sponsoring Agency Code	
		15. Supplementary Notes	
16. Abstract An investigation has been conducted in the Langley 16-Foot Transonic Tunnel to determine the effects of empennage surface location and vertical tail cant angle on the aft-end aerodynamic characteristics of a twin-engine fighter-type configuration. The configuration featured two-dimensional convergent-divergent nozzles and twin-vertical tails. The investigation was conducted with different empennage locations that included two horizontal and three vertical tail positions. Vertical tail cant angle was varied from -10° to 20° for one selected configuration. Tests were conducted at Mach numbers from 0.60 to 1.20 and at angles of attack from -3° to 9° . Nozzle pressure ratio was varied from jet off to approximately 9, depending upon Mach number. Tail interference effects were present throughout the range of Mach numbers tested and were found to be either favorable or adverse, depending upon test condition and model configuration. At a Mach number of 0.90, adverse interference effects accounted for a significant percentage of total aft-end drag. Interference effects on the nozzle were generally favorable but became adverse as the horizontal tails were moved from a mid to an aft position. The configuration with nonaxisymmetric nozzles had lower total aft-end drag with tails-off than a similar configuration with axisymmetric nozzles at Mach numbers of 0.60 and 0.90.			
17. Key Words (Suggested by Authors(s)) Tail interference Empennage location Twin noise Afterbody drag Nonaxisymmetric nozzles		18. Distribution Statement  Until February 1987 Subject Category 02	
19. Security Classif.(of this report) Unclassified	20. Security Classif.(of this page) Unclassified	21. No. of Pages 77	22. Price